UNDERSTANDING ACTIVE ABL KINASE CONFORMATIONS: APPLICATION TO DISCOVERY OF SMALL MOLECULE ALLOSTERIC MODULATORS

by

Prerna Grover

Bachelor of Engineering in Biotechnology, Panjab University, 2009

Submitted to the Graduate Faculty of

Medicine in partial fulfillment

of the requirements for the degree of

Doctor of Philosophy

University of Pittsburgh

2015

UNIVERSITY OF PITTSBURGH

SCHOOL OF MEDICINE

This dissertation was presented

by

Prerna Grover

It was defended on

April 13, 2015

and approved by

Jeffrey L. Brodsky, Ph.D., Dissertation Committee Chair, Biological Sciences

J. Richard Chaillet, M.D., Ph.D., Microbiology and Molecular Genetics

Qiming Jane Wang, Ph.D., Pharmacology and Chemical Biology

Ora A. Weisz, Ph.D., Cell Biology

Thomas E. Smithgall, Ph.D., Dissertation Advisor, Microbiology and Molecular Genetics

UNDERSTANDING ACTIVE ABL KINASE CONFORMATIONS: APPLICATION TO DISCOVERY OF SMALL MOLECULE ALLOSTERIC MODULATORS

Prerna Grover, Ph.D.

University of Pittsburgh, 2015

The c-Abl protein-tyrosine kinase regulates diverse cellular signaling pathways involved in cell growth, adhesion, and responses to genotoxic stress. Abl is well known in the context of Bcr-Abl, the active fusion tyrosine kinase, which causes chronic myelogenous leukemia (CML) and other leukemias. The tyrosine kinase activity of Abl is tightly regulated by auto-inhibitory interactions involving its non-catalytic SH3 and SH2 domains. Mutations that perturb these intramolecular interactions result in kinase activation. This study examined the effect of activating mutations on the biochemistry and solution structure of Abl core proteins. In an active myristic acid-binding pocket mutant (A356N), the relative positions of the regulatory N-cap, SH3 and SH2 domains were virtually identical to those of the assembled wild-type core despite differences in catalytic activity and thermal stability. In contrast, a dramatic structural rearrangement in an active gatekeeper mutant (T315I) was observed with the positions of the SH2 and SH3 domains reversed relative to wild-type. These results show that Abl kinases can adopt multiple conformations in solution and kinase activation does not necessarily require destabilization of the assembled core structure.

Small molecules that allosterically regulate Abl kinase activity through its non-catalytic domains may represent selective probes of Abl function. I developed a screening assay to identify chemical modulators of Abl kinase activity that either disrupt or stabilize the regulatory interaction of the SH3 domain with the SH2-kinase linker. This fluorescence polarization (FP)

assay is based on a recombinant Abl protein containing the regulatory domains (Ncap-SH3-SH2-linker, N32L) and a short fluorescein-labeled probe peptide that binds the SH3 domain. The probe peptide binds the recombinant Abl N32L protein in vitro producing a robust FP signal. Mutation of the SH3 binding site (W118A) or introduction of a high-affinity linker both resulted in loss of the FP signal. Pilot screens were performed with two chemical libraries (2800 compounds total), and thirteen compounds were found to specifically inhibit the FP signal. Secondary assays showed that one of these hit compounds enhances Abl kinase activity *in vitro*. These results show that screening assays based on the regulatory domains of Abl can identify allosteric modulators of kinase function.

TABLE OF CONTENTS

LIST OF TABLES

LIST OF FIGURES

ACKNOWLEDGEMENTS

I cannot believe that it's almost time for my thesis defense! While graduate school has been an incredible journey, it has been filled with many ups and downs. I couldn't have made it to this day without the support of many people, both inside the lab and outside, and I would like to express my sincere gratitude and appreciation.

First and foremost, I'd like to express heartfelt gratitude for my advisor Dr. Thomas Smithgall. Thank you for giving me many opportunities and for your mentorship and support throughout my tenure in your lab. Your enthusiasm for science, your sharp scientific acumen, and the breadth of your knowledge have always been a source of inspiration for me. Thank you for your guidance in helping me learn to focus on finding the solutions to a problem, and to constructively think and write about science. I shall always be grateful for your belief in me that always motivated me to work harder.

I would like to thank my dissertation thesis committee members for their ongoing guidance and support. I really appreciate the time and effort you invested into my scientific career, thank you for asking me insightful questions in the committee meetings and for helping me develop my thesis project. Dr. Jeffrey Brodsky, thank you for agreeing to be the chair of my thesis committee and for your guidance and suggestions for future career options. Dr. Richard Chaillet, thank you for your commitment and support for my research since the early days of my comprehensive examination. Dr. Ora Weisz, thank you for your commitment and for your sincere concern for my research progress. Dr. Jane Wang, thank you for your enthusiasm for my research project, and for your continued encouragement through the years.

I would like to thank our collaborators who have contributed to different parts of my thesis project and helped make it a complete story. Dr. John Engen and Dr. Roxana Iacob, thank you for conducting mass spectrometric analysis for the Abl proteins. Dr. Lee Makowski and Dr. John Badger, thank you for performing and analyzing the SAXS experiments for the Abl proteins. Dr. Haibin Shi, thank you for performing SPR experiments and analyzing data for compound binding to Abl proteins. Dr. Carlos Camacho and Matt Baumgartner, thank you for performing molecular dynamic simulations and generating docking models for compound binding to Abl proteins.

I would like to thank current and former members of the Smithgall lab for their continued support through the years: Dr. Lori Emert-Sedlak, Dr. John-Jeff Alvarado, Dr. Haibin Shi, Dr. Jerrod Poe, Dr. Sherry Shu, Dr. Sabine Hellwig, Dr. Heather Rust, Dr. Malcom Meyn III, Dr. Linda O'Reilly, Dr. Patty George, Dr. Shoghag Panjarian, Dr. Purushottam Narute, Dr. Xiong Zhang, Dr. Jamie Moroco, Dr. Sreya Tarafdar, Mark Weir, Kindra Whitlatch, Eleanor Johnston, Ravi Patel, and Kathleen Makielski. Thank you all for sharing many chats and lunches and walks, and for making it fun to work in the Smithgall lab. Shoghag, thank you for welcoming me to the lab and helping me get started on my research project, and for your enthusiasm for my 'Hallosteric' compounds. Also, thank you for being a great friend and for sharing your love and concern in all the years that I have known you! Lori, thank you for your help during the early stages of my screening assay development and protein purifications, and for all the chats about science and life. John-Jeff, thank you for helping me get started with the thermal melt assays, and for your cheerful presence in the lab. Jerrod, thank you for helping me get started with data analysis for the high throughput screens. Jamie, thank you for helping me get started with the ADP Quest assay. Sherry, thank you for being a great friend and support through the years, and for sharing the many walks and talks. I have appreciated our conversations about science as well as life, and you have been a source of inspiration.

I would like to thank the faculty members in the Program in Integrative Molecular Biology and the Department of Microbiology and Molecular Genetics for providing a great scientific environment. I would specially like to thank Dr. Gary Thomas and Laurel Thomas for many conversations about science, life and career, and for their constant encouragement. I also want to

extend a special thank you to students in the PIMB program for all the fun conversations about science and life, and for being great friends. I would also like to thank the dissertation support group for supporting me in the toughest times and for reminding me about the light at the end of the tunnel.

I would like to thank the staff in the Program in Integrative Molecular Biology and the Department of Microbiology and Molecular Genetics for all their work behind the scenes that ensures that we can focus on our experiments and research. Thank you Joann Polk, John Viaropulos, Susanna Godwin, Jennifer Walker, Christian Yates, Mary Lou Meyer, Diane Vaughan, Joe Llaneza and all the other staff members.

I could not have made it this far without the support of friends and family. I would like to thank many friends, old and new, for always being available to talk and share life's ups and downs. Thank you for helping me stay sane through these years: Jess, Dushani, Monika, Manasi, Rounak, Amita, Kathleen, Tarun, Madhav, Reety, Nisha, Sriranjini, Krishna Samavedam, Krishna Subramaniam, Amitabh, Sumreet, Sonam, Nitesh, Navjeet, Priyanka, Dhananjay, and Sonal Gaur. I want to thank volunteers at the non-profit organization AID (Association for India's Development) for keeping me grounded and focused on the bigger picture of life.

I would like to thank my immediate and extended family who have been my greatest support all these years. I want to thank my parents for always believing in me, and for encouraging me to reach for the stars. Thank you for all the sacrifices and the hard work, I wouldn't have been here if it weren't for all that you've done. I want to thank my siblings, Anandita, Arundhatii, and Raghav, and my brothers-in-law Rohit and Ritesh for their faith in me, for their constant understanding and acceptance, and for always cheering me on. I want to thank my extended family, my grandparents, my *mamas* and *mamis* and cousins for their support and encouragement. I also want to thank Abhishek, for being there through thick and thin. Thank you for always making me laugh and for making the hardest times bearable!

1.0 INTRODUCTION

1.1 C-ABL KINASE OVERVIEW

c-Abl was identified as the cellular homolog of the v-Abl oncogene in the Abelson murine leukemia virus (A-MuLV) that causes lymphosarcoma in mice [1–3]. Subsequently, it was found that the c-Abl gene is involved in human leukemias caused by chromosomal translocation t(9,22) that gives rise to the Philadelphia chromosome (discussed later in section 1.4), and encodes a non-receptor protein tyrosine kinase [4,5]. The mammalian c-Abl gene (or Abl 1), and its closest relative Arg (Abl related gene or Abl 2), are ubiquitously expressed. Both c-Abl and Arg are alternatively spliced in the first exon, and encode two splice variants of the protein – 1a and 1b that have distinct N-terminal sequences [6]. The 1b form of c-Abl is myristoylated at the N-terminal glycine residue of the protein, while the 1a form is not myristoylated and is shorter by 19 amino acids. This thesis focuses on the 1b isoform of the c-Abl protein, and will be referred to hereafter as Abl .

The domain organization of the c-Abl 1b protein is shown in Figure 1 [7,8]. The N-terminal half of the protein contains a unique N-terminal region, followed by Src-homology 3 (SH3) and Src-homology 2 (SH2) domains, an SH2-kinase linker, and the kinase domain. The kinase domain is followed by the C-terminal half of the protein that includes proline-rich

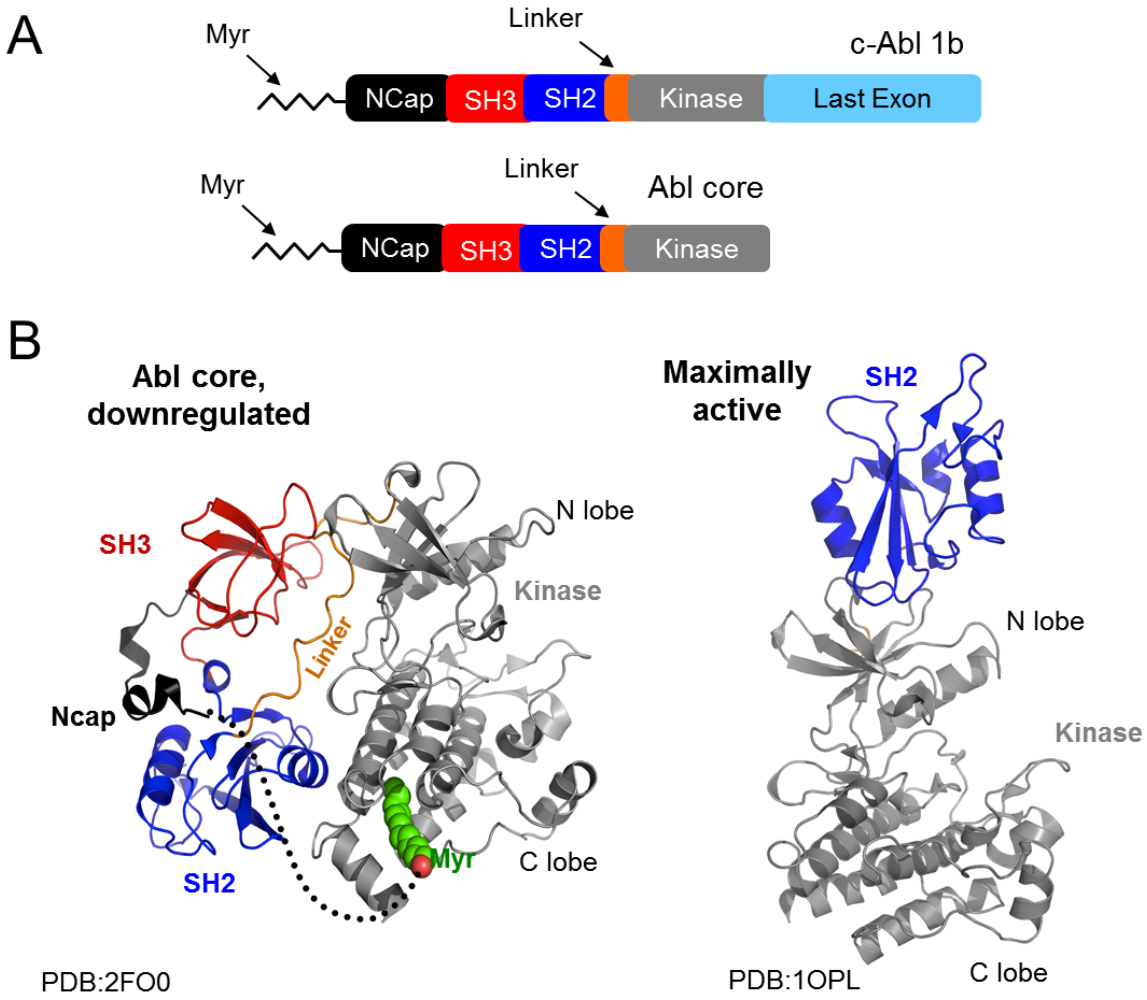

Figure 1. The organization and regulation of Abl proteins.

(A) *Top:* The modular domain organization of the c-Abl 1b protein is shown. It consists of a myristoylated N-cap, SH3 and SH2 domains, SH2-kinase linker, kinase domain, and a last exon region that includes proline rich regions, DNA and actin binding domains, nuclear localization and export signals. *Bottom:* The Abl core protein, which includes the N-terminal half of the protein as shown, was found to be sufficient for regulation of Abl kinase activity. (B) *Left:* The crystal structure of the assembled down-regulated conformation of the Abl core (PDB: 2FO0, [9]) is shown, with the disordered portion of the N-cap represented as a dotted line. The autoinhibited Abl core is stabilized by three critical intramolecular interactions. The linker forms a PP II helix and binds the Abl SH3 domain, while the SH2 domain interacts with back of the C-lobe of the kinase domain through extensive hydrogen bonding interactions. The myristoylated N-cap binds a hydrophobic pocket in the C-lobe of the kinase domain, and acts as a clamp packing the SH3 and SH2 domains against the back of the kinase domain. *Right:* In a maximally activated conformation of the Abl core, also called the 'top-hat' conformation, the SH2 domain is reoriented to the top of the kinase domain and stabilizes the active conformation of the kinase. The location of the SH3 domain and the linker could not be identified in this structure.

regions, nuclear localization and export signals, and DNA and actin binding domains. Through the SH2 and SH3 domains as well as the protein binding domains in the C-terminal region, Abl interacts with diverse classes of proteins such as transcription factors, actin, pro-apoptotic proteins, proteins in the DNA-damage repair pathway, and adaptor proteins. Consequently, Abl is involved in the regulation of several signaling pathways that regulate cell proliferation and survival, actin remodeling, cell adhesion and migration, and responses to DNA-damage and oxidative stress [7]. Moreover, the Abl protein is temporally localized to different sub-cellular compartments such as the nucleus, cytoplasm, and plasma membrane, depending on the cellular environment and activating stimuli. For example, while nuclear Abl is activated in response to DNA damage, and involved in cell cycle control and apoptotic promotion (discussed later in section 1.3), cytoplasmic Abl is activated at the cell periphery in response to integrin engagement and growth factor stimulation (discussed later in section 1.2.3.3) [7,10].

1.2 STRUCTURE AND REGULATION OF C-ABL

As described above, Abl plays an important role in the regulation of multiple cellular processes in cells. Consequently, its kinase activity is tightly regulated by multiple mechanisms. Aberrant activation of Abl as a result of chromosomal translocations can lead to leukemias in humans, as discussed later in section 1.4. The following sections will discuss the key structural elements essential for the physiological regulation of Abl kinase activity.

1.2.1 Regulation by intramolecular interactions

The kinase 'core' of the Abl protein consists of the N-terminal half of the protein, including the N-terminal cap, the SH3 and SH2 domains, the SH2-kinase linker, and a bi-lobed kinase domain (Figure 1) [11]. This Abl core protein was found to be necessary and sufficient for auto-inhibition of the Abl protein tyrosine kinase activity. Subsequent X-ray crystal structures revealed three critical intramolecular interactions that are important for Abl auto-inhibition (Figure 1) [9,12,13]. Each of the elements involved in these intramolecular interactions are discussed below.

1.2.1.1 N-terminal cap (N-cap)

The N terminus of the Abl protein contains a unique 80 amino acid residue region called the N-terminal cap (referred to as N-cap hereafter). Mutagenesis studies showed that deletion of this N-cap region leads to kinase activation, thus suggesting that this region is important for inhibiting Abl kinase activity [13]. Further investigation into the mechanism of action revealed that the N-cap is myristoylated at the N-terminal glycine residue and mutation of this glycine residue to alanine (G2A) leads to a loss of myristoylation and kinase activation, suggesting that myristoylation is important for Abl regulation [14]. Furthermore, deletion mutagenesis of the N-cap revealed that residues 15-56 are not essential for the regulation of Abl kinase activity.

The first crystal structure of the Abl core was solved in 2003 and revealed that the myristate moiety binds a deep hydrophobic pocket in the C-lobe of the kinase domain [12]. Mutations in the hydrophobic pocket in the kinase domain that disrupt myristate binding also lead to kinase activation [14]. Introducing polar residues in this hydrophobic pocket, including replacement of Ala356 with asparagine (A356N) or Val525 with aspartate (V525D), result in kinase activation, possibly through the loss of myristate binding. Interestingly, the crystal

structure showed that binding of the myristate moiety induces bending of the α-helix I in the C-lobe of the kinase domain, and this conformational switch is important for auto-inhibitory interactions between the SH2 domain and the kinase domain (discussed later in section 1.2.1.3) [12].

In addition to the kinase domain, the N-cap also makes important contacts with the SH3 and SH2 domains, and the SH3-SH2 connector that joins these domains. In the first crystal structure of Abl, the entire N-cap region, from the SH3 domain to the myristate moiety, was disordered [12]. Subsequently, a higher resolution crystal structure of the Abl core, with an internal deletion of residues 15-56, was solved where residues 65-82 were modeled into the electron density [9]. In this structure, amino acid residues 2-14 and 57-64 were still disordered and were predicted to form an inherently flexible structure that is shown as the dotted region in Figure 1. The crystal structure revealed that several residues in the N-cap, including Trp67, Leu73, and Leu74, interact with a patch of hydrophobic residues on the SH2 domain, while Lys70 interacts with several residues in the SH2 domain through hydrogen bonding. These interactions are important for kinase regulation since disruption of these interactions by individual mutations of Lys70 or Leu73 to alanine leads to kinase activation [9,13,14]. Interestingly, the crystal structure revealed that a serine residue at position 69 in the N-cap is phosphorylated. This phosphoserine residue forms hydrogen bonds with Ser145 and Trp146 in the SH3-SH2 connector. While mutation of the N-cap Ser69 to alanine (S69A) had a weak effect, mutation to glutamate (S69E) had a strong activating effect on Abl kinase activity. This suggests an important role for the Ser69 residue in kinase regulation, although the identity of the kinase responsible for this modification *in vivo* is not clear. In conclusion, the N-cap plays an important regulatory role in Abl auto-inhibition where the myristoylated N-terminal part of the

N-cap interacts with the C-lobe of the kinase domain, while the C-terminal portion interacts with the SH3-SH2 connector and the SH2 domain and acts as a clamp to stabilize the Abl SH3-SH2 regulatory subunit against the back of the kinase domain.

1.2.1.2 SH3 domain

The SH3 domain is a small modular domain present in signaling proteins consisting of about 60 amino acids [15]. The structures of many SH3 domains have been studied by X-ray crystallography and NMR spectroscopy, and a typical SH3 domain contains five anti-parallel β-strands that form two perpendicular β-sheets [16,17]. In addition, there are two charged loops called the RT loop and the n-Src loop that vary across SH3 domains from different proteins.

SH3 domains interact with other proteins through proline-rich regions that form poly-proline type II helices (PP II). This principle was first discovered in a phage-display screen for binding partners of the Abl SH3 domain, and defined a consensus sequence for Abl SH3 binding as XPXXXPPPFXP, where X is any amino acid [18,19]. The ligand-binding site in the SH3 domain consists of a cluster of conserved hydrophobic amino acids that form three shallow pockets, surrounded by the n-Src and n-RT loops that confer specificity and determine the orientation of ligand binding [17]. SH3 domains serve multiple functions, including scaffolding for signaling pathways, substrate recognition, and regulation of enzymatic activity.

The Abl SH3 domain is important for regulation of Abl kinase activity, and deletion of the SH3 domain results in constitutive kinase activation [20–22]. The Abl SH3 domain regulates kinase activity by interacting with the SH2-kinase linker, which forms a PPII helix (Figure 2) [12]. Mutations in the ligand binding surface of the SH3 domain that are predicted to disrupt this SH3:linker interaction, such as P131L and W118A, lead to kinase activation [22,23]. Moreover,

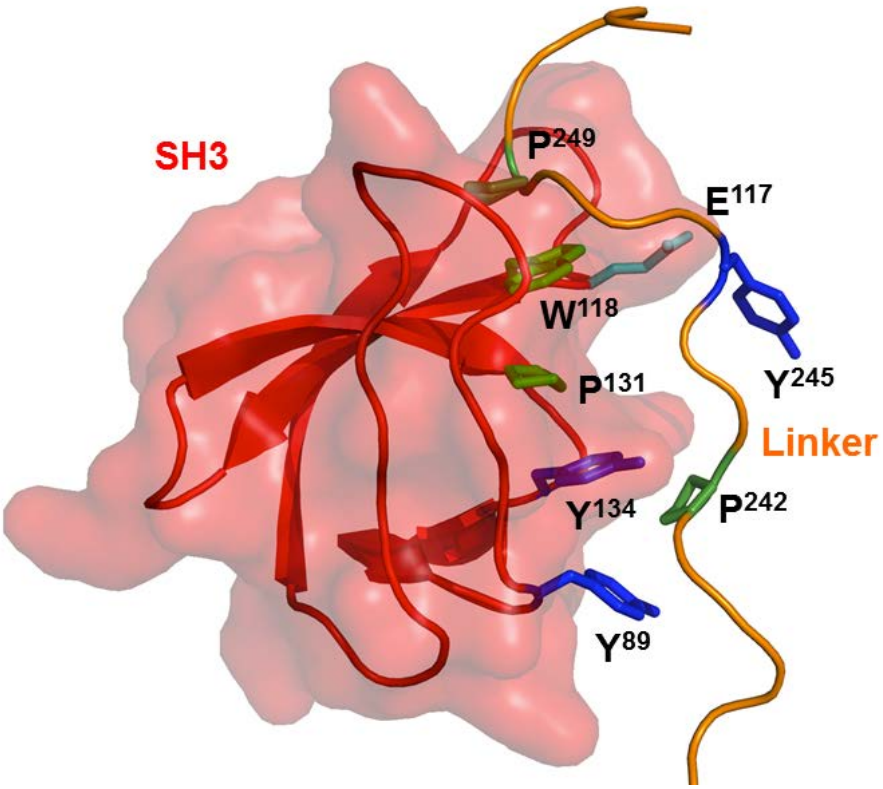

Figure 2. Mutations that disrupt the Abl SH3:linker interaction cause kinase activation.

A model of the interface between the SH3 domain and the SH2-kinase linker, derived from the down-regulated Abl core crystal structure (PDB: 2FO0 [9]), is shown. The positions of residues in the SH3 domain and linker, which are important for Abl regulation, are color-coded and presented as sticks. *Green:* Mutations of W118 and P131 in the SH3 domain and proline residues 242 and 249 in the linker cause disruption of the SH3:linker interaction, and consequent kinase activation. *Cyan:* Mutation of E117 in the SH3 domain disrupts the ionic interaction with K313 (located in the N-lobe of the kinase domain) and results in kinase activation. *Blue:* Phosphorylation of tyrosine residues 89 and 134 in the SH3 domain, and Y245 in the linker are correlated with kinase activation. The phosphorylation of Y89 and Y134 interferes with SH3:linker interaction.

phosphorylation of tyrosine residues in the Abl SH3 domain, such as Tyr134 and Tyr89, are also predicted to disrupt the SH3:linker interaction and are associated with kinase activation [24,25]. In addition, SH3 domain Glu117 makes an ionic contact with kinase domain N-lobe Lys313. This interaction also contributes to kinase auto-inhibition since mutating these residues (E117K or K313E) disrupts this salt bridge and leads to kinase activation [23].

1.2.1.3 SH2 domain

SH2 domains are small modular protein domains containing about 100 amino acids, and are present in most non-receptor protein tyrosine kinases and other signaling proteins [15]. SH2 domains were first identified as homologous non-kinase domain sequences shared by the oncoproteins Src and Fps, and later found to be present in many other proteins [26]. Structurally, a typical SH2 domain contains a central hydrophobic anti-parallel β-sheet, which is flanked by two α-helices [15]. SH2 domains bind protein or peptide ligands containing a phosphotyrosine (pY) residue, followed by specific amino acids that define selectivity [27]. The ligand binding surface of the SH2 domain consists of two pockets – one contains a conserved arginine residue and binds the phosphotyrosine side chain, while the other interacts with hydrophobic residues C-terminal to the phosphotyrosine. While the first phosphotyrosine binding pocket is highly conserved, the second recognition pocket is variable across different proteins and confers binding specificity. By virtue of their ability to recognize and bind unique phosphotyrosine containing motifs, SH2 domains play multiple roles in proteins and signaling pathways. They play an important role in the regulation of enzymatic activity by auto-inhibitory interactions, recognition of enzymatic substrates, and have scaffolding functions in signaling pathways.

The crystal structure of the Abl core revealed that the SH2 domain in Abl interacts with the back of the C-lobe of the kinase domain through extensive hydrogen bonding and hydrophobic interactions [12]. These interactions are dependent on the restructuring of the C-terminal helix αI, which is induced by binding of the myristoylated Ncap to the C-lobe as described above [9,12,14]. Mutations in the SH2 domain or the C-lobe of the kinase domain that disrupt this interaction were found to lead to kinase activation [14]. In a maximally activated conformation of Abl that lacks all intramolecular interactions, the SH2 domain was found to reorient its position to the top of the N-lobe of the kinase domain [9]. The SH2 domain, in this "top-hat" conformation, interacts with specific residues in the N-lobe of the kinase domain and stabilizes this active conformation. A similar stabilization of the active conformation by SH2-N-lobe interaction is also seen in the non-receptor tyrosine kinase, Fes.

1.2.1.4 SH2-kinase linker

The SH2-kinase linker forms a PPII helix and acts as an internal ligand for the Abl SH3 domain, thus contributing to the down-regulated conformation of the Abl kinase core [12]. Even though similar SH3:linker interactions are also observed in the structures of downregulated Src-family kinases, there are important differences in the SH2-kinase linker sequences. In contrast to Hck, a member of the Src kinase family, the Abl SH2-kinase linker contains a tyrosine residue at the second proline position in the 'PXXP' motif, and this Tyr245 points away from the SH3 domain and packs in a hydrophobic crevice in the kinase domain [12]. Moreover, the Abl linker contains two additional residues near the N-lobe of the kinase domain, Trp254 and Glu255, which contribute towards the unique conformation exhibited by the Abl SH2-kinase linker. Furthermore, hydrogen exchange mass spectrometry studies have shown that the Abl SH2-kinase

linker binds the SH3 domain in the absence of the kinase domain [28], which is not the case for Hck.

The SH3:linker interaction is important for the regulation of Abl kinase activity, as mutation of linker proline residues (P242E and P249E) disrupts SH3:linker interaction and leads to kinase activation (Figure 2) [23]. Moreover, phosphorylation of Tyr245 in the linker has also been associated with kinase activation, and mutation of this residue (Y245F) leads to a decrease in kinase activity [29]. In contrast, a recent study from our laboratory has shown that increasing the proline content of the linker enhances SH3:linker interaction (this engineered high affinity linker is referred to as HAL hereafter [30]) (Figure 3). Remarkably, introduction of this HAL sequence into the Abl core protein overcame the effects of certain activating mutations such as A356N. A356N is a mutation in the hydrophobic pocket of the C-lobe of the kinase domain that disrupts binding of the myristoylated N-cap resulting in kinase activation (discussed earlier in section 1.2.1.1) [14]. When the HAL sequence is combined with this A356N mutation, the kinase activity of the HAL-A356N Abl core is significantly reduced in comparison to the A356N Abl core with a wild-type linker [30]. This observation suggests that SH3-linker interaction has a dominant influence on the overall structure and activity of the kinase domain. Furthermore, the SH3:linker interaction was also found to regulate inhibitor sensitivity of the oncogenic fusion protein, Bcr-Abl (discussed later in section 1.4.2). Remarkably, the introduction of this HAL sequence into Bcr-Abl sensitized Bcr-Abl transformed cells to apoptotic induction by both ATP-competitive and allosteric inhibitors of the Abl kinase.

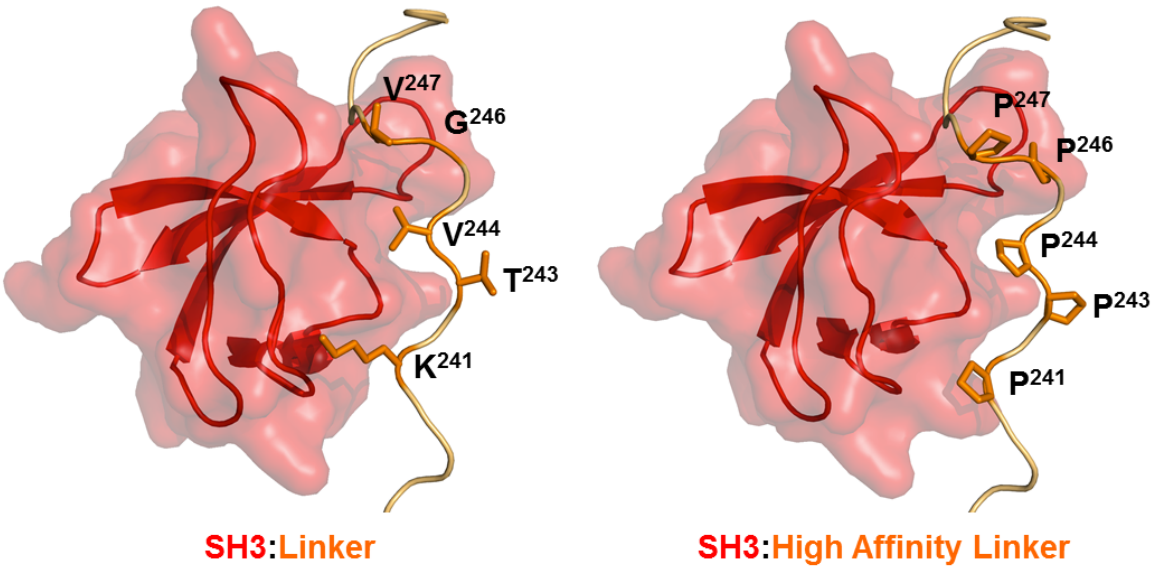

WT	APKRNK^{241}PTVYGV^{247}SPNYDKWE
HAL	APKRNP^{241}PPPYPP^{247}SPNYDKWE

Figure 3. Increased proline content in the SH2-kinase linker enhances SH3:linker interaction.

Left: A model of the wild-type SH3:linker interface derived from the down-regulated Abl core (PDB: 2FO0, [9]) is shown. The side chains of the linker residues that were modified in the high affinity linker (HAL) mutant are shown as sticks. *Right:* A model of the SH3:HAL interface shows the positions of the five proline substitutions [30]. The sequence of the wild-type and the high affinity linker are shown in the box at the bottom, with the modified residues highlighted in red. These linker proline substitutions enhance intramolecular binding to the SH3 domain as shown by hydrogen exchange mass spectrometry and FP assay (see main text for details).

1.2.1.5 Kinase domain

The catalytic or kinase domains of serine, threonine, and tyrosine kinases are evolutionarily conserved in both primary amino acid sequence as well as structure [31]. Like other kinases, the kinase domain of Abl is bi-lobed, consisting of a smaller N-terminal lobe (N-lobe) and a larger C-terminal lobe (C-lobe). The N-lobe of the kinase consists of a β-sheet composed of 5 strands, and a single α-helix known as the αC helix, while the C-terminal lobe (C-lobe) is primarily helical. The hinge region in between the two lobes is also conserved, and contributes to the catalytic function of the kinase. The N-lobe and the hinge region define the site where ATP binds, which includes the phosphate binding loop or P-loop. Both lobes contribute conserved residues that are important for the catalytic transfer of γ-phosphate from ATP to the tyrosine residue in the substrate. In addition, the C-lobe contains the peptide substrate binding site, and the activation loop.

The relative positions of the two lobes of the kinase domain and conserved residues in these structural features play an important role in the catalytic reaction and the dynamic interchange between the inactive and active conformations of the kinase domain. Interestingly, while most kinases adopt similar active conformations, the inactive conformations of the kinase domains are remarkably diverse, thus providing opportunities for selective inhibitor discovery [32–35]. The crystal structures of the Abl kinase domain bound to ATP-competitive inhibitors dasatinib and imatinib (discussed later in sections 1.4.4 and 1.4.3, respectively) highlight the features of the active and inactive conformations adopted by the Abl kinase domain (Figure 4) [32,36]. In the active conformation shown in Figure 4A, a conserved glutamate residue (Glu286) in the αC helix forms an ionic interaction with Lys271 in the N-lobe. This interaction is

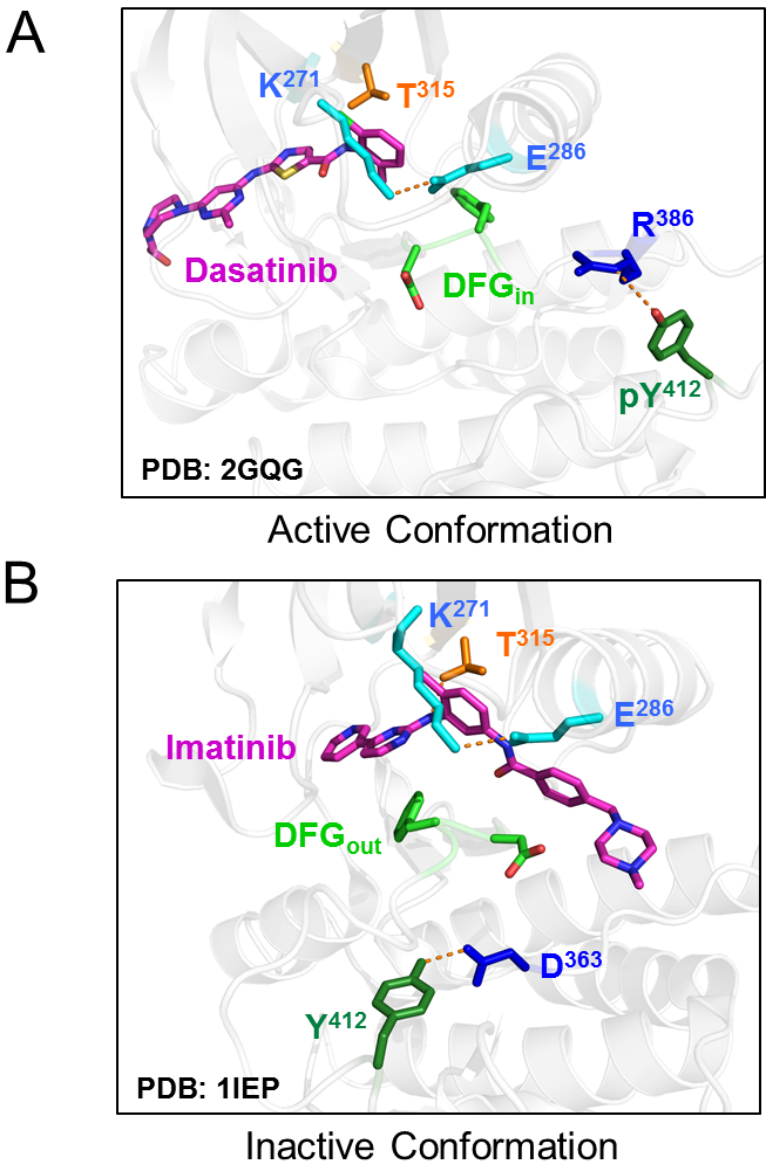

Figure 4. Active vs. inactive conformation of the Abl kinase active site.

(A) The crystal structure of dasatinib (pink carbons) bound to the Abl kinase domain (PDB: 2GQG, [36]) highlights the features of the active kinase conformation. The conserved DFG motif is flipped in and Asp381 coordinates a magnesium ion important for catalysis. The ionic interaction between Lys271 and Glu286 is important for coordinating the phosphate group of ATP. The phosphorylated Tyr412 forms a hydrogen bond with Arg386, and contributes to stabilization of the active conformation. (B) The crystal structure of imatinib (pink carbons) bound to the Abl kinase domain (PDB: 1IEP, [32]) shows the features of the inactive conformation of the active site. The DFG motif is flipped out, while ionic interaction between K271 and E286 is maintained. The activation loop is folded into the active site, and Tyr412 forms a hydrogen bond with the conserved Asp363 (catalytic aspartate). Imatinib also forms a key hydrogen bond with the gatekeeper residue Thr315.

important for coordinating the phosphate group of ATP and is conserved in the active conformations of protein kinases. Interestingly, this ionic interaction is maintained in the imatinib bound inactive conformation as well (Figure 4B), in contrast to c-Src. However, in another crystal structure of the Abl kinase domain bound to an ATP-peptide conjugate, the kinase domain adopts a Src-like inactive conformation where the αC helix is switched out and this Glu-Lys salt bridge is disrupted [37]. The activation loop in the C-lobe contains a tyrosine residue (Tyr412) that undergoes autophosphorylation upon activation. Phosphorylation of Tyr412 stabilizes an 'open' conformation of the active site through an ionic interaction with a neighboring arginine residue, allowing access to the peptide substrate (Figure 4A). On the other hand, in the inactive 'closed' kinase conformation, the activation loop is folded back into the active site and Tyr412 forms a hydrogen bond with a conserved aspartate residue (Asp363) in the catalytic loop (Figure 4B). This conformation of the activation loop mimics substrate binding, and stabilizes the inactive conformation of the kinase. Furthermore, the position of a highly conserved aspartate-phenylalanine-glycine (DFG) motif also plays an important role in determining the active vs. inactive kinase conformation. In the active conformation, Asp381 is oriented towards the active site (also called the 'DFG in' conformation) and coordinates a magnesium ion important for catalysis (Figure 4A). In the inactive conformation, Asp381 is flipped away from the active site (also called 'DFG out') and Phe382 occludes the active site, thus preventing catalytic activity (Figure 4B). This DFG out conformation is also important for the specificity of imatinib binding to Abl (discussed later in section 1.4.3.1).

The gatekeeper residue is a structurally conserved feature in the ATP binding site that regulates the binding of nucleotide and small molecule inhibitors to the ATP binding site [38–41]. A majority of kinases contain threonine or a larger amino acid in this position, and the size

of the residue regulates access to a pre-existing cavity in the ATP-binding pocket. While mutations in this residue are commonly known to confer resistance to targeted inhibitors of multiple kinases, these mutations have sometimes been reported to be present before inhibitor treatment [42,43]. These mutations are thus predicted to independently influence kinase activity and correlate with kinase oncogenic potential. Consistent with this hypothesis, a threonine to methionine mutation at the gatekeeper position in the epidermal growth factor receptor (EGFR) is associated with lung cancer [42]. In an attempt to understand the mechanism of this activation, a recent study found that substitution of the gatekeeper position with bulky hydrophobic residues such as isoleucine or methionine stabilizes the 'hydrophobic spine' of the active kinase conformation, thus promoting kinase activity [44]. On the other hand, substitution with smaller residues such as glycine or alanine resulted in either no change or a modest increase in kinase activity, respectively. The threonine to isoleucine gatekeeper mutation in Bcr-Abl (T315I) is clinically relevant since it causes resistance to most Abl kinase inhibitors and will be further discussed in section 1.4.3.2. Similar to mutations in EGFR, platelet derived growth factor receptor (PDGFR), and Src, a threonine to isoleucine substitution in Abl results in an increase in kinase activity. Remarkably, Abl with the T315I mutation is able to transform Ba/F3 cells to the same extent as Bcr-Abl [44]. An additional study found that the phosphorylation status of tyrosine residues in the P loop of the kinase domain is distinct for Bcr-Abl gatekeeper mutants and suggested altered substrate specificity for these kinases [45]. Furthermore, a recent study from our group investigated the conformational dynamics of the Abl T315I mutant and found that this mutation induces dynamic conformational changes not only at the site of the mutation, but also at interface of the SH3 domain and the linker [46]. To summarize, these studies

demonstrate that the gatekeeper position in the Abl kinase domain has significant influences on both kinase regulation and inhibitor sensitivity.

1.2.1.6 C-terminal region

In contrast to Src-family kinases, Abl has a large C-terminal region following the kinase domain [7,8]. This region, encoded by a single exon and known as the last exon region, contains several motifs important for diverse functions exhibited by Abl. These include proline-rich motifs that interact with the SH3 domains of signaling adaptors such as Crk, a DNA binding domain, three functional nuclear localization signals, a nuclear export signal, and F-actin and G-actin binding domains. These domains are important for mediating interactions with other signaling molecules, and for determining Abl subcellular localization as required for biological functions.

1.2.2 Conformational dynamics of Abl proteins

The X-ray crystal structures of the Abl core discussed above provides valuable insight into the intra-molecular interactions regulating Abl kinase activity [9,12]. However, X-ray crystallography only presents a singular static view of the protein structure, in its assembled, downregulated state. Protein kinases, like many other biomolecules, are not rigid entities and undergo dynamic changes between different conformations in solution. Thus, an analysis of conformational dynamics is essential to our understanding of the different activation states of the protein in solution. To this end, this section will discuss the different techniques that are used to evaluate conformational dynamics of proteins in solution, and their application to the study of Abl kinase dynamics.

1.2.2.1 Small Angle X-ray Scattering (SAXS)

Small angle X-ray scattering is a valuable technique for the characterization of large protein structures that are not amenable to crystallization or NMR analysis [47–50]. It is especially useful to investigate the conformational states of large structures with multiple domains, and can provide a low resolution picture of the relative orientation of these domains, or the shape and size of molecular assemblies of these protein domains. The X-ray scattering patterns can be analyzed to predict the average ensemble of multiple conformational states. While the radius of gyration (R_g) of a molecule is useful in estimating the relative size of the molecule, *ab initio* calculation of low-resolution 3-dimensional molecular envelopes can aid in predicting the overall shape. This approach to determination of molecular envelopes is attractive because the shapes of the reconstructed molecular envelopes are independent of any specific, previously known atomic model.

SAXS has been used to investigate the conformation of an active mutant Abl core protein, referred to as $Abl^{activated}$ or ΔNcap-2PE, which lacks the N-cap and myristoylation site, and includes two mutations in the SH2-kinase linker (P242E, P249E) that disrupt the SH3:linker interaction [9]. The molecular envelope generated from SAXS analysis predicted a reorientation of the SH2 domain to the top of the N-lobe of the kinase domain, in an extended “top-hat” conformation, while the exact positions of the SH3 domain and the SH2-kinase linker could not be modeled. This study also used SAXS to analyze the Abl kinase domain and the downregulated Abl core and found that the predicted conformations from SAXS are consistent with the X-ray crystal structures. Additionally, this study examined another active mutant Abl core protein, $Abl^{SH2\text{-}mutant}$, which includes mutations in the SH2 and kinase domains (I164E, T291E, Y331A) that disrupt the SH2:kinase domain interface in the top-hat conformation, in

addition to the absence of N-cap and the SH3:linker interaction as described above for Abl^{activated}. This protein was predicted to sample multiple conformational states, and the molecular shape could not be reconstructed for structural interpretation. It is pertinent to note here that all the proteins in this study were purified in the presence of a small molecule ATP-site inhibitor (PD166326) to prevent protein aggregation, and the presence of this small molecule bound to the active site in the kinase domain could potentially influence the conformational state of the proteins in solution.

A recent study utilized a combination of SAXS and nuclear magnetic resonance spectroscopy (NMR) to investigate the conformations adopted by a modified Abl core protein, Abl ΔN-cap, which lacks the N-cap including the myristoylation signal [51]. This study examined the effect of imatinib (an ATP-competitive tyrosine kinase inhibitor discussed in section 1.4.3) and GNF-5 (an allosteric inhibitor that acts through the myristic acid binding pocket and is discussed further in section 1.4.5) on the Abl ΔN-cap conformation in solution in comparison to the apo form of the kinase. The Abl ΔN-cap apo form adopts a 'closed' conformation similar to the down-regulated Abl core crystal structure, and the radius of gyration (R_g) for the Abl ΔN-cap apo (27Å) is similar to the Abl core (28Å) [9,51]. Despite this protein lacking two of the three intra-molecular interactions that are important for down-regulation (discussed earlier in section 1.2.1), namely the myristoylated N-cap and the SH2:kinase domain interactions, this protein adopts a closed conformation suggesting that the SH3:linker interaction may be sufficient to maintain Abl in a down-regulated conformation. Interestingly, the presence of imatinib leads to an 'open' conformation where the SH3 and SH2 regulatory domains appear to be displaced from the back of the kinase domain, and the radius of gyration is increased to 31Å. However, this effect of imatinib leading to a displacement of the regulatory SH3-SH2

domains could possibly be due to the absence of the N-cap and the myristic acid moiety. In contrast to imatinib, addition of GNF-5 does not have any significant influence and the conformation is very similar to the Abl ΔN-cap apo form. Remarkably, addition of GNF-5 to the complex of Abl ΔN-cap and imatinib leads to a reversal to the 'closed' conformation similar to the Abl ΔN-cap apo form. This effect is consistent with GNF-5 acting through the myristic acid binding pocket and inducing stabilization of this complex.

1.2.2.2 Hydrogen Exchange Mass Spectrometry (HXMS)

Hydrogen exchange mass spectrometry is a valuable technique to analyze protein conformation and dynamics in solution [52]. This technique is not limited by protein size or solubility constraints that are seen for NMR spectroscopy and X-ray crystallography studies, requires relatively small quantities of proteins, and can provide information about protein dynamics on a wide time scale. HXMS uses heavy or deuterated water (D_2O) and it measures the rate of exchange of the backbone amide hydrogen atoms with deuterium in solution. Solvent-exposed amide hydrogen atoms and ones that are involved in weak hydrogen bonds undergo a rapid exchange. In contrast, amide hydrogen atoms that are buried in the interior of the protein, or are involved in forming stronger hydrogen bonds exchange more slowly. The exchange reaction can be quenched at multiple time points, and the rate of exchange can be measured by mass spectrometry since deuterium has a larger mass than hydrogen. Several studies from our laboratory, in collaboration with Dr. John Engen's research group at Northeastern University, have used HXMS to examine the conformational dynamics of Abl proteins and will be summarized here.

Initial HXMS studies with Abl proteins investigated the conformational dynamics of the Abl regulatory domains in the absence of the kinase domain. One of these studies found that the presence of the SH2-kinase linker, which binds to the SH3 domain in cis, slows down the rate of cooperative unfolding of the SH3 domain, thus providing the first evidence for interaction between the SH3 domain and the linker in the absence of the kinase domain [28]. Moreover, this study also tested different lengths of the linker, and identified the minimum number of residues required for SH3 domain engagement. Another HXMS study investigated the effect of the N-cap on deuterium uptake by the Abl regulatory domains (SH3 alone, SH3-SH2 or 32, SH3-SH2-linker or 32L) [53]. The N-cap was found to have a stabilizing influence on the SH3 domain but only in the presence of the SH2 domain, and this effect was further enhanced in the presence of the linker. This observation suggests that the N-cap stabilizes SH3:linker interaction, consistent with the overall structure of the downregulated Abl core. Moreover, a recent study examined the effect of increased proline content in the linker on SH3:linker interaction using the the high affinity linker (HAL) discussed earlier in section 1.2.1.4. This study showed that increased linker proline content resulted in enhanced SH3 engagement, measured as stabilization of the SH3 domain to deuterium uptake [30].

Earlier work from our lab has shown that Src family kinases phosphorylate multiple tyrosine residues in the Abl regulatory domains, including the tyrosine residue at position 89 in the SH3 domain [25]. In the down-regulated Abl core crystal structure, this tyrosine residue is present at the SH3:linker interface, suggesting that phosphorylation of this residue could potentially disrupt SH3:linker interaction. In support of this idea, phosphorylation of this residue enhances Bcr-Abl kinase activity, and HXMS studies found that phosphorylation of this residue results in linker disengagement as measured by the rate of cooperative unfolding of the SH3

domain [24]. Moreover, phosphorylation of Tyr89 also disrupts binding of Abl binding protein, ABI1 to the Abl SH3 domain.

Other studies have used HXMS to investigate the effect of mutations on the conformational dynamics in the Abl core proteins [30,46]. In agreement with the crystal structure of the down-regulated wild-type Abl core, HXMS analysis of this protein found that the N-cap, linker, activation loop, and portions of the SH3 and SH2 domains that are exposed on the surface and predicted to be solvent exposed, are fairly dynamic and undergo rapid deuterium exchange [46]. On the other hand, this analysis also revealed that a region including the C-lobe of the kinase domain and the SH2:kinase domain interface is protected from deuterium exchange, and hence represents a more stable or rigid part of the protein structure. Additionally, this study also examined the effect of the gatekeeper mutation, T315I (discussed in sections 1.2.1.5 and 1.4.3.2), and found an increase in deuterium uptake not only in the vicinity of the mutation site, but also in the RT-loop of the SH3 domain. Another HXMS study examined the effect of an activating mutation, A356N in the myristic acid binding pocket (discussed in section 1.2.1.1), and found an increase in deuterium uptake in the N-lobe of the kinase domain adjacent to the active site, in addition to changes at the site of mutation [30]. Moreover, this study also examined the effect of the high affinity linker (HAL), discussed in section 1.2.1.4 and above in the context of the Abl 32L proteins, on the Abl core protein dynamics. The introduction of HAL into the wild-type Abl core resulted in a decrease in deuterium uptake in parts of the SH3 and SH2 domains as well as in parts of the N-lobe and C-lobe of the kinase domain close to the active site, thus suggesting a global stabilization of the inactive Abl core conformation. Remarkably, this study found that introduction of the HAL into the A356N Abl core mutant reverses the dynamic effects of this

mutation on Abl core conformation. Together, these studies provide evidence for allosteric communication between different parts of the Abl kinase core that are responsible for regulation.

HXMS has also been useful in investigating the stabilizing influence of small molecule inhibitors on Abl core dynamics. For example, HXMS studies have examined the effect of GNF-5 (an allosteric inhibitor acting through the myristic acid binding pocket, discussed later in section 1.4.5), alone and in combination with an ATP-competitive tyrosine kinase inhibitor, dasatinib (discussed later in section 1.4.4) [54,55]. The binding of GNF-5 to the Abl core protein was found to induce conformational changes not only in the drug-binding site but also at a distance in the ATP-binding site. Moreover, additional studies showed that binding of a combination of GNF-5 and dasatinib to the mutant Abl core T315I protein induces similar conformational changes as those when dasatinib was bound to the wild-type Abl core. Thus, these results suggest that binding of allosteric inhibitors to the myristic acid binding pocket in Abl core mutants helps to stabilize the inactive conformation or remodel the conformation of the Abl active site making it accessible to ATP-competitive inhibitors.

1.2.2.3 Nuclear Magnetic Resonance Spectroscopy (NMR)

NMR is a valuable technique to determine structures of proteins and other biomolecules in solution, and to study protein dynamics and folding [56,57]. Besides X-ray crystallography, this is the only other technique that provides atomic resolution for structure determination. While NMR is useful for proteins that are not amenable to crystallization, it is constrained by requirements of a large amount of protein at high concentration, and magnetic field strength places an upper limit on the size of proteins for which structures can be resolved (typically around 40 kDa).

The first few NMR studies with Abl proteins focused on the regulatory domains since they could be easily expressed with heavy isotope labeling in bacterial expression systems. The solution structures of the Abl SH2 and SH3 domains were first solved by NMR [58,59]. Additionally, the NMR solution structure of the regulatory SH3-SH2 unit in the absence of the kinase domain revealed that the domains are flexible relative to each other [58,60]. There is very little structural information available about the protein domains present in the C-terminal half of the protein that is encoded by the last exon region of Abl, except the actin binding domain whose solution structure was solved using NMR [61]. Moreover, NMR has also been useful to study inter-molecular domain interactions in proteins, and was used to identify the proline-rich motif in the Crk SH2 domain that binds to the Abl SH3 domain, and validate the multi-domain interaction between Crk II and Abl [62].

In 2005, a method to isotopically label proteins expressed in Sf9 insect cells was optimized and used to express the Abl kinase domain for NMR studies [63]. This was followed by an elegant study to determine the solution structure of the Abl kinase domain in complex with four different ATP-competitive inhibitors – imatinib, nilotinib, and dasatinib, and PD180970 [64]. These solution structures found that imatinib and nilotinib bind Abl in the DFG-out conformation (also discussed in sections 1.2.1.5, 1.4.3, and 1.4.4), while dasatinib predominantly binds Abl in the DFG-in active conformation (also discussed in sections 1.2.1.5 and 1.4.4), thus providing solution validation for the X-ray crystal structures. Furthermore, a combination of solution NMR, X-ray crystallography, and HXMS was utilized to demonstrate that GNF-2, an allosteric inhibitor of Abl (discussed later in section 1.4.5), binds the myristic acid binding pocket in the C-lobe of the kinase domain [55]. Recently, solution NMR and X-ray crystallography was also used to confirm that the Ile164 residue in the Abl SH2 domain is

involved in the binding interface with the monobody 7c12 (discussed later in section 1.4.5), and the monobody acts by destabilizing one of the active conformations of the Abl kinase [65].

Finally, a recent study utilized a combination of SAXS and NMR to investigate the conformations adopted by the largest Abl protein to be studied by NMR so far [51]. This study examined the effect of imatinib (an ATP-competitive tyrosine kinase inhibitor discussed in section 1.4.3) and GNF-5 (an allosteric inhibitor that acts through the myristic acid binding pocket and is discussed further in section 1.4.5) on a modified Abl core protein, Abl ΔN-cap, that lacks the N-cap including the myristoylation signal. As discussed in detail above in section 1.2.2.1, the Abl ΔN-cap apo form adopts a 'closed' conformation similar to the down-regulated Abl core crystal structure, while the presence of imatinib leads to an 'open' conformation where the SH3 and SH2 regulatory domains appear to be displaced from the back of the kinase domain. Remarkably, addition of GNF-5 to the complex of Abl ΔN-cap and imatinib leads to a reversal to the 'closed' conformation similar to the Abl ΔN-cap apo form. This effect is consistent with GNF-5 acting through the myristic acid binding pocket and inducing stabilization of this complex through reassembly of the downregulated state.

1.2.3 Physiological regulation of Abl kinase function

As discussed in section 1.1, Abl is ubiquitously expressed and involved in regulating multiple cellular functions. Consequently, the kinase activity of Abl is tightly regulated *in vivo* by multiple mechanisms. While section 1.2.1 discusses the auto-inhibitory interactions that are important for Abl regulation, this section will discuss the cellular stimuli that result in Abl activation.

1.2.3.1 Phosphorylation

The kinase activity of Abl is regulated by phosphorylation and dephosphorylation of critical tyrosine residues in the activation loop and regulatory domains. In the absence of activating stimuli, neither endogenous nor overexpressed Abl is phosphorylated [20,21,23,29]. However, when Abl is activated in response to intracellular or extracellular signals, there is a corresponding increase in tyrosine phosphorylation.

In the inactive Abl kinase, the activation loop folds into the active site and Tyr412 (also discussed earlier in section 1.2.1.5) forms a hydrogen bond with the conserved Asp363 to stabilize the inactive conformation and prevent substrate and ATP binding [31,33]. Activation loop Tyr412 can undergo autophosphorylation as well as be phosphorylated by other tyrosine kinases including members of the Src family [66,67]. Phosphorylation of Tyr412 stabilizes the active kinase conformation, while replacement with phenylalanine impairs kinase activation [29]. In addition to Tyr412, phosphorylation of Tyr245 in the SH2-kinase linker is also required for maximal Abl kinase activity, and mutation of this residue has been shown to inhibit kinase activation *in vitro* [29]. However, this phosphorylation-induced activation is not mediated by disruption of SH3:linker interaction as observed by HXMS studies [24]. Phosphorylation of several other tyrosine residues is implicated in the regulation of Abl kinase activity. Tyr134 in the SH3 domain is directly involved in binding the PXXP motif, and phosphorylation of this residue is predicted to disrupt SH3:linker interaction [22,25]. Similarly, phosphorylation of SH3 domain Tyr89 has been shown to interfere with SH3:linker interaction and cause kinase activation [24,25]. Additionally, phosphorylation of Tyr283 in the N-lobe of the kinase domain or Ser94 in the SH3 domain are predicted to disturb the closed packing of the SH3 domain against the N-lobe of the kinase domain and disturb the inhibitory intra-molecular interactions

[22]. In contrast to the activating effect of phosphorylation of residues discussed above, phosphorylation of Ser69 in the N-cap plays a role in stabilizing the down-regulated conformation of the Abl kinase core (also discussed earlier in section 1.2.1.1) [9]. The sites of phosphorylation are modeled on the structure of the down-regulated Abl core and presented in Figure 5.

In addition to autophosphorylation and phosphorylation by other tyrosine kinases, Abl is also regulated by the action of tyrosine phosphatases such as protein tyrosine phosphatase non-receptor type 6 (PTPN6), type 12 (PTPN12), and type 18 (PTPN18) [8].

1.2.3.2 Interaction with binding partners

Multiple protein partners interact with Abl, and may play a role in regulating its kinase activity [8]. Some of these binding partners are also substrates of Abl, and may play a role in complex regulatory networks. On one hand, some proteins interact with the Abl SH3 and SH2 domains, through their polyproline motifs or phosphotyrosine sites, respectively. On the other hand, other proteins interact with the Abl proline-rich or phosphotyrosine sites through their SH3 or SH2 domains, respectively. Additionally, interactions may also occur through other binding domains in the C-terminal region of the Abl protein. Sometimes, a single protein uses multiple mechanisms to interact with Abl. One such example is the adaptor protein Crk II, which contains a single SH2 and two SH3 domains. Crk II interacts with the proline-rich motifs in the C-terminal region of Abl through the Crk II SH3 domain, and is phosphorylated by Abl kinase at a specific tyrosine residue (Tyr 221). These events cause a conformational change, exposing a PXXP motif in the SH2 domain of Crk which binds the Abl SH3 domain causing kinase activation [62,68]. Abl interacting proteins – 1 and 2 (ABI1 and ABI2) were the first identified

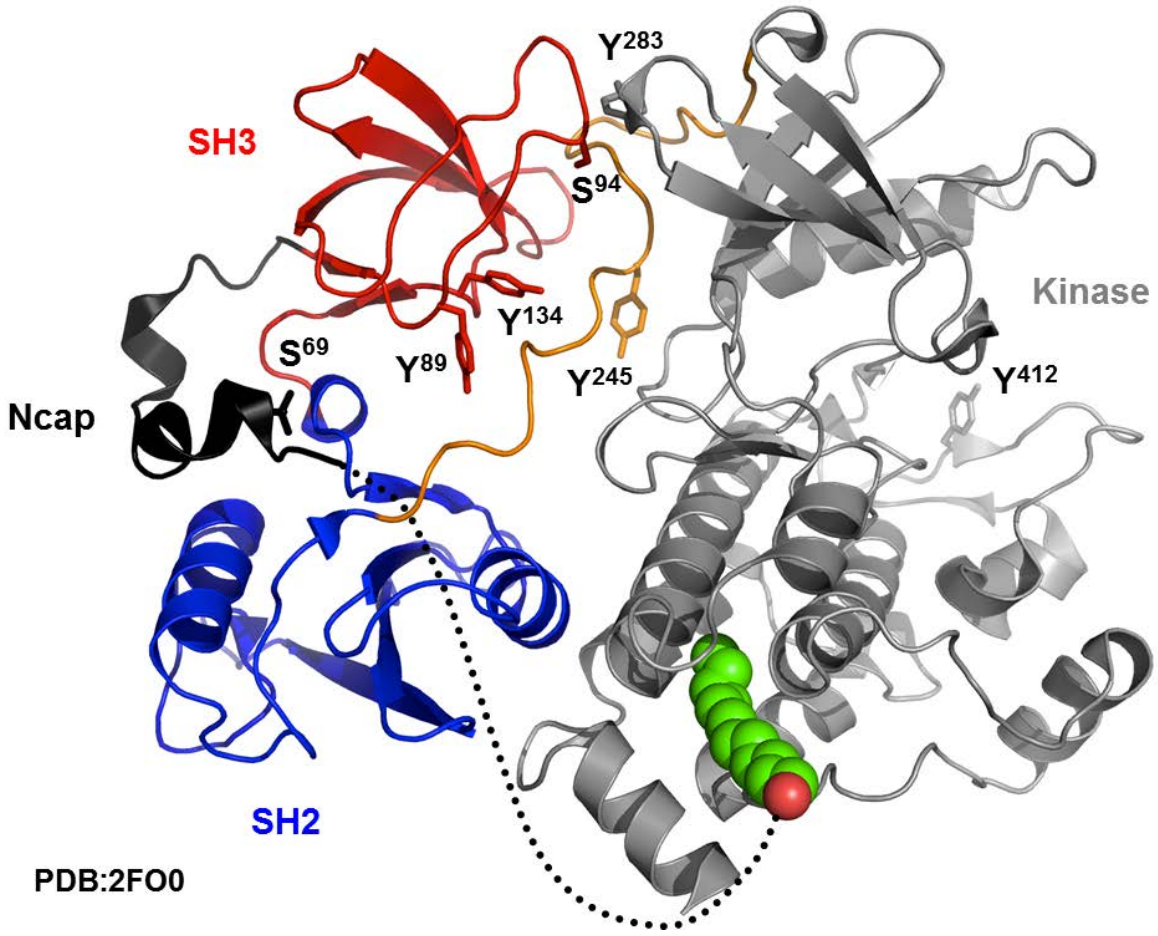

Figure 5. Regulatory phosphorylation sites in the Abl core.

The location of the tyrosine and serine residues that are important for Abl regulation are modeled on the down-regulated structure of the Abl core (PDB: 2FO0, [9]). Phosphorylation of these residues (except Ser69) is correlated with an increase in kinase activity. Ser94, Tyr89, and Tyr134 are located in the SH3 domain (red), Tyr245 is located in the SH2-kinase linker (orange), and Tyr283 and Tyr412 are located in the kinase domain (gray). The phosphorylation of Ser69, located in the N-cap (black), is important to stabilize the downregulated conformation of the kinase.

binding protein partners of the SH3 domain of Abl, and their effect on the kinase activity of Abl is not clear [69,70]. They interact with the Abl SH3 domain through their PXXP binding motifs, as well as bind the proline rich motifs in the C-terminal region of Abl through their SH3 domains. On one hand, ABI 1 binding has been shown to be associated with Abl oligomerization and enhanced phosphorylation of Abl substrates, thus suggesting that it plays a role in Abl activation. On the other hand, ABI1 can also inhibit the transforming activity of v-Abl and phosphopeptides derived from ABI1 have been found to have an inhibitory effect on Abl activity [70,71]. Another binding partner of Abl is the RAS effector protein RIN1 that binds both the SH3 and SH2 domains in Abl through its PXXP motif and a phosphotyrosine site respectively, leading to Abl kinase activation [72]. Some proteins have also been implicated in the negative regulation of kinase activity, such as Tusc2 (or Fus1) and Prdx1 (or PAG) [73,74]. Interestingly, Prdx1 was shown to bind the Abl SH3 domain as well as the kinase domain and inhibit Abl kinase activity [73]. These studies have important implications for the discovery of small molecules that allosterically regulate Abl function, because interaction with the SH3 domain or other regulatory motifs may result in either Abl activation or inhibition.

1.2.3.3 Growth factor induced activation

Abl is activated by stimulation of cells with PDGF and EGF, and is involved in mediating the mitotic and chemotactic responses to these factors [66,75].

When cells are treated with PDGF, Abl kinases are recruited to the cytoplasmic domain of PDGFR within minutes, and the subsequent Abl activation requires Src and phospholipase C-γ1 (PLC-γ1) activities [66,75–77]. Src is known to phosphorylate Abl at multiple tyrosine residues including the activation loop Tyr412, and other tyrosine residues in the regulatory

domains and cause kinase activation [76]. Moreover, PLC- γ1 is also important for Abl activation since PLC- γ1 activation leads to depletion of phosphatidylinositol 4,5-bis-phosphate (PIP_2), which is a substrate of PLC- γ1 as well as an inhibitor of Abl [77]. Furthermore, Abl-deficient mouse embryonic fibroblasts are unable to reorganize the actin cytoskeleton and exhibit delayed S-phase entry on PDGF stimulation [66,78].

Abl is also activated upon stimulation with EGF, though the exact mechanism of activation is uncertain [66,79]. Interestingly, a high affinity binding site for the SH2 domain of Abl is present in all four members of EGFR family, and Abl has been found to be associated with EGFR in several cell lines [79,80]. These studies suggest that Abl may directly associate with EGFR, and this interaction is predicted to stabilize Abl in an open and active conformation. Furthermore, a recent study found that active Abl phosphorylates EGFR and subsequently inhibits its endocytosis from the cell surface, thus suggesting that activated Abl promotes increased cell-surface expression of EGFR [81].

1.3 C-ABL IN DNA DAMAGE

Abl is known to be activated in response to several genotoxic stresses such as ionizing radiation and exposure to DNA damaging agents such as cisplatin, methylmethane sulfonate (MMS), mitomycin C (MMC), and doxorubicin [82–84]. In response to genotoxic stress, nuclear Abl is activated by several kinases involved in the DNA damage repair (DDR) pathways such as ataxia telangiectasia-mutated (ATM), and DNA-dependent protein kinase (DNA-PK) [85–87]. ATM, a serine/threonine kinase related to phosphinositide 3-kinases (PI3K), interacts with Abl through its SH3 domain and phosphorylates Abl on Ser465 in response to ionizing radiation [85,86]. This

phosphorylation event is required for Abl activation since a S465A mutation abrogates this IR-induced activation, and Abl activation is not seen in ATM deficient cells [85,86]. Interestingly, Abl is known to interact with and phosphorylate modulators of both DNA-damage induced apoptosis and DNA-damage repair pathways. In addition, activation of Abl has been shown to promote the DDR pathway in some studies, while it has been shown to inhibit this process in others. The sections below will examine the role of Abl in promoting cell survival or cell death in response to DNA-damage.

1.3.1 Role of Abl in the DNA damage repair pathway

Multiple proteins involved in the DNA-damage repair pathway have been found to interact with Abl, and many of them are Abl kinase substrates [8]. Many initial studies found that Abl phosphorylation of these proteins leads to inhibition of the DNA-damage repair process. Rad51, an important protein involved in the homologous recombination (HR) pathway to repair double-stranded breaks (DSBs) in DNA, interacts with the Abl SH3 domain through two PXXP motifs, and Abl phosphorylates Tyr54 and Tyr315 on Rad51 [88]. The phosphorylation of Tyr54 inhibits the ability of Rad51 to bind single stranded DNA, and its function in mediating DNA-strand exchange [88]. On the other hand, phosphorylation of Tyr315 has been shown to stabilize the association between Rad51 and chromatin, suggesting a positive influence on Rad51 activity [89]. Thus, the exact effect of the Abl kinase on Rad51 activity in DNA damage repair is not clear. In addition to Rad51, Abl phosphorylates DNA-PK, an important mediator of the non-homologous end joining (NHEJ) DNA repair process, and disrupts its ability to form a complex with DNA, thus leading to reduced NHEJ repair [90]. Moreover, Abl phosphorylates WRN, a RecQ helicase that is involved in DNA metabolism, and inhibits its exonuclease and helicase

activities, thus inhibiting NHEJ DNA repair process [91]. Abl also interacts with BRCA1, a protein associated with DSB repair, and this interaction is disrupted in response to IR [92]. To summarize, most of these studies suggest that Abl has an inhibitory effect on the DNA damage repair processes.

DNA damage repair is predicted to happen in two phases – a short phase of fast rejoining kinetics which repairs the majority of lesions and lasts about 2 hours, followed by a longer phase of slow rejoining kinetics. Interestingly, a recent study examined the effect of Abl on the DNA-damage response over time [93]. Pre-treatment with imatinib, a selective inhibitor of Abl kinase activity discussed later in section 1.4.3, led to a higher rate of DSB repair and clonogenic survival in response to ionizing radiation as compared to control cells. Moreover, a pronounced effect was seen at later time points suggesting that Abl inhibits the second phase of slower DNA repair. In contrast, a recent study with primary non-immortalized mouse embryonic fibroblasts (MEFs) presented evidence supporting a role for Abl positively regulating the DNA-damage repair process [94]. Lack of Abl expression in these primary MEFs was found to result in reduced ATM and ATR kinase activity, nuclear foci formation, and DNA repair. These observations suggest that Abl activation, in response to DNA damage, plays a secondary role in the activation of ATM and ATR kinases. To summarize, while several studies suggest that Abl has an inhibitory effect on DNA-damage repair, a few studies provide evidence for a positive regulatory effect on these processes. Moreover, a kinetic analysis of Abl activation and its influence on the DNA-damage repair pathways may aid in a better understanding of the function of Abl in this process. Discovery of selective small-molecule activators of Abl kinase activity may enable such studies.

1.3.2 Abl signals inducing apoptosis

In response to genotoxic stress, Abl has been shown to interact with several proteins that mediate apoptotic cell death. Interestingly, Abl-deficient cells or cells expressing a kinase-dead mutant of Abl are resistant to IR-induced apoptosis [95]. While there is no clear evidence for a direct association of Abl with p53, Abl is known to induce apoptosis in response to DNA damage by both p53-dependent and p53-independent mechanisms [96–99]. Moreover, Abl also phosphorylates Mdm2 and neutralizes its inhibitory effect on p53, thus leading to p53 stabilization and accumulation [100,101]. Additionally, another member of the p53 family of tumor-suppressors, transcription factor p73, interacts with the Abl SH3 domain through its PXXP motif [102–105]. Upon treatment with ionizing radiation, Abl phosphorylates p73, leading to accumulation of p73 and apoptotic induction. Furthermore, in response to DNA damage, Abl also phosphorylates and stabilizes YAP1, a transcriptional co-activator that works with p73 to induce expression of pro-apoptotic genes [106]. These findings suggest that Abl is required for induction of apoptosis in response to DNA damage, and that multiple proteins may contribute to this effect. Interestingly, a recent study found that inhibition of Abl kinase activity using imatinib leads to an increase in the clonogenic survival of irradiated cells, suggesting that Abl inhibition confers resistance to radiation treatment [93].

1.4 BCR-ABL AND CHRONIC MYELOGENOUS LEUKEMIA

1.4.1 Disease overview

Chronic Myelogenous Leukemia (CML) is a clonal hematopoietic stem cell disorder that arises from a single transformed myeloid progenitor cell. The estimated number of new cases in the United States in 2015 is about 6,660 (12.3% of all leukemias) and the number of estimated deaths is around 1140 (4.7% of all leukemias) [107]. CML usually affects older adults with the average age at diagnosis being 64 years. Owing to the discovery of targeted drugs such as imatinib (discussed in detail in sections 1.4.3 and 1.4.4), the 5-year survival rate for CML patients has significantly improved from about 31% in the early 1990s to about 60% for patients diagnosed between 2004-2010 [107].

Clinically, chronic myelogenous leukemia is classified into three diseases phases, on the basis of the number of immature white blood cells, also called ‘blasts’, in the blood or bone marrow [108–110]. Most patients are diagnosed in the chronic phase of the disease, which is characterized by the expansion of mature myeloid cells, especially granulocytes, and is usually asymptomatic. This stage is diagnosed by a high number of mature granulocytes in the peripheral blood, weight loss, and splenomegaly. Patients in the chronic phase typically have less than 15% blasts in the blood or bone marrow, and usually respond well to imatinib treatment. If left untreated, the chronic phase usually last for about 2 to 5 years, and the disease progresses to the accelerated and blast crisis phases. Both the accelerated and blast phases of the disease are characterized by a decrease in hematopoietic cell differentiation, and accumulation of immature blasts in the bone marrow and peripheral blood (>15%). The accelerated phase lasts about 6 to 18 months, while the blast phase only lasts about 3 to 6 months. The transition to accelerated and

blast phases is accompanied by accumulation of genetic aberrations. Patients in blast crisis are characterized by poor appetite, splenomegaly, and proliferation of blast cells to other organs. In the advanced stages of disease, patients usually don't respond well to treatment.

1.4.2 Bcr-Abl: origin and mechanism of activation

The Philadelphia chromosome is the cytogenetic hallmark of chronic myelogenous leukemia, and was the first cytogenetic change to be associated with cancer [111]. The Philadelphia chromosome is formed by a reciprocal translocation between chromosomes 9 and 22 [112,113]. This translocation, described as t(9;22)(q34;q11), juxtaposes the Bcr and Abl genes, leading to the expression of a fusion oncogenic tyrosine kinase, Bcr-Abl [4,5,111,114]. The Philadelphia chromosomal translocation is known to occur at three different breakpoint regions in Bcr [minor(m), major (M), micro (μ)], thus giving rise to three variants of the Bcr-Abl fusion protein – p185, p210, or p230 respectively [114]. These different types of Bcr-Abl include varying lengths of the Bcr gene fused to the Abl sequence, and consequently varying domains from the Bcr protein, and are associated with different disease pathologies [115]. The p185 Bcr-Abl includes the coiled-coil oligomerization domain, the SH2 domain binding site, and the serine/threonine kinase domain, and is associated with about 10% cases of acute lymphocytic leukemia (ALL). The p210 form of Bcr-Abl includes a Bcr-derived pleckstrin homology domain and a Dbl/Cdc24 guanine exchange factor homology domain, in addition to the coiled coil, SH2 domain binding site, and serine/threonine kinase domain, and is associated with about 95% of CML and about 20% of ALL cases (Figure 6). The p230 form of Bcr-Abl includes the Rac GAP domain of Bcr, in addition to the above described domains, and is associated with chronic

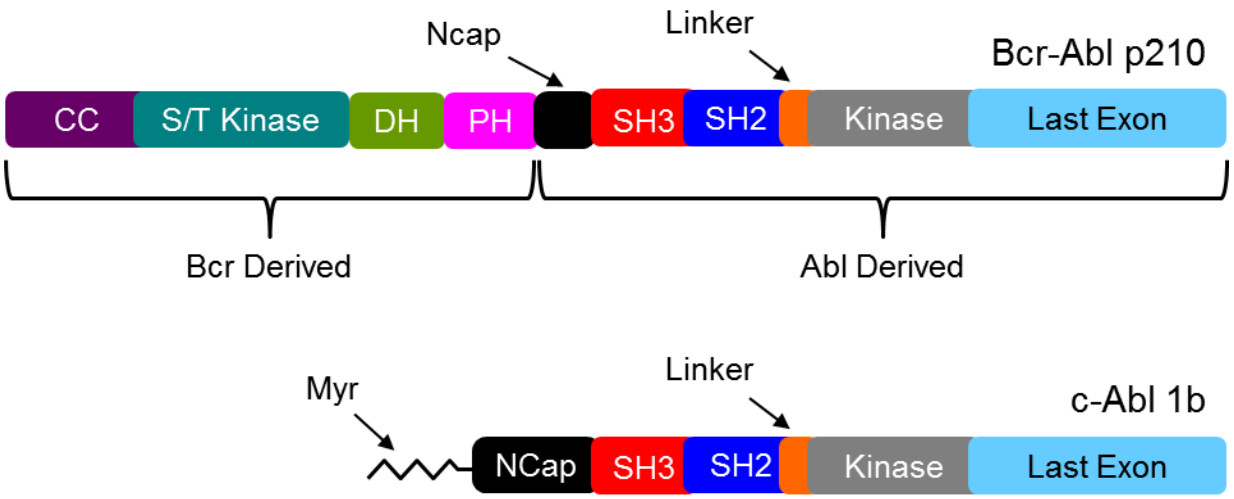

Figure 6. The modular domain organization of the Bcr-Abl p210 protein.

Bcr-Abl, an oncogenic protein tyrosine kinase, is the result of a chromosomal translocation that causes the fusion of Bcr and Abl proteins. The p210 variant of Bcr-Abl, responsible for CML, consists of multiple Bcr-encoded domains as shown – a coiled-coil domain (CC), a serine/threonine (S/T) kinase domain, a Dbl/Cdc24 guanine nucleotide exchange factor homology (DH) domain, and a pleckstrin homology (PH) domain. These Bcr domains are followed by Abl-encoded domains – partial N-cap, SH3 and SH2 domains, a SH2-kinase linker, kinase domain, and the last exon region containing proline rich regions, nuclear localization and export signals, and DNA and actin binding domains. The domain organization of the c-Abl 1b protein is shown at the bottom for reference.

neutrophilic leukemia (CNL). The discussion below is limited to the p210 form of Bcr-Abl responsible for CML.

The N-terminal fusion of Bcr to Abl results in the partial deletion of the N-cap region, leading to a loss of myristoylation that serves an important function in inhibiting Abl kinase activity (discussed earlier in section 1.2.1.1). Bcr-Abl does include the SH3 and SH2 domains, kinase domain, and the C-terminal region of Abl. Moreover, the addition of Bcr domains upstream of the Abl tyrosine kinase plays an important role in kinase activation and is required for Bcr-Abl oncogenicity [116,117]. An important example is the coiled-coil domain at the N-terminus of the Bcr protein [118,119]. This domain causes oligomerization of kinase molecules, leading to auto-phosphorylation, and kinase activation. Remarkably, disruption of Bcr-Abl oligomerization by deletion or mutation of the coiled-coil domain leads to a decrease in Bcr-Abl kinase and transforming activities.

Although Bcr-Abl exhibits constitutive tyrosine kinase activity, several studies suggest that some of the regulatory intra-molecular interactions seen in Abl may persist in Bcr-Abl. X-ray crystallization studies of imatinib bound to Abl have shown that it selectively binds the inactive conformation of the kinase domain (discussed in section 1.4.3.1), suggesting that it must trap Bcr-Abl in the same inactive conformation [32,33]. Moreover, mutations in the regulatory domains of Abl that disrupt the down-regulated conformation of Abl kinase core have been shown to cause resistance to imatinib [120]. Furthermore, enhanced SH3:linker intra-molecular interaction sensitizes Bcr-Abl-transformed cells to apoptosis by both ATP-competitive and allosteric inhibitors [30]. These studies suggest that Bcr-Abl may sample a dynamic range of conformations in solution, with the equilibrium being controlled by the same mechanisms that regulate Abl auto-inhibition (e.g. SH3-linker interaction).

Bcr-Abl expression is sufficient to induce factor-independent growth and survival in mouse fibroblasts, human myeloid progenitor cells, and primary bone marrow cells [108,121–123]. Moreover, transplantation of Bcr-Abl-transduced bone marrow cells in mice gives rise to CML-like myeloproliferative disease (MPD) [124]. Furthermore, the tyrosine kinase activity of Bcr-Abl is critical for leukemogenesis, since kinase-dead Bcr-Abl-transduced cells do not induce MPD in mice [108]. Bcr-Abl acts as the oncogenic driver by interacting with signaling proteins and activating multiple signaling pathways involved in mitogenic signaling, altered cell adhesion and motility, disruption of DNA-damage repair processes, inhibition of apoptosis, and increases degradation of negative regulators of kinase activity [125]. Examples of some of these pathways include Ras and mitogen-activated protein kinase (MAPK), Janus kinase (JAK) – signal transducer and activator of transcription (STAT), phosphoinositide 3-kinase (PI3K), and Src-family kinases, which are normally under strict physiological control by hematopoietic cytokines and growth factors.

1.4.3 Imatinib: targeted Bcr-Abl kinase inhibitor

One of the first examples of the selective inhibition of tyrosine kinase activity using small molecules was provided by the discovery of a class of compounds called tyrphostins that selectively inhibited EGFR kinase activity [126]. Subsequent studies reported a 2-phenylaminopyrimidine compound as an inhibitor of the PDGFR [127]. Imatinib (Gleevec, STI-571; Novartis) was developed as a derivative of 2-phenylaminopyrimidine to be a more potent inhibitor of PDGFR, and was subsequently found to inhibit the kinase activity of Abl tyrosine kinases and the stem cell factor receptor kinase (c-Kit) [128]. In a seminal study published in 1996, Brian Druker and colleagues reported that imatinib selectively inhibited the growth of Bcr-

Abl-positive cells and the growth of Bcr-Abl positive tumors *in vivo* [129]. Remarkably, it had no effect on the growth of non-transformed parental cells, or Bcr-Abl-negative transformed cells. Moreover, imatinib was found to inhibit hematopoietic colony formation by Bcr-Abl-positive cells obtained from patient samples. The success of these pre-clinical studies led to the first clinical trial with imatinib in 1998 [130]. In the initial phase I clinical trial, imatinib was remarkably successful with 53 out of 54 (98%) patients in chronic phase achieving complete hematologic response (CHR) after 4 weeks of treatment. This initial response was maintained in 96% of the patients for over a year. Moreover, 21 out of 38 (55%) patients in the accelerated or blast crisis phases achieved partial hematologic response as well. In a phase II clinical trial, 91% patients in chronic phase showed CHR, and 89% of these showed no disease progression. However, patients in the accelerated phase and blast crisis achieved only 69% and 21% hematologic responses, respectively. The phase III clinical trial compared the efficacy of imatinib with the standard treatment at the time (interferon-α plus cytarabine), and found that patients treated with imatinib showed a significantly higher complete cytogenetic response rate (CCyR) with 96.7% of patients in chronic phase showing no disease progression after 18 months. Based on the overall efficacy and survival rate, imatinib was approved for treatment of CML by the FDA in 2001 [131]. The success of imatinib was followed by the development of several second and third generation ATP-competitive tyrosine kinase inhibitors of Abl kinases that will be discussed in section 1.4.4.

1.4.3.1 Imatinib: mechanism of action

Crystal structures of the Abl kinase domain in complex with imatinib were solved to elucidate the mechanism of imatinib binding and specificity [32,33]. These studies revealed that imatinib binds between the N- and C-lobes of the kinase domain close to the activation loop and the helix

αC. Moreover, the drug specifically binds to a unique conformation of the kinase domain where the activation loop is pointed inward and the DFG motif is flipped outward (discussed earlier in section 1.2.1.5). The DFG-out conformation prevents ligation of a critical magnesium ion that is required for catalysis. Moreover, imatinib forms a hydrogen bond with Asp381 of the DFG motif, which helps stabilize its binding to Abl. Furthermore, imatinib binding is stabilized by other hydrogen bonding interactions with Met318, Thr315 (gatekeeper residue), Glu286, His361, and Ile360, and several van der Waals interactions. A comparison of the inactive and active conformation of kinases has been helpful in understanding specificity exhibited by imatinib towards Abl [32,35]. While protein tyrosine kinases from different kinase families in the active state exhibit quite similar conformations, they adopt distinct conformations in the inactive state. Thus, imatinib achieves selective binding by stabilizing this distinct and relatively unique inactive conformation of Abl.

1.4.3.2 Mechanisms of resistance to imatinib

While the high rates of hematologic and cytogenetic responses to imatinib have been very promising, resistance to imatinib treatment has been a major concern. About 20-30% of CML patients are predicted to develop resistance to imatinib over the course of their treatment [132,133]. The mechanisms of resistance to imatinib can be divided into two types – Bcr-Abl-dependent, and Bcr-Abl-independent mechanisms.

Imatinib resistance: Bcr-Abl-dependent mechanisms

One possible mechanism of Bcr-Abl dependent resistance to imatinib is through Bcr-Abl gene amplification, that results in over-expression of the Bcr-Abl protein. In the first set of 11 patients reported to show resistance to imatinib, 3 patient samples showed gene amplification as tested

using fluorescent in situ hybridization (FISH) [134]. In a larger set of 66 patient samples tested for Bcr-Abl amplification, only 2 patient samples showed amplification [135], suggesting that this mechanism is relatively uncommon.

A second mechanism that is commonly seen is the emergence of mutations in Bcr-Abl that render the kinase refractory to imatinib. In the first report on patients who developed resistance to imatinib, 6 out of 11 patients were found to have a single nucleotide change in Bcr-Abl, resulting in a mutation where the gatekeeper threonine residue at position 315 was mutated to isoleucine [134]. Based on the crystal structure of imatinib bound to the Abl kinase domain, this mutation not only prevents formation of a critical hydrogen bond between the tyrosine residue and imatinib, but the side chain of the isoleucine residue also introduces a steric clash that prevents imatinib binding [32]. T315I has turned out to be the most recalcitrant imatinib-resistance mutation, and is responsive to only one of the clinically available ATP-competitive drugs which was designed to specifically inhibit this mutant kinase (ponatinib; discussed below in section 1.4.4). Furthermore, this T315I mutation has also been shown to enhance the kinase activity of the Abl and Bcr-Abl proteins as discussed earlier in section 1.2.1.5. Since this initial study, numerous other mutations in the kinase domain have been reported to cause resistance to imatinib treatment. These include mutations that either directly disrupt imatinib binding (e.g. T315I), or alter the kinase conformation such that it is incompatible for imatinib binding. Mutations belonging to the latter category are predominantly found in specific regions in the kinase domain such as the P-loop (e.g. Glu255, Tyr253), activation loop (e.g. His396), or at the SH2-kinase interface (e.g. Met351), but a few have also been reported in the regulatory domains (e.g. Ser154, Thr212) [132,136,137]. The most commonly mutated residues, representing 60-70% of all mutations in clinical samples, are found in the kinase domain and include Gly250,

Tyr253, Glu255, Thr315, Met351, and Phe359 [132]. Interestingly, some of these mutations have been shown to enhance Bcr-Abl's transforming potential [45,138].

A comprehensive experimental study examining the effect of random mutagenesis of Bcr-Abl on the sensitivity of Bcr-Abl-transformed cells towards imatinib revealed many novel mutations that confer resistance to imatinib [120]. A majority of the mutations reported in the clinic were identified in this screen as well. Interestingly, this study found mutations not only in the drug binding site, but also in the regulatory domains of the Abl core. The positions of these mutated residues are distributed across all domains in the Abl kinase core and are presented in Figure 7. These mutations are predicted to cause resistance through an allosteric mechanism that promotes kinase activation. This is consistent with the inability of imatinib to bind the active (DFG-in, discussed earlier in section 1.2.1.5) conformation of the kinase domain [32,33].

Imatinib resistance: Bcr-Abl-independent mechanisms

Bcr-Abl-independent resistance accounts for about 50% of imatinib-resistant cases of CML and can be attributed to a multitude of different mechanisms [132,139]. One possible mechanism is the reduction in intracellular drug levels due to a decrease in drug influx in the presence of α-1 acid glycoprotein in the membrane, increase in drug efflux through P-glycoprotein mediated active transport levels, or changes in drug metabolism by cytochrome P450 isoenzymes. Other mechanisms of resistance include activation of other tyrosine or serine/threonine kinases downstream of Bcr-Abl signaling, leukemic stem cells refractoriness, and minimal residual disease in leukemic stem cells.

Some patients exhibit resistance to imatinib despite inhibition of Bcr-Abl kinase activity, and this could be due to activated downstream signaling pathways [135]. Several studies have implicated Lyn, Fyn, and Hck, members of the Src kinase family, in imatinib resistance in CML.

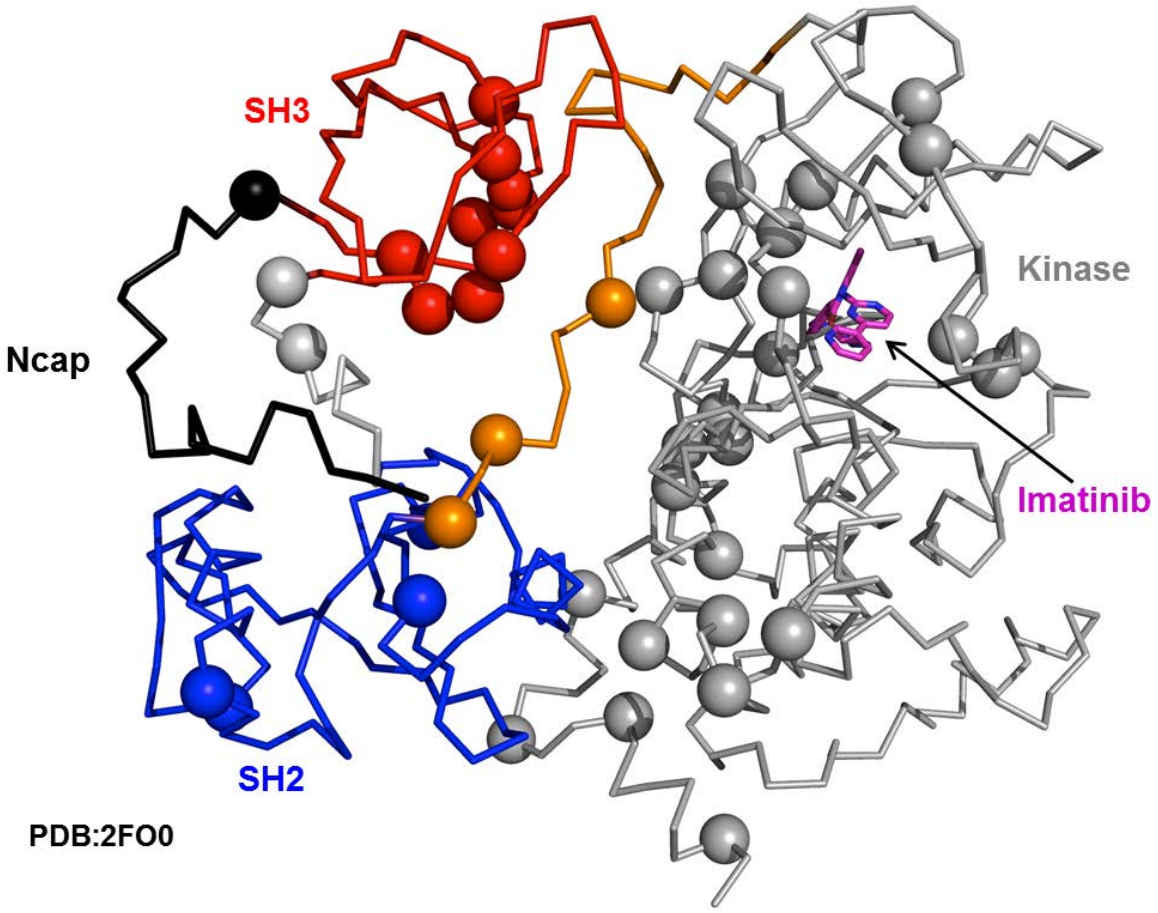

Figure 7. Point mutations in the Abl kinase core induce resistance to imatinib.

The location of residues, which render Bcr-Abl transformed cells resistant to imatinib upon mutation, are mapped onto the down-regulated structure of the Abl core (PDB: 2FO0). These mutations were identified in an unbiased *in vitro* screen [120]. Note that many of these mutations are located in the regulatory domains of the Abl core, indicating an allosteric mechanism of resistance through the drug binding site. The position of imatinib (carbons in magenta) in the active site was mapped by aligning the kinase domain of this structure with that of an imatinib-bound kinase domain crystal structure (PDB: 1IEP).

In an early study, K562 CML cells were cultured in increasing concentrations of imatinib to develop drug resistance. These resistant cells, in comparison to imatinib-sensitive cells, were found to have higher Lyn activity, and inhibition of Lyn kinase expression resulted in reduced proliferation and survival of these cells [140,141]. Moreover, imatinib resistance has been associated with upregulation of Hck, Lyn, or Fyn expression and/or activity levels in clinical samples from patients with accelerated or blast phase CML disease [140,142–144]. Additionally, a recent study found that Fyn potentially contributes to Bcr-Abl-induced genomic instability, leading to CML progression into blast phase of the disease [145]. In addition to these studies, work from our laboratory has shown that Fyn, Lyn, and Hck phosphorylate multiple tyrosine residues in the activation loop as well as regulatory domains of Abl [25]. The phosphorylation of some of these residues is predicted to disrupt regulatory intra-molecular interactions in the Abl core leading to kinase activation [24,25]. Moreover, recent studies from our lab have shown that overexpression of Hck in K562 CML cells leads to resistance to imatinib treatment and is correlated with increase in tyrosine phosphorylation in the Bcr-Abl SH3 domain (Tyr89) and activation loop (Tyr412). Furthermore, selective inhibition of Hck results in reversal of these phosphorylation events and restores imatinib sensitivity [146,147]. To summarize, these studies suggest an important role for Src-family kinase-mediated imatinib resistance in CML in the absence of mutations in the Bcr-Abl kinase domain. The success of dasatinib, a dual Bcr-Abl and Src-family kinase inhibitor (discussed below in section 1.4.4), in CML treatment suggests that inhibition of Src-family kinase activity can contribute towards reducing the incidence of drug resistance to tyrosine kinase inhibitors. In addition to SFKs, other signaling pathways such as MAPK, PI3K, and JAK-STAT, have also been implicated in resistance to imatinib [148].

The vast majority of chronic phase CML patients achieve complete cytogenetic response (CCyR) following imatinib treatment, but relapses are commonly observed after imatinib cessation, due to the persistence of a 'residual' population of CML stem and progenitor cells [148]. In patients who have achieved MMR or CMR with imatinib treatment, 0.09% to 1.61% Bcr-Abl positive leukemic stem cells are found to persist as observed in engraftment studies in immunodeficient mice [149]. Multiple studies have shown that tyrosine kinase inhibitors are able to inhibit Bcr-Abl kinase activity in leukemic stem cells [150,151]. However, in contrast to differentiated cells, these cells do not undergo apoptosis following drug treatment [151]. This suggests that these cells may not be totally dependent on Bcr-Abl for growth, and hence cannot be eliminated by tyrosine kinase inhibitor treatment and contribute to the minimal residual disease. Thus bone marrow transplantation remains as the only true cure for CML.

1.4.4 Second and third generation ATP-competitive inhibitors of Bcr-Abl

Although chronic use of imatinib leads to drug resistance in a large number of patients as discussed above, it has served as an important prototype for selective targeting of tyrosine kinases. Moreover, the X-ray crystal structure of imatinib bound to Abl has provided valuable insight into imatinib's mechanism of action, and has been used to develop second- and third-generation tyrosine kinase inhibitors (TKIs).

Nilotinib (Tasigna, AMN107; Novartis) is one such second generation ATP-competitive TKI that is a structural analog of imatinib and selectively binds the inactive (DFG-out) conformation of the kinase. Nilotinib is about 50 times more potent than imatinib for Bcr-Abl inhibition *in vitro*, and like imatinib, inhibits c-Kit and PDGFR as well [152]. Nilotinib is able to inhibit a majority of the imatinib-resistant Bcr-Abl mutants. However, the gatekeeper mutant

(T315I) is completely resistant to nilotinib, and a few other kinase domain mutants including Y253H, E255K/V, and F359C/V are less sensitive to nilotinib [109,153,154]. Nilotinib was approved for second-line treatment of chronic and accelerated phase CML patients who are resistant to imatinib in 2007, and for front-line chronic phase CML therapy in 2010.

Dasatinib (Sprycel, BMS-354825; Bristol-Meyers Squibb), another second-generation ATP-competitive TKI, is a dual Abl and Src family kinase inhibitor. In contrast to imatinib and nilotinib, dasatinib binds the active (DFG in) conformation of the kinase domain, and is about 300 fold more potent than imatinib against cells expressing Bcr-Abl [36,155]. Dasatinib is also able to bind and inhibit a majority of imatinib-resistant Bcr-Abl mutants, with the exceptions of the gatekeeper mutant T315I which is completely resistant, and V299L and F317L mutants that are not as sensitive [109,156]. Dasatinib was approved for second-line treatment of all CML patients who are resistant to imatinib in 2006, and for front-line chronic phase CML therapy in 2010.

Bosutinib (Bosulif, SKI-606; Pfizer), is another second generation ATP-competitive TKI that can inhibit Abl as well as Src family kinases. Unlike the other three inhibitors described above, bosutinib does not inhibit c-Kit and PDGFR [157,158]. Bosutinib also inhibits a majority of imatinib-resistant mutants, but the gatekeeper T315I mutant is recalcitrant to this drug as well. In 2012, bosutinib was approved for second-line treatment of CML patients who are resistant or intolerant to the other TKIs.

Ponatinib (Iclusig, AP24534; Ariad) is a third generation ATP-competitive TKI and the first approved inhibitor with activity against the Bcr-Abl T315I mutant [159]. Ponatinib, similar to imatinib, binds the inactive conformation of the Abl kinase domain through extensive hydrogen bonding and hydrophobic interactions, though drug binding does not require the

formation of a hydrogen bond with the Thr315 residue. Moreover, in contrast to imatinib, ponatinib interacts with the sidechain of the mutant T315I residue through a hydrophobic interaction and is thus able to bind and inhibit the Bcr-Abl T315I mutant. Ponatinib is about 500-fold more potent than imatinib for Bcr-Abl inhibition, and showed an impressive response in the phase I and II clinical trials with patients who had been pre-treated with the other TKIs and those harboring the T315I mutation [160,161]. Ponatinib was approved for second-line treatment for patients in all disease phases of CML who were resistant or intolerant to other TKIs in 2012. However, long-term exposure to ponatinib was found to result in an increased incidence of arterial thrombotic events in patients from the phase II study [160,161]. As a result, a large randomized phase III clinical trial comparing imatinib and ponatinib was suspended until more information is available about drug efficacy and safety. Currently, ponatinib is approved with restrictions and additional safety guidelines for patients harboring the Bcr-Abl T315I mutant, or those that are resistant to all other TKI therapies.

Another class of inhibitors, known as switch pocket inhibitors (DCC-2036; Deciphera Pharmaceuticals), bind the residues Arg386/Glu282 in the switch region and prevent Abl from adopting an active conformation [162]. DCC-2036 is able to inhibit a majority of the imatinib-resistant mutants, including the gatekeeper T315I mutant. A phase I clinical trial was initiated with CML patients harboring the T315I mutation to assess the safety and tolerability of prolonged drug exposure, and the results of the study are awaited.

1.4.5 Allosteric inhibitors of Bcr-Abl

In addition to the tremendous efforts invested in the development of tyrosine kinase inhibitors targeting the active site of the kinase, a few studies have identified small molecules that act at

allosteric sites that are distant from the active site. Allosteric inhibitors are predicted to target regulatory mechanisms and sites that are relatively unique to individual kinases, and thus may exhibit reduced off-target effects, improve selectivity, and hence be better tolerated and have fewer side effects.

The first allosteric inhibitor of Bcr-Abl, GNF-2, was discovered by Nathanael Gray and co-workers using a high-throughput cytotoxicity assay and Bcr-Abl-transformed cells in 2006 [163]. Subsequent biochemical and structural studies showed that GNF-2 binds to the myristic acid binding pocket of Abl and stabilizes the inactive conformation of the kinase [55]. Surprisingly, GNF-2 was unable to inhibit several imatinib-resistant mutants of Bcr-Abl, including the T315I mutation. However, a combination of GNF-2 with nilotinib was effective in inhibiting the Bcr-Abl T315I mutant, as well as many other imatinib resistant mutants. Moreover, a combination of GNF-5 (a GNF-2 analog with improved pharmacokinetics) and nilotinib was able to effectively reduce splenomegaly, white blood cell counts, and STAT5 phosphorylation in a murine bone marrow transplantation model of CML. Furthermore, this combination also resulted in an overall increased survival of animals in this study. Structural characterization of GNF-5 revealed conformational changes in the ATP binding site on compound binding, supporting allosteric communication between the myristic acid binding pocket and the ATP binding site (as discussed earlier in section 1.2.2.2) [54].

Besides identification of small molecules, a few research groups have developed peptides or monobodies to further understand and manipulate the allosteric regulation of Bcr-Abl. In one study, disruption of the N-terminal coiled-coil region of Bcr-Abl using a peptide was shown to inhibit the oligomerization of Bcr-Abl resulting in decreased kinase activity, and increased sensitivity to both imatinib and GNF-2 [164]. In another study, the interface between the SH2

domain and N-lobe of the kinase domain in the maximally activated ‘top-hat’ conformation of Bcr-Abl was disrupted using a monobody, HA4-7c12, resulting in inhibition of Bcr-Abl kinase activity and decreased survival of CML cell lines [65]. While intra-cellular delivery of these reagents restricts their clinical applicability, they are useful tools to understand the importance of allosteric interactions in Bcr-Abl activity regulation.

1.5 ROLE OF C-ABL IN SOLID TUMORS

In contrast to the role of Bcr-Abl in CML and other leukemias, the exact role of Abl in solid tumors is not as clear. There are a few reports about amplification, over-expression, and activation of Abl and/or Arg kinases in solid tumors [165]. Abl kinases are usually activated downstream of hyperactive receptor tyrosine kinases such as the PDGFR, EGFR, ERBB2 (or HER2), or insulin-like growth factor 1 receptor (IGF1R) [80,166–169]. Since Abl is involved in the regulation of diverse cellular processes, it is not surprising that it also plays a role in multiple facets of tumor growth and metastasis. In recent years, many research groups have been investigating the role of Abl kinases in diverse aspects of tumor pathology such as proliferation and survival, response to cellular stresses such as DNA damage, epithelial-to-mesenchymal transition (EMT), tumor invasion, and tumor metastasis. While the role of Abl in response to DNA damage is discussed earlier in section 1.3, this section will focus on the role of Abl in promoting or suppressing tumor growth and survival.

1.5.1 Abl as a promoter of tumor growth

The activation of Abl kinases has been associated with changes in cell growth and survival. Depletion of Abl expression in breast cancer cells using siRNA showed that Abl is required for anchorage independent growth in breast cancer cells [169]. Moreover, Abl was also found to be required for anchorage independent growth of gastric and hepatocellular carcinoma cells [170]. While the exact mechanisms of Abl-induced cell proliferation are still being investigated, some signaling pathways that have been shown to be involved include RAC, p38, and ERK5 [171].

1.5.2 Abl as a suppressor of tumor growth

In contrast to the role of Abl in promoting the growth of tumor cells, a few studies have shown a role for Abl in suppressing the growth of breast cancer cells. In a breast cancer xenograft mouse model, stimulation of EpHB4 receptor tyrosine kinase with ephrin B2 resulted in Abl activation, and a decrease in tumor growth through an Abl-Crk pathway [172]. Imatinib treatment blocked this effect, and Abl-dependent Crk phosphorylation was shown to be required for the effect of ephrin B2 on the growth arrest and apoptotic induction seen in breast cancer cells. Interestingly, another study reported that expression of a constitutively active form of Abl in a murine breast cancer cell line enhanced TGFβ induced growth arrest in 3D cell cultures, and inhibited the growth of tumor xenografts [173]. Moreover, active Abl kinase also suppressed TGFβ induced secretion of matrix metalloproteinase enzymes and inhibited cell migration in 3D cell culture.

The discrepancy in the role of Abl in promoting vs. suppressing growth or invasiveness of solid tumors can be explained by the heterogeneity of solid tumors in terms of diverse activated signaling pathways, cell type, and tumor microenvironment. The function of Abl in

solid tumors could potentially depend on a combination of these factors and requires more investigation with selective modulators of Abl kinase activity.

1.6 HYPOTHESIS AND SPECIFIC AIMS

The kinase activity of Abl is tightly regulated by multiple intra-molecular interactions, and disruption of these interactions leads to kinase activation. Although Bcr-Abl exhibits constitutive tyrosine kinase activity, several studies strongly suggest that some of the regulatory intra-molecular interactions seen in Abl may persist in Bcr-Abl. The positions of the regulatory SH3 and SH2 domain have been established in either the down-regulated Abl core conformation or the maximally activated mutant kinase. However, the reorientation of the regulatory domains and their positions as a consequence of kinase activation under different cellular circumstances are not known. Conformation dynamic studies using HXMS have shown that effects of mutations in the Abl core are allosterically communicated to other sites in the kinase core. Furthermore, recent NMR analysis has shown that when the ATP-site inhibitor imatinib is bound to the Abl kinase domain, the structure becomes more dynamic with respect to the SH2 and SH3 domains. Based on these studies, I propose the hypothesis that Abl kinase activation does not require complete disruption of all intra-molecular interactions and reorientation of regulatory domains.

Interaction between the SH3 domain and the SH2-kinase linker of Abl has been shown to be critical for regulation of Abl kinase activity. On one hand, disruption of the SH3:linker interaction by mutations or phosphorylation of tyrosine residues has been shown to activate Abl kinase, and induce resistance towards imatinib in Bcr-Abl transformed cells. On the other hand, enhanced SH3:linker interaction (as seen in our engineered HAL forms of Abl) overcomes the

effects of activating mutations in Abl, and sensitize Bcr-Abl transformed cells to both ATP-competitive (e.g. imatinib) and allosteric (GNF-2) inhibitors. Thus, I propose the hypothesis that a small molecule that acts through the regulatory domains of Abl and influences SH3:linker interaction can be a potential agonist or antagonist of Abl kinase activity. Such compounds will represent valuable new probes to better understand the role of Abl signaling in complex cellular environments (e.g., DNA damage response; breast cancer metastasis) and may represent new drug leads for Abl-related cancers.

My thesis project tested these hypotheses with the following specific aims:

Specific Aim 1:

To investigate the effect of activating and stabilizing mutations on Abl core kinase activity, enzyme kinetics, thermal stability, and conformation in solution.

Specific Aim 2:

To develop a fluorescence-polarization assay to screen chemical libraries to identify allosteric modulators of Abl kinase activity that act through the regulatory domains.

2.0 THE C-ABL KINASE ADOPTS MULTIPLE ACTIVE CONFORMATIONAL STATES IN SOLUTION*

2.1 SUMMARY

Protein-tyrosine kinases of the Abl family have diverse roles in normal cellular regulation and drive several forms of leukemia as oncogenic fusion proteins. In the crystal structure of the c-Abl kinase core, the SH2 and SH3 domains dock onto the back of the kinase domain, resulting in a compact, fully assembled state. This inactive conformation is stabilized by the interaction of the myristoylated N-cap with a pocket in the C-lobe of the kinase domain. Mutations that perturb these intramolecular interactions result in kinase activation. Here we present X-ray scattering solution structures of multi-domain Abl kinase core proteins modeling diverse active states. Surprisingly, the relative positions of the regulatory Ncap, SH3 and SH2 domains in an active myristic acid binding pocket mutant (A356N) were virtually identical to those of the assembled wild-type kinase core, indicating that Abl kinase activation does not require dramatic reorganization of the downregulated core structure. In contrast, the positions of the SH2 and SH3 domains in the clinically relevant imatinib-resistant gatekeeper mutant T315I appear to be switched relative to their positions in the wild-type protein. Thus Abl kinase activation can occur with (T315I) or without (A356N) global allosteric changes, revealing the potential for previously unrecognized signaling diversity.

*SAXS data were collected by Lee Makowski, Department of Chemistry and Chemical Biology, Northeastern University and analyzed by John Badger, DeltaG Technologies, San Diego, CA.

2.2 INTRODUCTION

The c-Abl tyrosine kinase is a modular signaling protein with multiple physiological roles ranging from regulation of the actin cytoskeleton to integration of DNA damage responses in the nucleus [8,174]. Abl is well known in the context of Bcr-Abl, the oncogenic tyrosine kinase responsible for chronic myelogenous leukemia (CML) and some cases of acute lymphocytic leukemia [175]. In CML, the normally tight regulation of c-Abl is lost as a result of fusion to Bcr sequences, and this uncontrolled kinase activity drives myeloid progenitor cell transformation and disease progression. Clinical management of CML has been revolutionized by the development of ATP-competitive inhibitors for the Abl kinase domain, of which imatinib (Gleevec) is the prototype [131]. The selectivity of imatinib for Bcr-Abl stems in part from its ability to trap a unique inactive conformation of the kinase active site [33]. Nevertheless, the evolution of drug-resistant mutants that affect imatinib binding has required the ongoing development of newer classes of Abl inhibitors. The so-called ‘gatekeeper’ mutant of Bcr-Abl, in which kinase domain position Thr315 in the imatinib binding site is replaced by isoleucine (T315I mutant), has been particularly difficult to target with small molecule inhibitors [134]. Other work has shown that the T315I mutation enhances both c-Abl and Bcr-Abl kinase activity, although the effect of this mutation on the overall structure and dynamics of c-Abl is less clear [46,138].

Crystallographic work on the Abl kinase 'core', which consists of an N-terminal cap region (N-cap), regulatory SH2 and SH3 domains as well as the kinase domain, has identified a compact, inactive conformation regulated by multiple interdomain contacts [9,12]. In this downregulated state, the SH2 and SH3 domains are docked onto the back of the kinase domain. Regulatory domain interactions are stabilized by addition of a myristic acid group to the N-cap, which inserts into a deep C-terminal lobe cavity unique to the Abl kinase domain. Mutations that perturb any of these intramolecular interactions lead to kinase domain activation, providing important validation of the crystal structure [14]. A model of the assembled, downregulated Abl core structure is presented in Figure 8A.

While X-ray crystallography has provided tremendous insight regarding the relative positions of the regulatory and catalytic domains in the downregulated state of the Abl core, the fate of these domains as a function of kinase activation is less clear. A single crystal structure of the Abl core that was activated by removal of all regulatory constraints revealed dramatic repositioning of the SH2 domain to the top of the kinase domain N-lobe (PDB ID: 1OPL, molecule B [12]), a result supported by other solution-based biophysical measurements [46].

Another attractive approach to investigate Abl structure is X-ray solution scattering, which enables structural characterization of protein forms that are not amenable to crystallization [47–50]. In particular, flexible conformations of large structures with multiple domains can be readily analyzed with this technique. Ensembles containing multiple conformational states may be identified from X-ray scattering patterns. In addition to well-known structural measures such as the radius of gyration (R_g) of the molecules in a sample, methodology for the *ab initio* calculation of low-resolution 3-dimensional molecular envelopes from intensity data has become

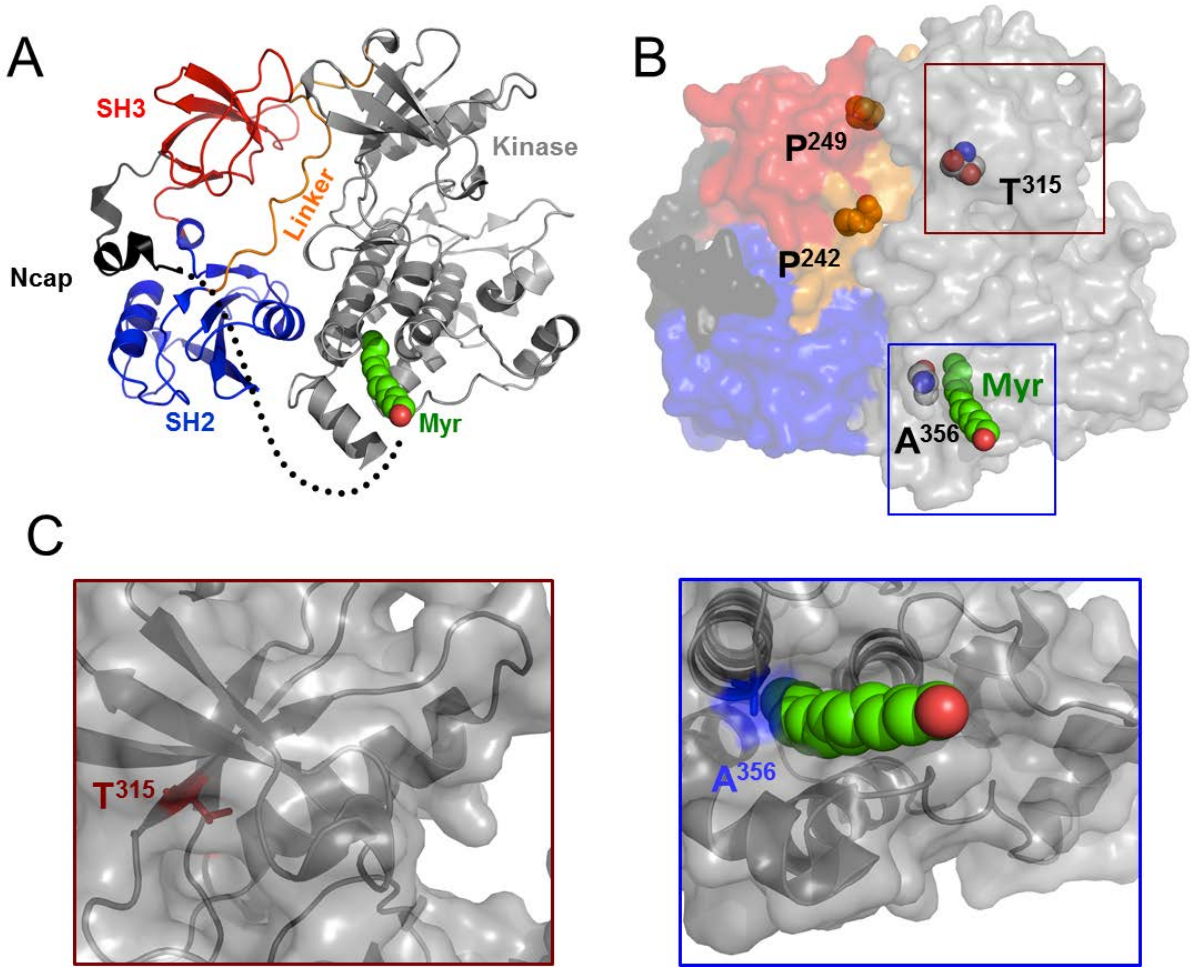

Figure 8. Abl core proteins.

A) Crystal structure of the assembled, downregulated Abl kinase core (PDB:2F0O [9]). The Abl core is composed of a myristoylated (Myr) N-cap, followed by the SH3, SH2, and kinase domains. The unstructured part of the N-cap that extends to the C-lobe of the kinase domain is represented as a dotted line. The SH2-kinase linker forms a polyproline type II helix which engages the SH3 domain. B) Positions of activating mutations of the Abl core used in this study. These include isoleucine substitution of the Thr315 gatekeeper position in the kinase domain (T315I), asparagine substitution of Ala356 (A356N) in the kinase domain C-lobe pocket that engages the myristoylated N-cap, and glutamic acid replacement of two prolines in the SH2-kinase linker (P242, P249) which were combined with deletion of N-cap residues 1-82 in the mutant ΔNcap-2PE. C) Enlarged views of boxed portions from the Abl core structure in panel B are shown to highlight the exact position of the Thr315 (left, brown box) and Ala356 (right, blue box) residues.

well-established [50]. This approach to determination of molecular envelopes is attractive because the shapes of the reconstructed molecular envelopes are independent of any specific, previously known atomic model.

Using the same hyperactive c-Abl protein (PDB ID: 1OPL, molecule B [12]) where SH2 was observed to be positioned on the top on the kinase domain N-lobe by X-ray crystallography, a molecular envelope was obtained by X-ray solution scattering. The conformation of Abl from those measurements yielded a fully extended conformation with the kinase, SH2, and SH3 domains in a linear arrangement, although the precise location of SH3 was not resolved [9]. Between the inactive assembled state and this fully disassembled state, X-ray solution scattering data from an SH2 mutant of the hyperactive construct identified an intermediate state (or set of states) that has resisted a specific structural interpretation [9]. In complementary studies, recent NMR analysis showed that when the ATP-site inhibitor imatinib is bound to the Abl kinase domain, the structure becomes more dynamic with respect to the SH2 and SH3 domains [51]. Taken together, these studies demonstrate remarkable dynamic interplay between the Abl regulatory and catalytic domains which raises the important question of the ensemble of possible active states attainable. Despite intense research efforts, our understanding of the structural transitions between the active and inactive states of Abl and the mechanisms that determine the equilibrium between them remains incomplete.

To characterize the range of active conformational states attainable by the Abl kinase, we created four recombinant Abl core proteins that model a graded range of active states. This approach allowed us to sample the core conformation at various points along the activation coordinate, in contrast to previous approaches that reference only a highly mutagenized active form that adopts a single extended conformation. X-ray scattering was used to determine the

solution structures of these proteins, which included: 1) the wild-type (WT) myristoylated Abl kinase core protein, identical in amino acid sequence and post-translational modifications to the one for which the crystal structure was solved by Nagar, *et al*. [9,12]; 2) an alanine to asparagine point mutant in the myristic acid-binding pocket of the kinase domain N-lobe (A356N), which interferes with insertion of the myristate group of the N-cap necessary for kinase downregulation (Figure 8C) [14]; 3) an imatinib-resistant mutant in which the gatekeeper threonine is substituted with isoleucine (T315I) Figure 8C [134]; and 4) a double mutant lacking a portion of the N-cap (amino acids 1-82) including the myristoylation site plus dual proline to glutamate substitutions in the SH2-kinase linker (prolines 242 and 249) which disrupt intramolecular docking of the SH3 domain (ΔNcap-2PE) [9,12]. The positions of these mutations are modeled on the crystal structure of the downregulated Abl core in Figure 8B, while Figure 8C shows enlarged views of the sites of mutation. These kinase proteins span a broad range of intrinsic catalytic activities, with the following rank order: wild-type < A356N < T315I < ΔNcap-2PE. Our X-ray scattering results demonstrate that activation of the Abl kinase domain does not necessarily require regulatory domain displacement or destabilization of the assembled core structure associated with downregulation. However, the clinically important imatinib-resistant mutation T315I causes an unexpected and dramatic rearrangement of the overall core structure, providing new insight into its heightened catalytic and signaling capabilities.

2.3 MATERIALS AND METHODS

2.3.1 Recombinant protein expression and purification

Construction of baculovirus vectors for insect cell expression of the Abl core proteins used in this study has been described elsewhere [9,30]. For protein production, Sf9 cells were co-infected with Abl core and YopH phosphatase baculoviruses to allow purification in the dephosphorylated state [30]. Abl proteins were purified from infected cell lysates using a combination of ion exchange and affinity chromatography and dialyzed against 20 mM Tris-HCl (pH 8.3) containing 100 mM NaCl and 3 mM DTT. Purity and mass of each purified protein was verified by SDS-PAGE and mass spectrometry.

2.3.2 Protein kinase activity measurements

Tyrosine kinase activity of recombinant Abl core proteins was assessed using the FRET-based Z'Lyte kinase assay system and Tyr-2 peptide substrate as described elsewhere [46]. The Tyr2 peptide substrate is labeled with fluorescein and coumarin at the N-terminal and C-terminal ends, and the emission ratio (ER) of the coumarin to fluorescein (FRET) fluorescence serves as the readout. Briefly, recombinant Abl kinase was incubated with ATP (50 μM) and Tyr2 peptide substrate (1 μM) for one hour. Assays were performed in quadruplicate in black 384 well plates (Corning #3676) in reaction volumes of 10 μL/well. Development reagent containing a selective protease was then added and the reaction was allowed to incubate for an additional hour. The development protease can selectively cleave the unphosphorylated peptide, resulting in disruption of FRET, and a high ER. On the other hand, phosphorylated peptide is not cleaved

and high FRET fluorescence results in a low ER. The assay includes a 0% phosphorylation control with unphophorylated peptide and no kinase, and a 100% phosphorylation control with a stoichiometrically phosphorylated Tyr2 peptide. The coumarin and fluorescein fluorescence is measured at the end of the assay, and the emission ratio for each well is normalized to the 0% and 100% phosphorylation controls.

2.3.3 Transient expression of Abl proteins in HEK 293T cells

The activity of Abl proteins expressed in HEK 293T cells was assessed as described previously [30]. Briefly, 10^6 HEK 293T cells were plated overnight in 6 cm dishes and then transfected with 2.5 µg plasmid DNA and X-tremeGENE9 DNA transfection reagent (Roche Applied Science). Twenty-four hours post-transfection, cells were lysed and protein concentrations were determined using the Bradford assay reagent (Pierce). Equal amounts of cell lysates from each condition were separated by SDS-PAGE and immunoblotting was performed to detect overall phosphotyrosine levels (pY99; Santa Cruz Biotechnology) and Abl expression levels (Abl polyclonal sc-131, Santa Cruz).

2.3.4 Kinetic protein kinase assay

The ADP Quest assay (DiscoverRx) [176], which fluorimetrically measures kinase activity as the production of ADP, was used to determine Abl kinase reaction velocities. Assays were performed in quadruplicate in black 384 well plates (Corning #3571) in reaction volumes of 10 µL/well. The Tyr2 substrate peptide (EAIYAAPFAKKK) was dissolved in the ADP Quest assay buffer (15 mM HEPES, pH 7.4, 20 mM NaCl, 1 mM EGTA, 0.02% Tween-20, 10 mM $MgCl_2$,

0.1 mg/ml bovine γ-globulins), while ATP stocks were prepared in 10 mM Tris-HCl (pH 7.0). The kinase reaction was initiated by the addition of ATP and read at 5 min intervals for 3 h in a SpectraMax M5 Microplate reader (Molecular Devices). To determine the substrate K_m, the ATP concentration was fixed at 50 μM and the substrate peptide was serially diluted from 0.2-200 μM. For ATP K_m determination, the substrate concentration was fixed at the respective substrate K_m for each of the kinases, and the ATP concentration was titrated over the range of 0.2-200 μM. The resulting progress curves were analyzed according to the method of Moroco et al. [177]. Briefly, raw fluorescence data were corrected for non-enzymatic ADP production (no kinase or substrate control) and kinase auto-phosphorylation (rate observed in the absence of substrate), and converted to pmol ADP produced using a conversion factor determined from an ADP standard curve generated under the same reaction conditions. The resulting values were plotted against time, and the linear portion of each progress curve was fit by regression analysis to determine the reaction velocity. Substrate and ATP K_m values were determined by non-linear regression analysis using the Michaelis-Menten equation (GraphPad Prism 6).

2.3.5 Differential Scanning Fluorimetry (DSF)

DSF measurements were performed using a StepOnePlus real-time quantitative PCR instrument (Applied Biosystems) and software (version 2.3). DSF assays (20 μl) were run in duplicate in sealed MicroAmp Fast 96-well qPCR plates (Applied Biosystems). DSF profiles were acquired with recombinant Abl core proteins (2 μM) in bicine buffer (10 mM bicine, 150 mM NaCl, pH 8.0) and SYPRO Orange (Sigma) diluted to a 5X working concentration. Parallel reactions without proteins were run in parallel to correct for background fluorescence. DSF reactions were allowed to equilibrate to 25 ^{o}C for 2 min, followed by an increase to 99 ^{o}C at a 1% temperature

ramp rate (1.6 ^{o}C/min) with continuous data collection. Background fluorescence was subtracted and mean fluorescence intensities were then plotted as a function of temperature. Melt curves were fit using the Boltzmann sigmoid function of GraphPad Prism 6, and T_m values were calculated as the midpoint of the thermal transition between the minimal and maximum fluorescence intensities.

Small molecules (20 μM) were pre-incubated with the Abl core proteins (1 μM) for 30 minutes in bicine assay buffer (10 mM bicine, 150 mM NaCl, pH 8.0). SYPRO Orange (Sigma) was added at 5X final concentration and fluorimetry profiles were acquired as described above. Control reactions without proteins were included to correct for background fluorescence.

2.3.6 X-ray solution scattering data collection

SAXS data were collected using the undulator-based beam line X9 at the National Synchrotron Light Source (NSLS) at Brookhaven National Laboratory configured with two detectors [178] in order to collect both SAXS and WAXS data simultaneously, over the range of $0.006 < q < 2.0$ Å^{-1}, where q is the momentum transfer ($q = 4\pi \sin(\theta)/\lambda$), 2θ is the scattering angle and λ is the wavelength of incident X-rays. Data were collected at an X-ray wavelength of 0.9184 Å. A Photonic Science CCD detector operated as the WAXS detector and a Mar 165 CCD as the SAXS detector. The SAXS detector was located 3.4 m from the sample. Samples were loaded into a 96-well plate and aspirated into the 1.5-mm diameter, thin-walled sample tube using an automated system previously described [178]. Preliminary data processing was carried out using the X9 software package to produce circularly averaged intensity profiles combining data from the two detectors and extending over the entire range of q values.

2.3.7 Reconstruction of molecular envelopes

Reconstructions of molecular envelopes from X-ray solution scattering data were performed using programs from the ATSAS software suite [179]. The particle distance distribution function, P(r), was calculated using GNOM [180] with data resolution limits and the maximum allowed inter-atomic distance, r_{max}, selected empirically so as to optimize the fit to the intensity data. In addition to scoring trials for P(r) using the output from GNOM, the shape of P(r) and the reciprocal space fit of P(r) to the observed data were also checked by visual inspection.

Three-dimensional models of connected beads were generated to fit the data using GASBOR [50] with the number of beads set approximately equal to the number of amino acids in the Abl constructs. Between 10 and 40 independent modeling runs were performed on each data set, depending on the consistency of solutions and, for key selected examples, to assess the reproducibility of features in the molecular envelopes by comparing sub-averages from replicated reconstruction runs. Grid objects and molecular surfaces corresponding to Abl molecular envelopes were obtained by aligning replicate reconstructions with the DAMSEL and SUPCOMB [181] programs. A locally developed program was used to convert these aligned reconstructions to contiguous grid objects in which the volumes filled by the molecular envelope are represented by a set of pseudo-atoms set on a cubic grid with a 4 Å interval. For the seven reconstructions carried out on the initial data collection run (run 1) the grid objects were generated by counting the number of aligned beads within 8 Å of each grid point and thresholding these number densities to give objects with approximately the same partial specific volume as calculated from the Abl sequence. The reconstructions for the four data sets collected in the second run (run 2) showed somewhat more scatter so the larger range of 16 Å was used to calculate bead number densities to obtain an appropriately smooth molecular envelope. Except

for the highly extended ΔNcap-2PE construct, analysis focused on the most extended set of examples collected under a single set of experimental conditions (run 1).

2.4 RESULTS

2.4.1 Biochemical characterization of the kinase activity of Abl kinase proteins

Recombinant Abl core proteins were expressed in Sf-9 insect cells, purified to homogeneity, and their masses and post-translational modifications (myristoylation; phosphorylation) were confirmed by mass spectrometry. Additional constructs incorporating a high affinity linker sequence ('HAL9') [30] that stabilizes intramolecular binding to the SH3 domain were expressed as controls. Using an in vitro kinase assay [46], we determined the concentration of each Abl kinase required for 50% maximal substrate phosphorylation (EC_{50}) as a relative measure of intrinsic protein kinase activity. As shown in Figure 9A, the kinases spanned a wide range of activities, with the WT (least active) and ΔNcap-2PE (most active) differing by nearly 60-fold. The A356N and T315I mutants exhibited intermediate activities, with the T315I mutant nearly 8-fold more active than the A356N mutant. Earlier studies have reported the activity of the A356N and T315I mutants in cell-based assays, but the activity of the ΔNcap-2PE Abl mutant has not been tested in cells [30]. We therefore expressed these mutant Abl proteins in HEK 293T cells, and examined Abl kinase activity by immunoblotting for the total phosphotyrosine content in the whole cell lysates. As shown in Figure 9B, we found that cells expressing mutant Abl proteins have higher phosphotyrosine content, correlating with an increase in kinase activity.

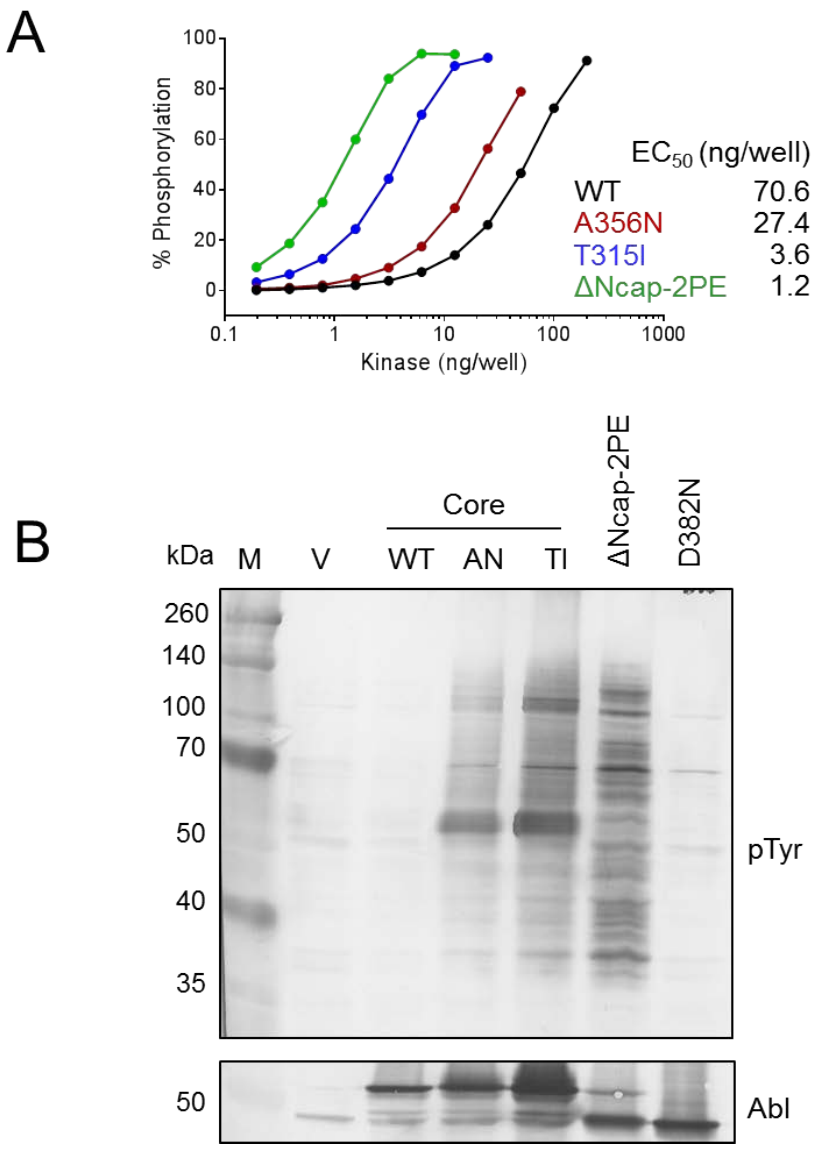

Figure 9. Kinase activity measurements for Abl proteins.

A) In vitro kinase assays of recombinant purified Abl proteins. Kinase activity was determined at ambient temperature using a FRET-based tyrosine kinase assay with a peptide substrate and increasing amounts of each recombinant Abl protein. Each condition was repeated in quadruplicate, and the extent of phosphorylation is expressed as mean percentage phosphorylation relative to a control phosphopeptide ± SD. Each kinase activation curve was best-fit by non-linear regression analysis, and the resulting EC_{50} values for half-maximal kinase activity are shown. (Note: The S.D. values are smaller than the diameter of the symbols, and therefore cannot be seen.) B) Kinase activity of Abl proteins in cells. Each Abl protein was expressed in 293T cells, and the overall protein tyrosine phosphorylation was assessed in the cell lysates by immunoblotting with an anti-phosphotyrosine antibody, with Abl blots performed as a control. The rank order of activity was the same in two independent experiments, and a representative blot is shown.

Cells expressing the wild-type Abl core protein, on the other hand, showed no increase in phosphotyrosine content in comparison to the vector-transfected (V) cells, indicating that the core is effectively downregulated in this system. The relative activities of the wild-type and mutant Abl core proteins are consistent with their intrinsic catalytic activities observed in the *in vitro* kinase assay (Figure 9A). To test whether the increased phosphotyrosine content seen with the ΔNcap-2PE Abl mutant is a consequence of enhanced Abl kinase activity, we introduced a mutation in a catalytic aspartate residue (D382N) that is predicted to render the kinase catalytically inactive [9]. As shown in Figure 9B, we observe a complete loss of phosphotyrosine content in cells expressing this ΔNcap-2PE D382N mutant protein, thus confirming that Abl kinase activity is directly responsible for the observed increase in phosphotyrosine content in HEK 293T cells.

We then proceeded to characterize the enzyme kinetics of the recombinant Abl core proteins using a fluorimetric kinetic kinase assay (ADP Quest, DiscoverRx) [176]. In contrast to the end-point kinase assay described above, the ADP Quest assay can be used to determine the enzymatic rate of reaction by measuring the accumulation of ADP, which results from phosphorylation of a peptide substrate, as a function of time. In addition to the wild-type, A356N, and T315I Abl core proteins, we also determined kinetic constants for the HAL9 Abl core and an Abl kinase domain protein that lacks the SH2 and SH3 regulatory domains [30]. To determine a protein concentration that gives a basal rate of reaction of about 9 pmol ADP produced per minute, we first conducted a kinase titration experiment. Figure 10A shows a representative experiment for the wild-type Abl core kinase at multiple protein concentrations, and the rate of reaction was found to increase with increasing concentrations of the kinase. We

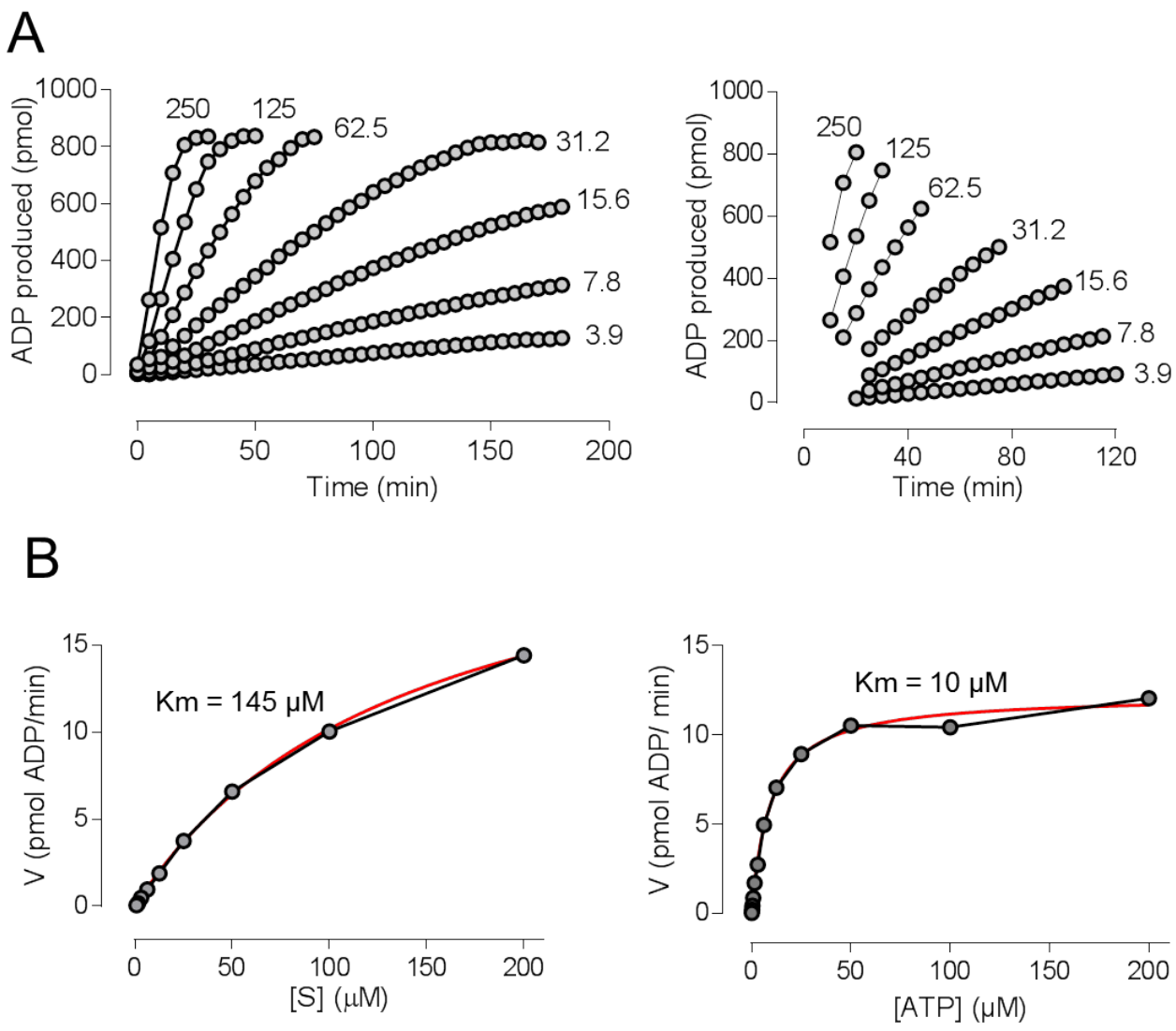

Figure 10. Characterization of wild-type Abl core enzyme kinetics.

A) Left: The time-course of ADP production for seven concentrations of Abl core wild-type was determined at ambient temperature using the ADP Quest kinetic kinase assay as described in the Materials and Methods. A representative experiment is shown. *Right:* The linear portion of each curve was analyzed by linear regression to determine the slope, which is equivalent to the rate of reaction in pmol APD produced/min. B) The rates of reaction for Abl core wild-type were determined at the indicated substrate peptide (*left*) and ATP (*right*) concentrations as described in the Materials and Methods. These rates were plotted as a function of concentration of the peptide substrate (*left*) and ATP (*right*) and exhibit saturation kinetics. The K_m values were determined by fitting these curves to the Michelis-Menten equation using non-linear regression analysis (red lines). The kinetic constants for the mutant Abl core proteins were determined similarly and are presented in Table 1.

observed similar trends for the other Abl proteins as well, and fixed the kinase concentrations to yield a basal rate of 9 pmol ADP produced per minute. We then determined the K_m values for the substrate peptide, EAIYAAPFAKKK, and ATP for each of the Abl kinase proteins. Figure 10B shows a representative experiment for K_m determination for the wild-type Abl core protein for the substrate peptide (left) and ATP (right), and both curves obey Michelis-Menten kinetics. Similar trends were observed for the other Abl kinase proteins as well, and the K_m values for each protein are summarized in Table 1. For the Tyr2 substrate peptide, the K_m values for the active Abl core mutants, A356N and T315I, are about three-fold lower than the wild-type Abl core, suggesting that these mutants have a higher affinity for this peptide substrate. The substrate K_m for the Abl kinase domain protein is about seven-fold lower than the wild-type Abl core, suggesting that the lack of regulatory constraints may make the active site more open to peptide binding. In contrast to these active proteins, the substrate K_m for the HAL9 Abl core protein is similar to the wild-type Abl core. The ATP K_m values are in similar range for the four Abl core proteins, while the Abl kinase domain protein has a four-fold higher K_m than the wild-type Abl core protein. The significance of this higher ATP K_m is also likely to reflect conformational differences in the ATP-binding site result from removal of the regulatory region.

2.4.2 Thermal stability of Abl proteins

We then compared the thermal stability of each recombinant Abl protein using a differential scanning fluorimetry (DSF) assay [182]. Each purified Abl protein was gradually heated in a quantitative PCR instrument in the presence of the reporter dye, SYPRO orange. As the temperature rises and the protein unfolds, the reporter dye gains access to the hydrophobic interior of the protein, resulting in an increase in dye fluorescence. The resulting rise in

Table 1. Kinetic constants for recombinant Abl core proteins.

The K_m values for the Tyr2 peptide substrate and ATP were determined for each Abl core protein using the ADP Quest assay as described under Materials and Methods. All experiments were performed twice, except for the wild-type Abl core, for which peptide substrate experiments were performed four times, and ATP experiments were performed three times. The table shows the mean K_m values $\pm$ S.E.

Abl Protein	Substrate Peptide K_m (μM)	ATP K_m (μM)
WT	144.6 $\pm$ 1.6	9.8 $\pm$ 0.1
A356N	49.1 $\pm$ 1.7	19.4 $\pm$ 0.3
T315I	42.2 $\pm$ 3.0	11.0 $\pm$ 1.4
HAL9	150.2 $\pm$ 5.4	21.2 $\pm$ 1.6
Kinase	20.9 $\pm$ 0.4	36.0 $\pm$ 3.5

fluorescence as a function of temperature eventually reaches a maximum, and the resulting protein 'melt curve' is fit by non-linear regression analysis to obtain a T_m value (temperature at which half-maximal thermal denaturation is observed). Figure 11A shows representative curves from a DSF experiment for the wild-type Abl core as well as the ΔNcap-2PE (least stable) and HAL9 Abl core (most stable) proteins. Interestingly, we observed a difference in the baseline fluorescence at 25 °C for the three proteins. The Abl ΔNcap-2PE protein exhibits higher baseline fluorescence in comparison to the wild-type, suggesting that the hydrophobic regions in the Abl ΔNcap-2PE protein are more accessible and it potentially adopts an open conformation. On the

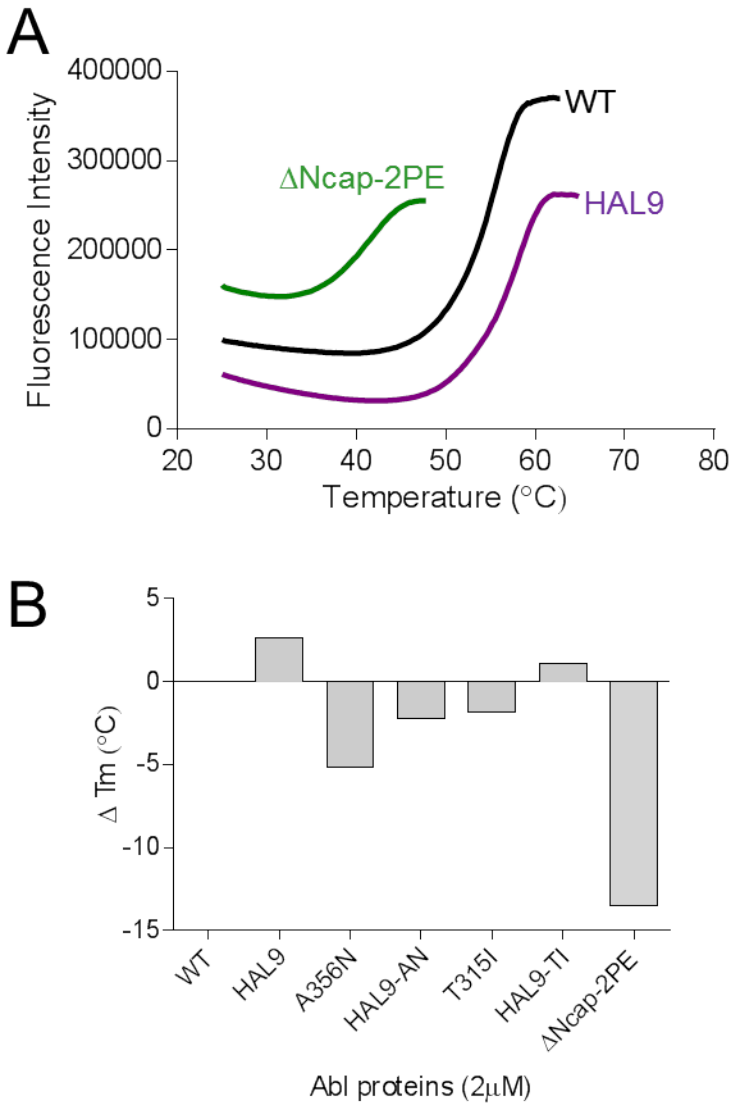

Figure 11. Thermal stability measurements for recombinant Abl proteins.

A) Differential scanning fluorimetry (DSF) assay. DSF was performed on the seven recombinant Abl kinase core proteins as described in Materials and Methods. Background-corrected fluorescence intensities for the wild-type Abl core, HAL9 Abl core, and the ΔNcap-2PE protein are plotted as a function of temperature for a representative assay. Thermal melt temperatures, or temperatures at which half-maximal fluorescence (T_m) was observed, were determined and are presented in Table 2. B) The changes in average melt temperature (ΔT_m) for each Abl protein, with respect to the wild-type Abl core as a reference, are presented here and in Table 2.

other hand, the lower baseline fluorescence observed with the Abl core HAL protein suggests that the hydrophobic regions in this protein are less accessible and it potentially adopts a relatively compact conformation. The thermal melt temperatures (T_m) for each protein were determined, and are summarized in Table 2. Additionally, we calculated the change in thermal melt temperature (ΔT_m) for each of these proteins with the wild-type Abl core protein as a reference. As shown in Figure 11B and Table 2, the T_m values for the wild-type (assembled) core and the fully disrupted ΔNcap-2PE mutant varied by more than 13 °C. This large decrease in the T_m of the ΔNcap-2PE mutant relative to WT is consistent with the loss of regulatory constraints and a resulting increase in dynamic behavior. The myristate binding pocket mutant (A356N), on the other hand, showed only a 5 °C reduction in thermal stability relative to wild-type, consistent with the more modest enhancement of kinase activity compared to ΔNcap-2PE. Remarkably, the T315I gatekeeper mutant showed a reduction in T_m of less than 2 °C relative to wild-type, suggesting that this mutant adopts a thermally stable albeit more active conformation. X-ray scattering data presented in the next section support this idea.

As shown in Figures 11A and 11B, the T_m value for the HAL9 Abl core protein is higher by almost 3 °C as compared to the wild-type Abl core. This is consistent with the stabilizing effect of the enhanced SH3:linker interaction on the wild-type Abl core protein, as observed earlier in HXMS studies [30]. In addition to the Abl proteins discussed above, we also tested the thermal stability of proteins that include the high affinity linker in the context of the A356N and T315I mutations, HAL9-AN and HAL9-TI respectively [30]. We observed that the combination of the high affinity linker with the active mutant Abl proteins results in an increase in T_m, suggesting that enhanced SH3:linker interaction leads to stabilization of these mutant proteins.

Table 2. Thermal melt temperatures (T_m) for recombinant Abl core proteins.

The T_m values were determined, for each Abl protein, using the DSF assay as described in the Materials and Methods. The T_m values are presented as mean $\pm$ S.E.M. [n=6 for Abl core WT; n=5 for Abl core HAL9; n=4 for Abl core A356N, T315I and HAL9-AN; and n=2 for Abl core HAL9-TI and ΔNcap-2PE]. The change in the average melt temperature (ΔT_m) was also calculated for each protein with the wild-type Abl core as a reference.

Abl Protein	**Melt Temperature T_m (°C)**	**ΔT_m (°C)**
WT	53.9 $\pm$ 0.2	0
HAL9	56.8 $\pm$ 0.2	2.8
A356N	48.8 $\pm$ 0.2	-5.2
HAL9-AN	51.7 $\pm$ 0.1	-2.2
T315I	52.4 $\pm$ 0.4	-1.5
HAL9-TI	55.0 $\pm$ 0.0	1.1
ΔNcap-2PE	40.4 $\pm$ 0.3	-13.5

These results are consistent with the earlier study where enhanced SH3:linker interaction was found to be dominant over these activating mutations and led to a reduction in their kinase activity in cell culture [30]. X-ray scattering data presented in the next section support these ideas.

2.4.3 X-ray scattering analysis

We next collected small and wide angle X-ray solution scattering data under a consistent set of conditions from each of the Abl core constructs. Calculations of the radii of gyration, R_g, show that the average solution structures of the WT and A356N proteins are the nearest to that expected for a spherical protein, while the R_g from T315I and ΔNcap-2PE correspond to shapes that are significantly more elongated (Table 3). The rank order of R_g for these samples is WT ≈ A356N < T315I << ΔNcap-2PE, which correlates closely with their intrinsic protein tyrosine kinase activity ranking (Figure 9). The smallest values for R_g were obtained for the three constructs that included the high-affinity linker (HAL9) sequence [30], consistent with the role of SH3:linker interaction in stabilizing the assembled structure of the downregulated kinase (Figure 11).

The values of R_g obtained from our experiments also compare favorably with previously published results (using the GNOM program) of R_g = 27.2 Å for the compact, inactive WT form and R_g = 31.7 Å for a structurally undetermined active form that may contain multiple active conformational states [9]. However, our data for the fully extended ΔNcap-2PE construct yielded an R_g = 39.4 Å, which is larger than the R_g value of 34.5 Å obtained for this construct in the previous study. This conformational form consists of a linear array of structural domains and some flexing between domains, perhaps in response to different experimental conditions or the presence of the stabilizing ligand used in this earlier work (and absent here), may account for this difference in R_g.

Table 3. Radii of gyration (R_g) for recombinant Abl core proteins.

Radii of gyration, R_g, were calculated from X-ray scattering curves as reported by the OLIGOMER program [183] and by the GNOM program [180] from the fitting of P(r). Systematic discrepancies were reduced by making comparisons between data sets collected under the same experimental conditions, with the exception of the data set for the ΔNcap-2PE control. The rank order for the R_g obtained with OLIGOMER is consistent with that obtained from GNOM with just one minor inversion that is within the estimated errors of the R_g determinations.

Abl Protein	R_g (Å; OLIGOMER)	R_g (Å; GNOM)
A356N	29.7	27.7
WT	29.7	28.1
T315I	31.5	28.7
ΔNcap-2PE	42.6	39.4
HAL9	26.9	26.8
HAL9 + A356N	27.3	27.1
HAL9 + T315I	28.5	27.1

2.4.4 Shape reconstructions from X-ray solution scattering data

Reconstructions of the molecular envelopes of each Abl structure from solution X-ray scattering were performed using standard methods in order to identify distinct conformational states and to

compare these states with the available Abl crystal structures. Conclusions regarding the relative similarities of the reconstructed molecular envelopes to each other were checked by calculation of overlaps with the SUPCOMB program [181]. Insights regarding the solution structure of each Abl core protein resulting from these reconstructions are summarized below.

Wild-type and A356N myristic acid binding pocket mutant. Reconstructions of the protein shapes from the WT Abl core protein and the A356N myristic acid binding pocket mutant differ only slightly from one another, and also agree quite well with the crystal structure of the inactive conformation (PDB: 2F0O; Figure 12A). Previously reported solution scattering data collected from a WT Abl sample containing a stabilizing ligand also resulted in a shape consistent with this crystal structure [9]. Although the A356N mutation enhances the intrinsic kinase activity of Abl both *in vitro* and in cells (Figure 9) [30], the shape of this reconstruction suggests that this mutation induces an active conformation without movement of the SH2 to the so-called 'top-hat' position, where it engages the kinase domain N-lobe and stabilizes an active conformation of the kinase domain [184]. This conclusion is supported by previous results from hydrogen exchange mass spectrometry, which revealed that an identical A356N Abl core protein shows very little difference in deuterium uptake relative to the wild-type form [30]. These results imply that activation of Abl by displacement of the myristate group from the N-lobe may result in an active state in which the core retains the assembled configuration.

T315I imatinib-resistant gatekeeper mutant. Unlike the A356N mutant, the shape of the T315I reconstruction is markedly different from that of the WT Abl core (Figure 12B). In this case, the reconstructed molecular envelope tends towards a 'squashed pear' form that is poorly fit by the crystal structure of the inactive conformation. Instead, the T315I envelope is better fit by the crystal structure of the disassembled Abl structure (PDB: 1OPL, molecule B [12]), in which

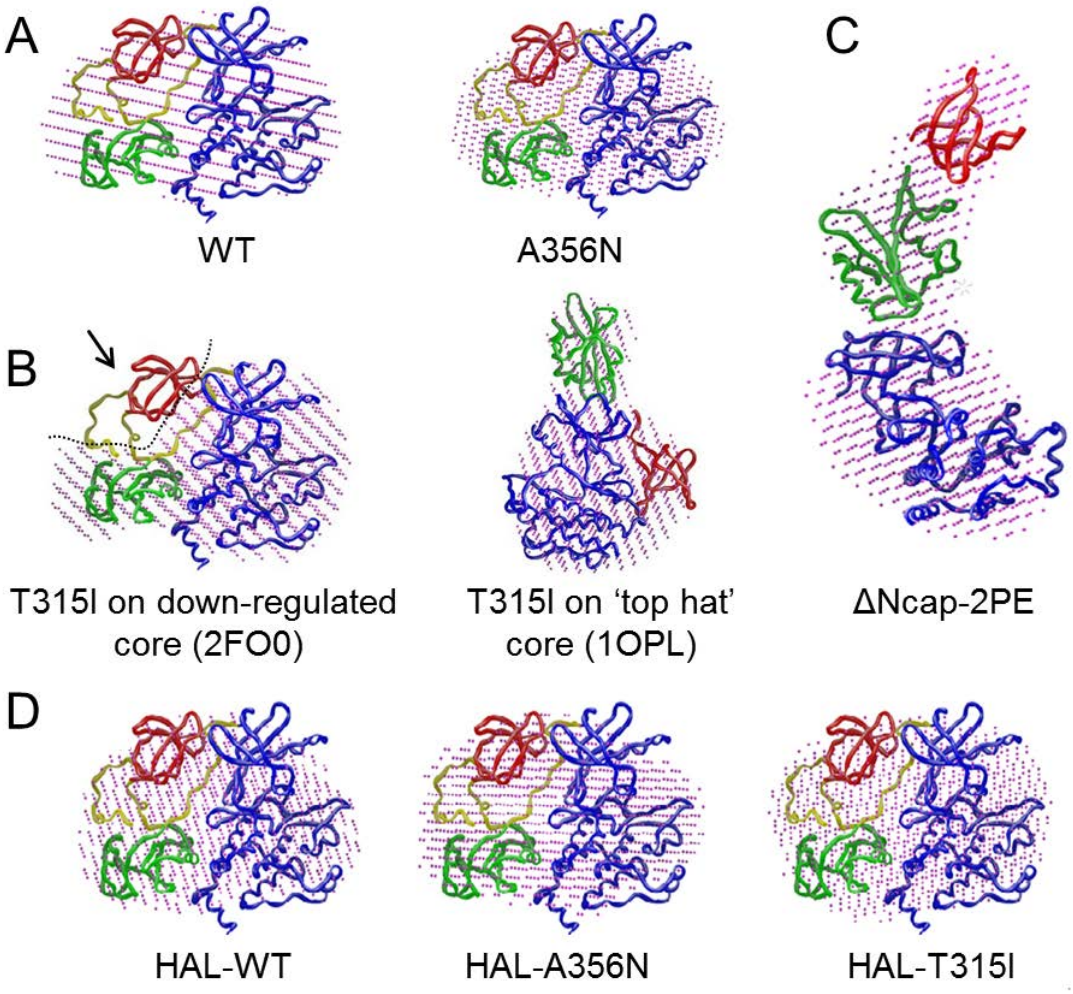

Figure 12. X-ray solution scattering reconstructions of molecular envelopes for Abl constructs and fits by atomic models.

For all models, the purple dots indicate the reconstruction volumes. The backbone chain traces for the kinase, SH2 and SH3 domains are displayed as blue, green and red tubes, respectively. The best overlap between model and reconstruction in all images was obtained using SUPCOMB [21] and the images were rendered with MIFit. (A) Reconstructions for wild-type and A356N mutant Abl core proteins superimposed on the main chain trace from the crystal structure of Abl in the inactive form (PDB ID: 2FO0 [9]). (B) *Left*: Reconstruction of the T315I gatekeeper mutant superimposed on the crystal structure of the assembled Abl core (PDB: 2FO0, [9]). Note that the T315I scattering envelope is fit poorly by the 2FO0 structure, leaving the position of the SH3 domain and N-cap unaccounted for (dotted line and arrow). *Right*: The T315I envelope is superimposed on the extended conformation of an active Abl structure (PDB: 1OPL, molecule B [10]). The SH3 domain was then manually fit in the remaining void adjacent to the kinase domain. (C) Reconstruction for the ΔNcap-2PE construct showing the fit of kinase and SH2 domains from the disassembled crystal structure (PDB ID: 1OPL, molecule B), with the SH3 domain fitted to

the unfilled volume. (D) Scattering envelopes for the high affinity SH2-kinase linker variant of the Abl core protein (HAL9) as well as variants that combine HAL9 with A356N (HAL9 + A356N) and T315I (HAL9 + T315I) Abl core constructs superimposed on the downregulated Abl structure (PDB: 2FO0 [9]). SAXS data and analysis courtesy of John Badger, DeltaG Technologies, and Lee Makowski, Department of Chemistry and Chemical Biology, Northeastern University.

the SH2 domain is juxtaposed to the kinase domain N-lobe. The SH3 domain was not visualized in this crystal structure but if the SH2-kinase linker is refolded, the remaining unfilled space in the envelope can be fit by the SH3 domain. This model strongly suggests that this single drug resistance mutation in the kinase domain has profound allosteric effects on the overall shape of the Abl core. This previously unobserved active state of Abl may contribute to the unique kinetic properties and altered substrate selection profile of the T315I mutation in the context of Bcr-Abl [138]. The model is also consistent with previous hydrogen exchange studies, which revealed subtle increases in SH3 domain deuterium uptake in the T315I mutant compared to WT Abl [46].

Hyperactive ΔNcap-2PE mutant. Analysis of scattering data from the ΔNcap-2PE construct revealed a molecular envelope with a highly elongated appearance, as expected from earlier work [9] (Figure 12C). The prior study modeled the ΔNcap-2PE protein using an Abl conformation based on PDB entry 1OPL (molecule B) for the kinase and SH2 domains, with the SH2 domain in the 'top-hat' configuration next to the kinase domain N-lobe as described above. The SH3 domain was fitted so as to occupy the remaining empty space adjoining the SH2 domain and extending to the full 115 Å length of the molecular envelope. The surface of our reconstruction more clearly defines the separate domains of this extended structural arrangement,

with a narrowing of the protein envelope at the boundaries of the kinase, SH2 and SH3 domains. These results provide an important control for the novel active structures observed with the A356N and T315I Abl cores.

2.4.5 Enhanced SH3-linker interaction reverses the structural changes induced by the T315I mutation

Recent work from our laboratory has shown that the strength of intramolecular SH3 domain interaction with the SH2-kinase linker has a dominant effect on Abl kinase activity and Bcr-Abl kinase inhibitor sensitivity [30]. This study reported a series of Abl and Bcr-Abl proteins with modified linkers containing extra proline residues to enhance internal SH3 docking. The HAL9 linker, described in the previous section, has five linker proline substitutions that reverse the activating effects of both the A356N and T315I mutations in cell based assays [30]. These observations predicted that X-ray scattering studies of the HAL9 forms of our active Abl mutants would show a return to the assembled inactive state associated with the crystal structure of the wild-type Abl core. To test this idea, we expressed and purified HAL9 versions of the Abl core protein on the WT, A356N and T315I backgrounds. X-ray scattering data were then collected on each of these proteins, and compared to results with the complementary constructs with wild-type linkers.

The shape of the reconstruction from the HAL9 construct that is otherwise wild-type (Figure 12D, left) is completely consistent with the crystal structure of the WT Abl core in the assembled inactive conformation (PDB ID: 2FO0; [9]). This result indicates that the introduction of five additional linker prolines enhances SH3 engagement without distorting the overall shape of the downregulated molecule. The shape of the reconstruction from the WT sample (Figure

12A) lies somewhere in between the shapes of the HAL9 (Figure 12D, left) and T315I (Figure 12B) structures, suggesting that in solution the WT form is poised between inactive and active conformational states. Intensity data and the resulting reconstruction of the HAL9 variant of the A356N protein (Figure 12D, middle) are also indistinguishable from those obtained for the HAL9 construct with a wild-type kinase domain. This observation is fully consistent with previous hydrogen exchange data showing that subtle dynamic changes resulting from the A356N mutation are abolished by incorporation of this high affinity linker sequence [30]. Remarkably, the intensity data and molecular reconstruction from the HAL9 protein incorporating the T315I mutation (Figure 12D, right) are also very similar to those obtained from the control HAL9 construct (Figure 12D, left). This result suggests that enhanced SH3-linker interaction reverses the dramatic structural rearrangement triggered by the T315I mutation (Figure 12B). Similarly, the compact shape of the HAL9 variant of the T315I protein is consistent with the observation that the enhanced activity of the T315I mutant is suppressed in cells when coupled to the HAL9 sequence [30]. The shape reconstructions for the three HAL proteins are also consistent with the radii of gyration, which are all smaller than the value observed for WT Abl (Table 3).

2.4.6 Effect of small molecules on thermal stability of Abl kinase proteins

Ponatinib is an ATP-competitive inhibitor of Abl that was rationally designed to bind to the Abl T315I mutant and inhibit its kinase activity [159]. Ponatinib, like imatinib, also selectively binds the inactive kinase conformation (DFG-out) of the protein. In order to investigate the effect of ponatinib on Abl core protein dynamics, we tested the effect of this drug on the thermal stability of the Abl core proteins. In addition to ponatinib, we tested the effect of two additional small

molecules – imatinib (the first generation ATP-competitive inhibitor) and DPH (a small molecule that activates Abl through the myristic acid binding pocket) on the thermal stability of these proteins [185]. Figure 13A shows representative thermal melt curves of the wild-type Abl core incubated with each of these three small molecules. The presence of imatinib and ponatinib results in a shift of the melt curve to the right, suggesting an increase in the thermal melt temperature (T_m) that correlates with increased protein stability. Moreover, we observed a more robust stabilization with ponatinib, which is consistent with its higher potency in inhibiting the wild-type Abl core. In contrast to the inhibitors, we observed a decrease in the Abl core T_m in the presence of DPH, suggesting that this compound destabilizes Abl as a function of activation. In addition to the wild-type Abl core, we also tested the effects of these small molecules on the mutant Abl core proteins, A356N and T315I, and calculated the change in T_m for each small molecule-protein complex with DMSO as a reference. As shown in Figure 13B, imatinib results in stabilization of both the wild-type and A356N Abl core proteins, but not the Abl T315I protein. This is consistent with the inability of imatinib to bind the T315I Abl mutant because of steric clash and loss of hydrogen bonding [32,33,134]. Moreover, we observe that DPH destabilizes the wild-type and T315I Abl core proteins, but not the A356N protein. Since the Ala356 residue is in the myristic acid binding pocket, this suggests that the mutation to asparagine at this site interferes with DPH binding. Ponatinib binding to Abl core induces a robust increase in protein stability for the three Abl core proteins tested in this study. These results provide important information about the effect of small molecules on Abl core protein stability and present a foundation for future analysis of Abl protein dynamics in the presence of these small molecules.

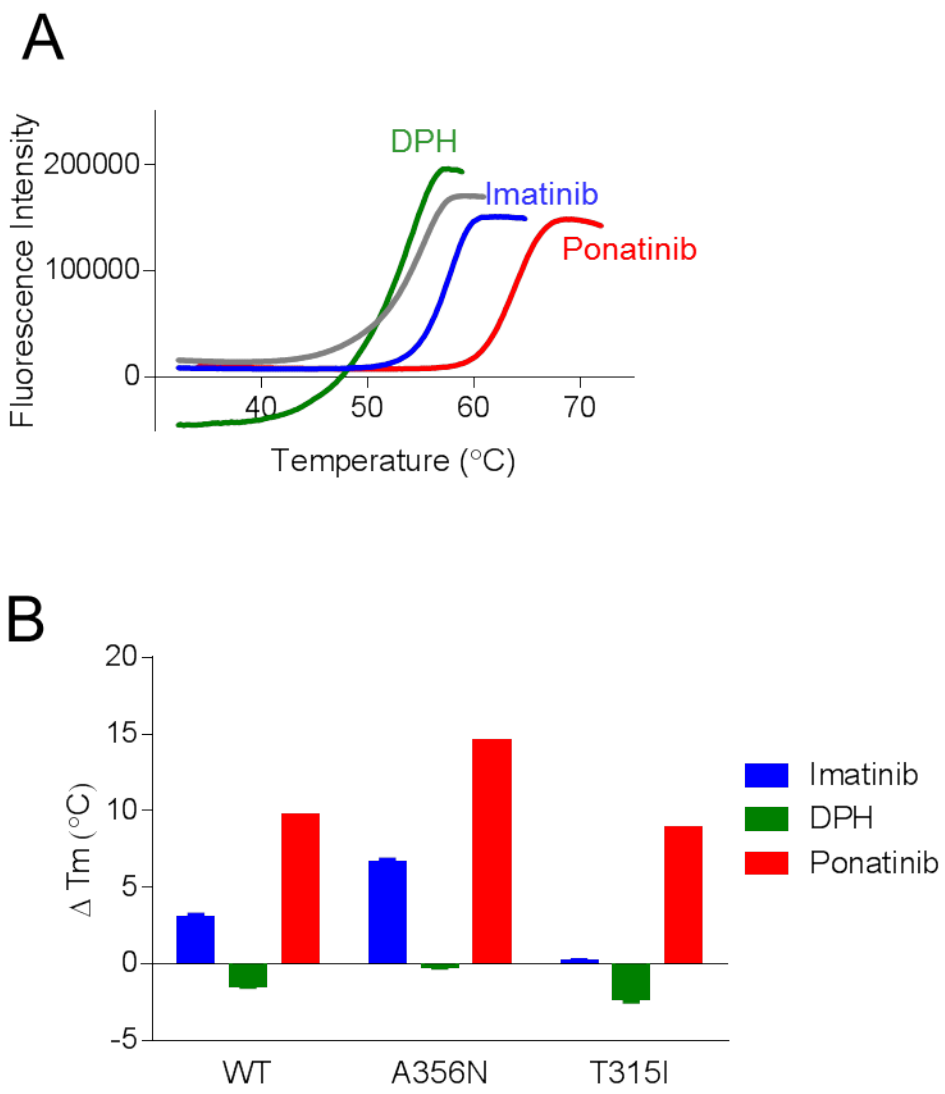

Figure 13. Effects of the Abl kinase inhibitors (imatinib and ponatinib) and activator (DPH) on thermal stability of recombinant Abl proteins.

A) Differential scanning fluorimetry (DSF) assay. DSF was performed on the wild-type Abl core protein in the presence of the indicated compounds as described in Materials and Methods. Background-corrected fluorescence intensities for each inhibitor-treated protein are plotted as a function of temperature in this representative assay. B) The change in melt temperature (ΔT_m) was calculated for the three Abl core proteins in the presence of the indicated compounds, with DMSO as a reference. The changes in melt temperature (ΔT_m) are presented as average values ± SE.

2.5 DISCUSSION

SAXS analyses of the diverse Abl core constructs presented here reveal a set of closely similar structures that differ in subtle yet important ways. Determination of R_g and the shapes of the molecular envelopes show an increase from compact to more elongated forms (Table 3 and Figure 12). The relatively smooth variation of these parameters among the WT, A356N and HAL9 proteins suggests that the differences in observed data correspond not to distinct conformations, but rather to differences in conformational equilibria in which two or more conformations are present in different proportions. As the proportion of the larger component increases, the value of R_g estimated from the X-ray scattering data will increase. Reconstructions of molecular envelopes from ensembles are difficult to anticipate, but can be estimated from data simulations if models of the dominant components are available [186].

Reconstructions of the most compact forms (Figure 12), obtained from constructs incorporating the HAL9 sequence, are all well fit by a crystal structure of the inactive form (PDB ID: 2FO0; [9]). The role of the additional prolines engineered into the linker is to provide additional stability for this structural form compared to WT. We surmise that the set of structural states corresponding to Abl samples containing the HAL9 sequence is highly dominated by this inactive conformation, even when combined with activating mutations at other sites (A356N and T315I). This observation suggests that enhancement of natural SH3:linker interaction with small molecules or antibodies may effectively inhibit these and other mutant forms of c-Abl and Bcr-Abl.

Data from the T315I and ΔNcap-2PE proteins are not consistent with a gradual change in conformational equilibria. Data collected from the T315I mutant shows that it exhibits a large and unanticipated departure from the inactive conformation. When calculated with GNOM, the

value of R_g obtained from the T315I data is slightly lower than the published value obtained from an SH2 mutant of a hyperactive form with '*molecular envelopes that resemble Abl*^{activated} (viz. ΔNcap-2PE) *although more compact*' [9]. We interpret this conformational change as due to a rearrangement of the SH2 and SH3 domains. When interpreted on the basis of the alternative Abl conformation identified from protein crystallography (PDB: 1OPL, molecule B), the kinase and SH2 domains fit well into the reconstruction but leave a large unfilled volume adjacent to the kinase domain. The volume of this region is approximately the same as that of the SH3 domain (not visible in the crystal), and we suggest that it identifies the positioning of the SH3 domain within this structure (Figure 12). This model appears feasible relative to the crystal data since, when modeled in this position, the SH3 domain fits in a volume that is not occupied by other domains in the 1OPL crystal cell as suggested previously by Nagar *et al*. [9].

An extended arrangement of kinase, SH2 and SH3 domains has also been reported for a crystal structure of the c-Src kinase that models a possible active state [187]. This c-Src structure is almost the same length as our Abl-T315I reconstruction but fits the contours of the molecular envelope less well than the model based on 1OPL molecule B (data not shown). Nevertheless, the possibility of some conformational flexibility between domains or the mixing of active and inactive populations of T315I might account for this level of misfit so this interpretation cannot be ruled out by the solution scattering data.

The structure of the highly active protein, ΔNcap-2PE, is most divergent from the other structures. The elongated reconstruction derived from the ΔNcap-2PE scattering data is consistent with previous results that associated a highly elongated appearance with this active form of the protein [9], but very different from that of T315I despite the high intrinsic kinase activities of both proteins (Figure 9). Altogether, our results show that the multi-domain Abl

proteins studied here can take on at least three distinct conformations (or families of closely related conformations): a compact conformation (WT, A356N, HAL); a highly elongated, active conformation (ΔNcap-2PE); and a novel, intermediate conformation exhibiting a previously unobserved arrangement of regulatory domains (T315I). Clearly Abl kinases, and by extension other multi-domain kinases including members of the Src and Tec families, likely adopt a wide range of active states in solution. This observation supports a previously unrecognized level of signaling diversity that may be exploitable for therapeutic gain.

Our results show that the small molecule ATP-competitive inhibitors, imatinib and ponatinib, stabilize the Abl core proteins by DSF assay. This is in contrast to a recent study where imatinib binding to Abl ΔNcap protein resulted in a more open and dynamic conformation with respect to the regulatory SH2 and SH3 domains [51]. This discrepancy could be explained by the difference in the proteins used for the two studies. While our study examined the effect of compounds on Abl core proteins that include the myristoylated N-cap, the study by Skora et al. [51] examined effect of imatinib on an Abl protein that lacks the N-cap and myristoylation signal. Based on our results in the thermal melt assay, it would be interesting to examine the solution structure of the myristoylated Abl core proteins in the presence of these small molecules using SAXS. X-ray scattering analysis of a complex of Abl core T315I and ponatinib could provide valuable insight into the relative orientation of the regulatory domains, and help understand the effect of ponatinib on Abl core conformational dynamics. In particular, it would be very interesting to determine whether the addition of panatinib is sufficient to restore the positions of the Ncap, SH3 and SH2 domains to those observed in the assembled, downregulated state.

3.0 FLUORESCENCE POLARIZATION SCREENING ASSAYS FOR SMALL MOLECULE ALLOSTERIC MODULATORS OF C-ABL KINASE FUNCTION*

3.1 SUMMARY

The c-Abl protein-tyrosine kinase regulates intracellular signaling pathways controlling diverse cellular processes and contributes to several forms of cancer. The kinase activity of Abl is repressed by intramolecular interactions involving its regulatory Ncap, SH3 and SH2 domains. Small molecules that allosterically regulate Abl kinase activity through its non-catalytic domains may represent selective probes of Abl function. Here we report a screening assay for chemical modulators of Abl kinase activity that either disrupt or stabilize the regulatory interaction of the SH3 domain with the SH2-kinase linker. This fluorescence polarization (FP) assay is based on a purified recombinant Abl protein consisting of the N-cap, SH3 and SH2 domains plus the SH2-kinase linker (N32L protein) and a short fluorescein-labeled probe peptide that binds to the SH3 domain. In assay development experiments, we found that the probe peptide binds to the recombinant Abl N32L protein *in vitro*, producing a robust FP signal that can be competed with an excess of unlabeled peptide. The FP signal is not observed with control N32L proteins bearing either an inactivating mutation of a conserved tryptophan residue in the SH3 domain or enhanced SH3:linker interaction. Pilot screens were performed with an FDA-approved compound library and the NCI Diversity Set III, and twenty-three compounds were identified that significantly

reduced the FP signal in comparison to the untreated controls. Secondary assays showed that one of these hit compounds, the antithrombotic drug dipyridamole, enhances Abl kinase activity *in vitro* to a greater extent than the previously described Abl agonist, DPH. Docking studies predicted that this compound binds to a pocket formed at the interface of the SH3 domain and the linker, suggesting that it activates Abl by disrupting this regulatory interaction. These results show that screening assays based on the non-catalytic domains of Abl can identify allosteric small molecule regulators of kinase function, providing a new approach to selective drug discovery for this important kinase system.

*Mass Spectrometric analysis was performed by Roxana Iacob and John Engen, Department of Chemistry and Chemical Biology, Northeastern University. Surface plasmon resonance data were collected and analyzed by Haibin Shi, Department of Microbiology and Molecular Genetics, University of Pittsburgh. Molecular dynamic simulation and docking studies were performed by Matthew Baumgartner and Carlos Camacho, Department of Computational and Systems Biology, University of Pittsburgh.

3.2 INTRODUCTION

The c-Abl protein-tyrosine kinase plays diverse roles in the regulation of cell proliferation, survival, adhesion, migration and the genotoxic stress response [7,8,188]. Abl kinase activity is perhaps best known in the context of Bcr-Abl, the translocation gene product responsible for chronic myelogenous leukemia (CML) and some forms of acute lymphocytic leukemia

[174,175]. The clinical management of CML has been revolutionized by selective ATP-competitive inhibitors of Bcr-Abl, of which imatinib is the prototype [131]. However, chronic use of kinase inhibitors often leads to drug resistance due to selection for mutations that disrupt drug binding or allosterically influence the conformation of the drug binding pocket [120].

The growing problem of imatininb resistance in Bcr-Abl has fueled efforts to identify compounds that work outside of the kinase active site. Such compounds offer advantages in terms of enhanced specificity, because they have the potential to exploit non-conserved regulatory features unique to c-Abl that persist in Bcr-Abl as well [30]. The kinase activity of Abl is tightly regulated *in vivo* by an auto-inhibitory mechanism. The Abl 'core' region, which includes a myristoylated N-terminal 'cap' (N-cap), SH3 and SH2 domains, an SH2-kinase linker and the kinase domain, is both necessary and sufficient for Abl auto-inhibition [13]. Subsequent X-ray crystal structures of the Abl core revealed three critical intramolecular interactions that regulate kinase activity [9,12,14] (Figure 14A and B). First, the SH2-kinase linker forms a polyproline type II helix that binds to the SH3 domain, forming an interface between the SH3 domain and the N-lobe of the kinase domain. Second, the SH2 domain interacts with the back of the kinase domain C-lobe through an extensive network of hydrogen bonds. Aromatic interactions between the side chains of SH2 Tyr158 and kinase domain Tyr361 also help to stabilize this interaction (see Panjarian et al. for an explanation of the Abl amino acid numbering scheme [189]). Finally, the myristoylated N-cap binds a deep hydrophobic pocket in the C-lobe of the kinase domain, clamping the SH3 and SH2 domains against the back of the kinase domain. Small molecules that occupy the myristic acid binding site in the C-lobe of the kinase domain have proven to be effective allosteric inhibitors of Bcr-Abl function [55,163].

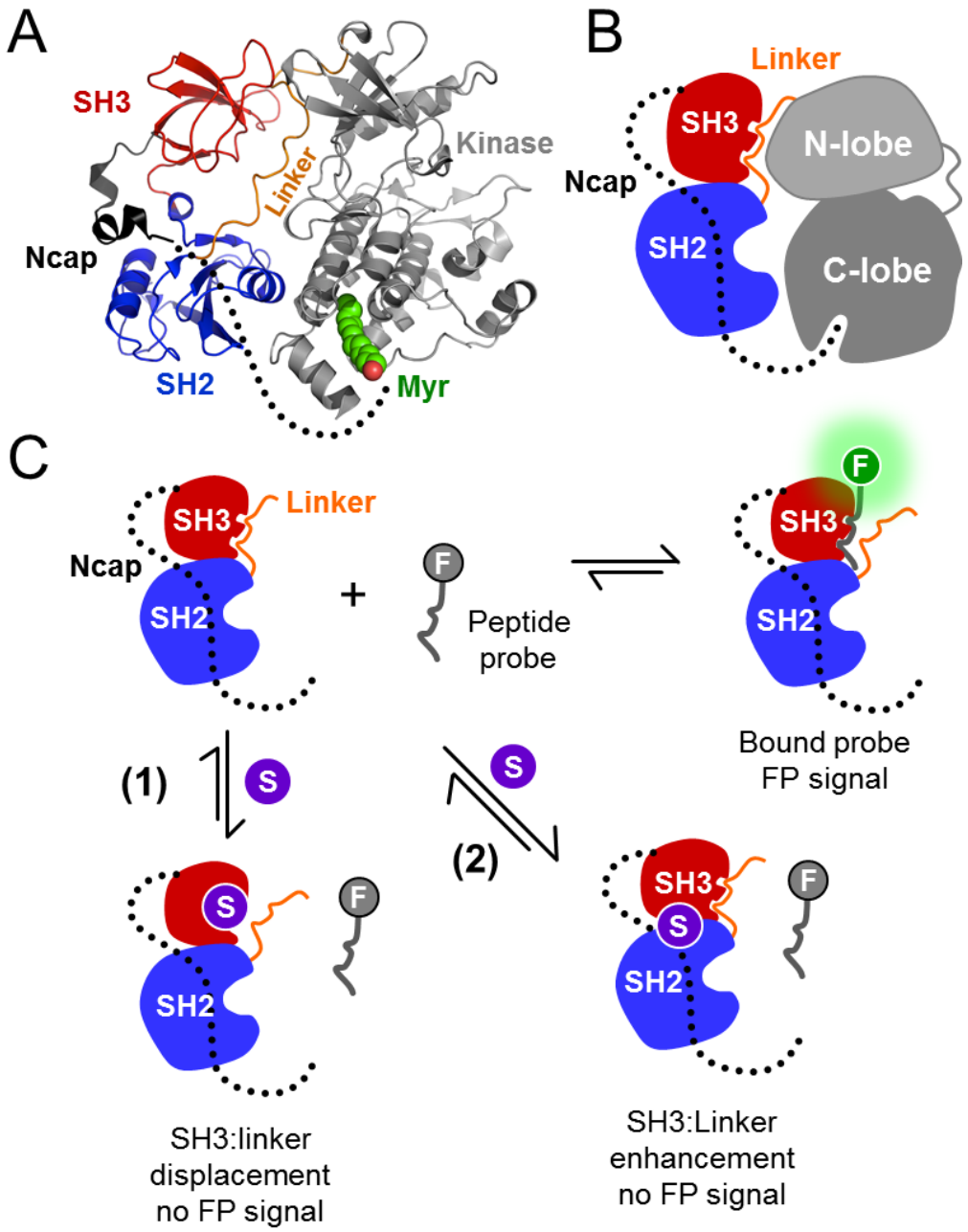

Figure 14. FP assay for small molecule modulators of Abl kinase function.

A) Crystal structure of the auto-inhibited Abl core (PDB: 2FO0, [9]). Key features include the N-cap, SH3 and SH2 domains, the SH2-kinase linker, and the kinase domain. The disordered portion of the N-cap is indicated by the dotted line. The N-terminal portion of the N-cap is myristoylated and engages a deep pocket in the kinase domain. B) Cartoon depiction of the intramolecular interactions regulating assembly of the downregulated Abl core. Note that the linker forms a polyproline helix that binds in cis to the SH3 domain. C) Fluorescence polarization (FP) assay. The FP assay combines a recombinant Abl Ncap-SH3-SH2-linker (N32L) protein and an SH3-binding

peptide probe labeled with a fluorescent moiety (F). The probe peptide binds the SH3 domain in the Abl N32L protein, resulting in an FP signal. Small molecules (S) may bind to the SH3 domain and block probe peptide binding directly; such molecules would be expected to disrupt SH3:linker interaction (case 1). Alternatively, small molecules may stabilize SH3:linker interaction, making the SH3 domain inaccessible to the probe peptide (case 2). In either case, small molecule binding is predicted to result in a loss of the FP signal.

Mutational analysis demonstrates that intramolecular SH3:linker interaction plays a central role in Abl auto-inhibition. Substitution of linker proline residues at positions 242 and 249 with glutamate disrupts SH3:linker interaction, resulting in Abl kinase activation [23]. In contrast, increasing the proline content of the linker enhances internal SH3 binding and overcomes the activating effects of mutations in the myristic acid binding pocket as well as the kinase domain gatekeeper residue (Thr315) [30]. Remarkably, enhanced SH3:linker interaction also dramatically sensitizes Bcr-Abl-transformed cells to inhibition by both imatinib and the allosteric inhibitor, GNF-2, which binds to the myristic acid binding pocket [30]. These findings suggest that small molecules enhancing or disrupting this natural regulatory mechanism may represent selective allosteric modulators of Abl kinase activity.

In contrast to the tremendous research efforts invested in discovering inhibitors for Abl kinase activity, few studies have explored the discovery of small molecules that activate Abl. Selective agonists may represent useful probes to examine the role of Abl kinase activity in normal cellular functions, such as DNA-damage repair pathways. Abl is activated in response to multiple forms of genotoxic stress and interacts with modulators of both DNA-damage induced apoptosis (e.g. p73) and DNA repair (e.g. Rad51), resulting in cell death or survival depending on the cellular environment [188]. Pharmacological activation of Abl may enhance the efficacy

of radiation therapy or genotoxic drugs by enhancing tumor cell death. Moreover, recent studies have shown that Abl inhibits the growth of breast cancer xenografts and promotes the phenotypic reversion of invasive breast cancer cells, suggesting that Abl agonists may have utility in combating cancer spread [165,173]. Clearly, selective and potent agonists are required to test the viability of Abl as a therapeutic target.

In this study, we report the development and validation of a high-throughput screening assay for the identification of small molecules that interact directly with the non-catalytic region of the Abl core. Our assay is based on the interaction of a fluorescent probe peptide with the SH3 domain in the context of a recombinant protein encompassing the regulatory region of the Abl core (Ncap-SH3-SH2-linker; referred to hereafter as the Abl 'N32L' protein). Interaction of the probe peptide with the Abl N32L protein results in fluorescence polarization, providing a convenient assay for SH3 occupancy in a format compatible with high-throughput chemical library screening. In theory, small molecules that bind to the SH3 domain and disrupt probe binding may also disrupt SH3:linker interaction in the context of Abl, resulting in kinase activation. On the other hand, compounds that enhance internal SH3 binding to the natural linker may represent allosteric inhibitors. Using this FP approach, we screened two small libraries – an FDA-approved compound library of 1200 compounds and a diversity set of 1600 compounds. One hit compound specifically inhibited the FP signal from the complex of the Abl N32L protein with the probe peptide, suggesting that it may interfere with SH3:linker interaction. This compound, a substituted pyrimido-pyrimidine known as dipyridamole, was confirmed to bind directly to the Abl N32L protein using both differential scanning fluorimetry and surface plasmon resonance. Dipyridamole was found to enhance the activity of a recombinant downregulated Abl core protein, but had no effect on an Abl core with engineered

high-affinity SH3:linker interaction. These observations suggest that dipyridamole binds to the Abl SH3 domain, resulting in linker displacement and kinase activation. This conclusion is supported by computational docking and molecular dynamics simulations, which predict a binding site for the compound at the SH3:linker interface and subsequent displacement of the linker. Our findings provide an important proof-of-concept that small molecules perturbing c-Abl SH3:linker interaction may allosterically influence Abl kinase activity, and provide a simple yet powerful assay method for their discovery.

3.3 MATERIALS AND METHODS

3.3.1 Expression and purification of recombinant Abl proteins

The coding sequence for the Abl Ncap-SH3-SH2-linker region (N32L; corresponding to residues 2-255 with an internal deletion of residues 15-56; numbering based on the crystal structure of the human c-Abl core; PDB: 2FO0 [9]) was amplified by PCR and subcloned into the bacterial expression vector, pET21a (EMD Millipore). A similar construct was prepared using the sequence of Abl with a high-affinity linker ('HAL9') substitution as described previously [30]. One glycine and six histidine residues (GHHHHHH) were introduced at the N-terminus of the coding sequence of these proteins during sub-cloning. An inactivating mutation of the SH3 domain (W118A) was introduced by site-directed mutagenesis using the QuikChange II method (Stratagene) and the pET21a-Abl N32L WT plasmid as a template. The Abl N32L proteins were expressed in *E.coli* strain Rosetta2(DE3)pLysS (EMD Millipore) and purified using immobilized

metal affinity chromatography. The purified proteins were then dialyzed against 20 mM Tris-HCl (pH 8.3) containing 200 mM NaCl and 1 mM DTT.

The wild-type and high-affinity linker ('HAL9') Abl core proteins (residues 1-531 with an internal deletion of residues 15-56) were expressed in Sf9 insect cells as previously described [30]. The Abl core proteins were purified using a combination of ion-exchange and affinity chromatography and dialyzed against 20 mM Tris-HCl (pH 8.3) containing 100 mM NaCl and 3 mM DTT.

The coding sequence for the Abl kinase domain (corresponding to residues 252-530; numbering according to the crystal structure of the human c-Abl core; PDB: 2FO0 [9]) was PCR amplified and subcloned into the bacterial expression vector pET21a (EMD Millipore). One glycine and six histidine residues (GHHHHHH) were introduced at the N-terminus of the protein during sub-cloning. The Abl kinase protein was expressed in *E.coli* Rosetta 2(DE3)pLysS (EMD Millipore) and purified as previously described by Seeliger et al [190]. The molecular weight and purity of all recombinant Abl proteins was confirmed by SDS-PAGE.

3.3.2 Peptide synthesis

Abl SH3 domain-binding peptides p41, p40, p8, and 3BP-1 [191,192] were synthesized by the University of Pittsburgh Genomics and Proteomics Core Laboratories. For the FP assay, the peptides were labeled with 6-carboxyfluorescein at their N-termini. Molecular weight and purity of all peptides were verified by mass spectrometry. Stock solutions (10 mM) were prepared in a 1:1 mixture of DMSO and FP assay buffer (20 mM Tris-HCl, pH 8.3) for labeled peptides and neat FP assay buffer for unlabeled peptides. Peptide stock solutions were stored at -20°C.

3.3.3 Fluorescence polarization assay

Fluorescence Polarization (FP) experiments were performed in quadruplicate in low volume black 384 well plates with a non-binding surface (Corning; catalog # 3676). Peptides and proteins were added to each well in FP assay buffer (20 mM Tris-HCl, pH 8.3) for a final assay volume of 20 μL and mixed by shaking for 5 min at ambient temperature. The FP signal in millipolarization (mP) units was measured at an excitation wavelength of 485 nM and emission wavelength of 515 nM in a SpectraMax M5 microplate reader (Molecular Devices) using the Softmax Pro software (version 5.4.1). Each plate was read three times and the values were averaged prior to analysis. Raw fluorescence intensity was also read at the same wavelengths for each assay.

3.3.4 Chemical library screening

Pilot screens with the FP assay were performed with two small molecule libraries. A library of 1200 FDA-approved small molecules was purchased from Prestwick Chemical, Inc. The Diversity Set III, a collection of 1597 compounds with chemically diverse scaffolds, was obtained from the Developmental Therapeutics Program, National Cancer Institute, National Institute of Health. Each library compound was screened at 10 μM and a final DMSO concentration of 1%. Compounds were added to 384-well assay plates first, followed by a pre-mixed complex of the Abl N32L protein (25 μg) and the p41 probe peptide (50 nM). Each plate also contained twenty-eight wells of the wild-type N32L protein plus p41 probe and DMSO as positive controls as well as twenty-eight wells of mutant Abl N32L-W118A protein plus p41 probe peptide and DMSO as negative controls. Each plate was mixed on the shaker for 5 min,

read three consecutive times, and the average FP signal for each well was calculated. To identify potential hit compounds, three measures were used: (i) average FP signal; (ii) control normalized percent inhibition, in which the FP signal with each compound was normalized to the mean FP signal of the positive and negative plate controls according to the formula: [(sample FP – mean FP_{WT}) / (mean FP_{W118A} – mean FP_{WT}) x 100] [193,194]; (iii) Z score, a statistical measure of variation of the mean sample FP signal that is independent of plate controls, calculated according to the formula: [(sample FP – mean $FP_{samples}$) / standard $deviation_{samples}$] [193,194]. The compounds were then ranked in order of increasing FP signal, decreasing control normalized percent inhibition, and increasing Z score. Potential hit compounds were then retested in quadruplicate using the FP assay under screening assay conditions.

3.3.5 Differential Scanning Fluorimetry (DSF)

Hit compounds (100 μM) were pre-incubated with the Abl N32L WT protein (1 μM) for 30 minutes in bicine assay buffer (10 mM bicine, 150 mM NaCl, pH 8.0). SYPRO Orange (Sigma) was added at 5X final concentration and fluorimetry profiles were acquired with a StepOnePlus real-time quantitative PCR instrument (Applied Biosystems) and software (version 2.3). Assays were performed in duplicate in sealed MicroAmp Fast 96-well qPCR plates (Applied Biosystems), and control reactions without proteins were included to correct for background fluorescence. Assays were equilibrated at 25 °C for 2 minutes, followed by an increase in temperature at the rate of 1% (1.6 °C/min) to 99 °C, with continuous data collection. Mean fluorescence intensities, after subtracting background fluorescence, were plotted against temperature. Non-linear regression analysis using the Boltzmann sigmoid function in GraphPad

Prism 6 was used to determine the T_m values, the midpoint of the melt curve between the minimum and maximum fluorescence intensities.

3.3.6 Surface Plasmon Resonance (SPR)

SPR analysis was performed on a BIAcore T100 instrument (GE Healthcare) using four-channel CM5 biosensor chips at 25 ºC. Recombinant purified Abl proteins were covalently attached to the CM5 chip via standard amine coupling chemistry [195,196]. Compounds 142 (dipyridamole; Prestwick Chemical) and 4B7 (NSC 288387; Fisher BioServices) were prepared in 20 mM Tris-HCl, pH 8.3, 150 mM NaCl and 0.1% DMSO and flowed past the immobilized Abl protein channel and a reference channel on the biosensor at a flow rate of 50 µL/min for 3 min over a range of concentrations. The initial binding reaction was followed by dissociation for 5 min, and the chip surface was regenerated using 20 mM Tris-HCl, pH 8.3, 150 mM NaCl, 0.1% DMSO, 0.05% Tween 20 and 1 mM DTT at a flow rate of 50 µL/min for 10 min. Sensorgrams were recorded in triplicate, corrected for buffer effects, and fitted with the 1:1 Langmuir binding model using the BIAevaluation software suite version 2.0.4 (GE Healthcare).

3.3.7 Protein kinase assays

The ADP Quest assay (DiscoverRx) [176], which fluorimetrically measures kinase activity as the production of ADP, was used to determine Abl kinase reaction velocities. Assays were performed in quadruplicate in black 384 well plates (Corning #3571) in reaction volumes of 10 µL/well. Recombinant kinase protein concentrations were fixed at 40 ng/well for the wild-type Abl core, 9 ng/well for the high affinity linker core, and 1.4 ng/well for the Abl kinase domain.

The Tyr2 substrate peptide (EAIYAAPFAKKK) was dissolved in the ADP Quest assay buffer (15 mM HEPES, pH 7.4, 20 mM NaCl, 1 mM EGTA, 0.02% Tween-20, 10 mM $MgCl_2$, 0.1 mg/ml bovine γ-globulins), while ATP stocks were prepared in 10 mM Tris-HCl (pH 7.0). The kinase reaction was initiated by the addition of ATP and read at 5 min intervals for 3 h in a SpectraMax M5 Microplate reader (Molecular Devices). To determine the substrate K_m, the ATP concentration was fixed at 50 μM and the substrate peptide was serially diluted from 0.2-200 μM. For ATP K_m determination, the substrate concentration was fixed at the respective substrate K_m for each of the kinases, and the ATP concentration was titrated over the range of 0.2 - 200 μM. The resulting progress curves were analyzed according to the method of Moroco et al. [177]. Briefly, raw fluorescence data were corrected for non-enzymatic ADP production (no kinase or substrate control) and kinase auto-phosphorylation (rate observed in the absence of substrate), and converted to pmol ADP produced using an ADP standard curve generated under the same reaction conditions. The linear portion of each progress curve was fit by regression analysis to determine the reaction velocity. Substrate and ATP K_m values were determined by non-linear regression analysis using the Michaelis-Menten equation (GraphPad Prism 6).

Each kinase protein was pre-incubated with the compounds 142 (10 μM), DPH (10 μM), 4B7 (10 μM) or imatinib (1 μM) for 30 min at ambient temperature. This was followed by the kinase assay with the substrate and ATP concentrations fixed at their respective K_m values. The pmol ADP produced were normalized to the amount of kinase present in each reaction, and plotted against time. The linear portion of each progress curve was then fit by regression analysis to determine the reaction velocity.

Half-maximal effective concentrations (EC_{50}) and activation constants (K_{act}) were determined for the Abl kinase core by both dipyridamole and the known Abl activator, DPH (5-

(1,3-diaryl-1H-pyrazol-4-yl)hydantoin; Sigma-Aldrich) [185]. The kinase was pre-incubated with each compound (10 nM to 100 μM) for 30 min at ambient temperature, followed by kinase assay with the substrate and ATP concentrations fixed at their respective K_m values. The rate of each reaction was plotted against compound concentration, and analyzed by non-linear regression analysis (GraphPad Prism 6) to determine the EC_{50} value. To determine the activation constant K_{act}, the basal rate of kinase activity was subtracted from the rates of reaction in the presence of each compound concentration, and plotted as a function of compound concentration. The resulting curves obeyed saturation kinetics and were best-fit by the following equation [177]:

$$V_a = V_{act} [L] / (K_{act} + [L])$$

where V_a is the reaction velocity in the presence of each activator concentration, V_{act} is the maximal reaction velocity, L is the activator concentration, and K_{act} is the activator concentration that yields half-maximal reaction velocity.

3.3.8 Molecular dynamics

To understand the dynamics of the recombinant N32L protein, for which there is no X-ray crystal structure, we ran unconstrained molecular dynamics (MD) simulations of residues 65-254 of the assembled, downregulated Abl core structure (PDB 2FO0). We disrupted the interaction between linker Pro249 and the SH3 domain by rotating the backbone bonds of linker Gly246. This glycine residue was chosen as a pivot point as it is more flexible and is located between Pro249 and the next strongly interacting residue (Val244) based on the predicted interaction

energy with the SH3 domain [197]. We also ran MD simulations of the (unmodified) isolated SH3 domain (residues 80-145) using the same parameters described below.

MD simulations were conducted with the *pmemd.cuda* [198] module of AMBER14 [199], using the force fields AMBER ff14SB and gaff (general amber force fields) [200]. An octahedral TIP3P water box was constructed with 12 Å from the edge of the box to the solute and the total system charge was neutralized by adding chloride ions. The non-bonded cutoff was specified at 10 Å. In the first energy minimization run, the solute was held fixed and the solvent was relaxed through 500 cycles of steepest descent followed by 500 cycles of conjugate gradient minimization. Subsequently, the system was minimized again with no constraints through 2,000 cycles of steepest descent followed by 3,000 cycles of conjugate gradient minimization. Following the energy minimization, a 50,000 step MD simulation was used to raise the system temperature to 300 K while holding the solute fixed with weak (10.0 kcal/mol) restraints on the solute atoms. The bonds involving hydrogens were held at a fixed length and an integration step of 2 fs was used. This simulation was followed by a second equilibration simulation at constant pressure for 50,000 steps. The final MD simulation of this equilibrated structure was run with no constraints for 100 ns.

3.3.9 Computational docking

The binding mode of hit compound 142 (dipyrimadole) was modeled to snapshots of the N32L and SH3 simulations by molecular docking using the program smina [201] with default docking parameters. The box was defined by the coordinates of linker residues 247-251 plus an outer shell of 8 Å after alignment to the SH3 domain of the crystal structure (PDB 2FO0).

3.4 RESULTS AND DISCUSSION

3.4.1 Abl fluorescence polarization (FP) assay design

In this study, we developed a screening assay for small molecule allosteric modulators of Abl kinase function. Our goal was to enable discovery of chemical scaffolds that interact with the regulatory region of the Abl kinase core, as opposed to the kinase domain, thereby providing a path to enhanced selectivity and allosteric control of kinase function. In addition, we wanted a flexible assay with the potential to identify both inhibitors and activators of Abl function. To accomplish these goals, we developed a fluorescence polarization (FP) assay based on the N-terminal region of Abl consisting of the Ncap, SH3 and SH2 domains, and the SH2-kinase linker (Abl N32L protein). Binding of a fluorescently labeled probe peptide to the SH3 domain (displacing the linker) should result in an increased FP signal due to the slowed rotation of the N32L target protein-peptide complex (Figure 14C). A small molecule that binds to the Abl N32L protein and enhances SH3 interaction with the linker in *cis* is predicted to prevent probe peptide binding, resulting in a decrease in the FP signal. Molecules in this class are predicted to act as allosteric inhibitors of Abl kinase activity, because they may enhance the natural negative regulatory interaction between the SH3 domain and the linker. Alternatively, compounds that interact with the SH3 domain and block probe peptide binding are also predicted to cause a decrease in the FP signal. By displacing SH3:linker interaction in the context of downregulated Abl, compounds of this type may act as allosteric activators of kinase activity. This assay design therefore has the potential to identify both types of Abl-binding compounds in a single chemical library screen. Their impact on Abl function can be easily distinguished in secondary assays for direct binding to the Abl domains, as well as functional assays.

3.4.2 Recombinant Abl regulatory proteins for FP assay development

The target protein for the Abl FP assay consists of the first 255 residues of c-Abl (isoform 1b), and encompasses the Ncap, the SH3 and SH2 domains, as well as the SH2-kinase linker as described above. This Abl N32L protein was expressed in bacteria in soluble form, purified to homogeneity, and its purity and identity were confirmed by SDS-polyacrylamide gel electrophoresis and mass spectrometry, respectively (Figure 15). Previous studies have established that regulatory SH3:linker interaction is maintained in this construct, despite the absence of the kinase domain [30,53]. In addition to the wild-type protein, two mutant forms of N32L were produced for use as controls. The first of these has an alanine substitution for a conserved tryptophan on the SH3 domain binding surface (W118A mutant; see Figure 16 for SH3 domain structure), which renders it unable to bind to the probe peptide and thus serves as a negative control. In the second mutant, five linker residues were replaced with prolines to enhance interaction with the SH3 domain [30]. This high-affinity linker (HAL) substitution suppresses the activating effects of kinase domain mutations and influences the conformation of the kinase domain, enhancing both imatinib and allosteric inhibitor action (discussed earlier in section 1.2.1.4). The HAL protein therefore represents a second negative control for probe peptide binding to the SH3 domain. Both the W118A and HAL forms of the Abl N32L protein were also expressed and purified from bacteria, and yielded soluble purified proteins of the expected mass (Figure 15).

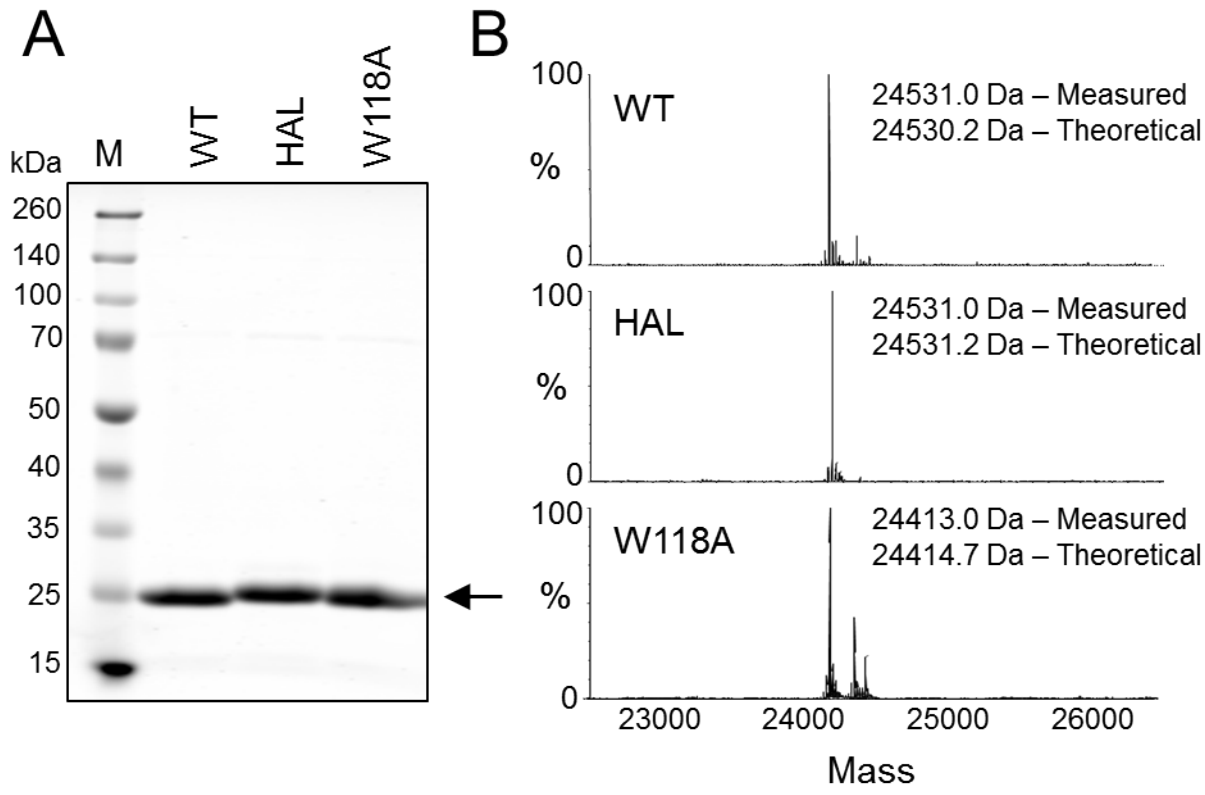

Figure 15. Recombinant Abl Ncap-SH3-SH2-linker (N32L) proteins.

Wild-type Abl-N32L protein and the corresponding high-affinity linker (HAL) and W118A mutants were expressed in *E. coli BL21* Rosetta cells using the pET system and purified by immobilized metal affinity chromatography. Protein purity and mass were verified by SDS polyacrylamide gel electrophoresis (A) and mass spectrometry (B). Mass spectrometry analysis was performed by Roxana Iacob and John Engen, Department of Chemistry and Chemical Biology, Northeastern University.

3.4.3 Structural basis for high affinity probe peptide binding to the Abl SH3 domain

A suitable probe for the Abl N32L FP assay required a short, proline-rich peptide with sequence specificity for the Abl SH3 domain. In addition, the probe peptide needed to bind to the SH3 domain with sufficient affinity to compete for *cis*-interaction of the SH3 domain with the natural linker (Figure 14). A survey of the literature identified four Abl SH3-binding peptides with the potential to serve as probes [191,192]. These peptides, designated p41, p40, p8, and 3BP-1, have K_D values for the Abl SH3 domain in the 0.4 to 34 μM range. The Abl SH3-binding peptide sequences are presented in Figure 16A, and are aligned with those of the wild-type and high-affinity SH2-kinase linkers of Abl.

To explore the potential of known Abl SH3 peptide ligands to compete for natural SH3:linker interaction, we first compared the structure of the Abl SH3:linker interface from the downregulated Abl core (PDB: 2FO0) [9] with the crystal structure of the p41 peptide in complex with the Abl SH3 domain (PDB: 1BBZ) [192]. The C-terminal half of the p41 peptide is comprised exclusively of proline, which facilitates both PPII helix formation as well as tight interaction with the hydrophobic SH3 binding surface (Figure 16B). In contrast, this region of the SH2-kinase linker is comprised of the less favorable SH3-binding sequence, KPTVY (Figure 16C). Specifically, p41 proline residues 9 and 10 fill the hydrophobic groove formed by the aromatic side chains of SH3 tyrosines 89 and 134; the linker is substituted with lysine in this position (Lys241). The main chain carbonyl of p41 Pro8 forms a stabilizing hydrogen bond with Tyr134. This position is substituted with threonine (Thr243) in the linker, which swings away from the SH3 surface. The N-terminal sequence of the p41 peptide forms a network of polar contacts involving SH3 residues Ser94, Asp96, and Trp118. None of these contacts are present

A

Peptide	Orientation	Sequence	SH3 K_D
p41	(C-N)	P^{10} PPPPSYSP^{2} A	1.5 µM
p40	(C-N)	P^{10} PPPPSYTP^{2} A	0.4 µM
p8	(C-N)	P^{10} PAPPPYTP^{2} A	5.0 µM
3BP-1	(C-N)	P^{10} PLPPPMTP^{2} A	34.0 µM
Abl WT linker	(N-C)	-RNK^{241}PTVYGVSP^{249}NYDKWE-	
Abl HAL	(N-C)	-RNP PPPYPPSP NYDKWE-	

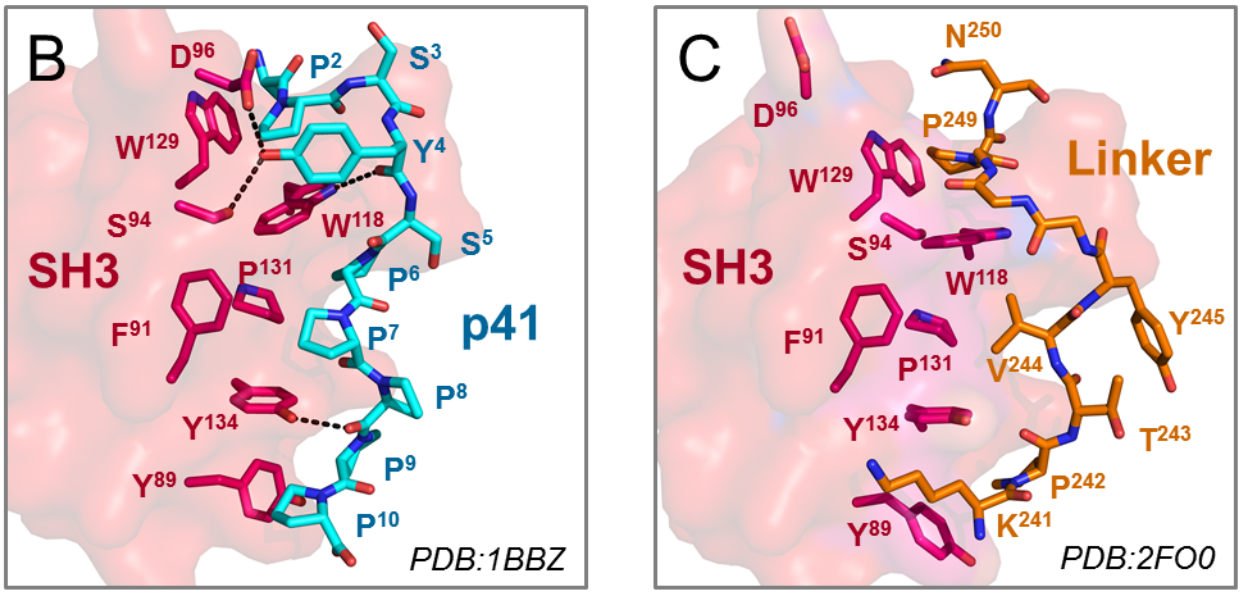

Figure 16. Peptide and linker interactions with the Abl SH3 domain.

A) Sequences of the Abl SH3 binding peptides, p41, p40, p8, and 3BP-1, and their published binding affinities for the Abl SH3 domain [191]. Sequences of the wild-type (WT) and high-affinity (HAL) SH2-kinase linker sequences are also shown at the bottom. The peptide sequences are presented in the C- to N-terminal orientation to align with those of the linkers. B) Crystal structure of the p41 peptide (cyan) bound to the Abl SH3 domain (PDB: 1BBZ) [202]. The SH3 surface is shown as a space filling model (red) and side chains of residues that interact with the p41 peptide are shown as sticks. C) Crystal structure of the SH2-kinase linker (orange) bound to the Abl SH3 domain (red) from the Abl core (PDB: 2FO0, [9]). Side chains of SH3 domain residues that interact with the p41 peptide as per panel B are shown as sticks. Note the lack of hydrophobic interactions and hydrogen bonds between the SH3 domain and the linker in comparison to the p41 peptide.

in the SH3:linker interface, and the side chain of SH3 Asp96 is rotated away from the linker. Taken together, these structural features strongly suggested that p41, or one of the closely related peptides (p40, p8, and 3BP-1), may interact with the Abl N32L target protein with sufficient affinity to displace the wild-type linker and provide a stable FP signal.

3.4.4 Selection of a probe peptide for the Abl N32L FP assay

To evaluate the suitability of the four Abl SH3 peptide ligands (p41, p40, p8, 3BP-1; Figure 16A) as FP probes, each peptide was synthesized and labeled with 6-carboxyfluorescein on its N-terminus. We first examined the baseline FP signal as well as the fluorescence intensity exhibited by each labeled peptide over a broad concentration range (1 - 1,000 nM) in the absence of the Abl N32L target protein. As shown in Figure 17A, probe peptide concentrations greater than 50 nM exhibited stable baseline FP readings with minimal well-to-well variation.

To test for Abl N32L protein interaction with each peptide in the FP assay, we held each probe peptide concentration at 50 nM and added the wild-type N32L protein over a range of concentrations. As shown in Figure 17B, both the p40 and p41 probe peptides produced a strong, saturable FP signal as a function of the N32L protein concentration. The p8 peptide also produced an FP response, albeit somewhat lower than that observed with p40 and p41, while the 3BP-1 peptide was inactive. These FP results correspond to the rank order of binding affinities previously reported for these peptides with the isolated SH3 domain [191,192]. Since the structure of the Abl SH3 domain in complex with p41 is known (Figure 16B), we chose the p41 peptide for FP assay optimization.

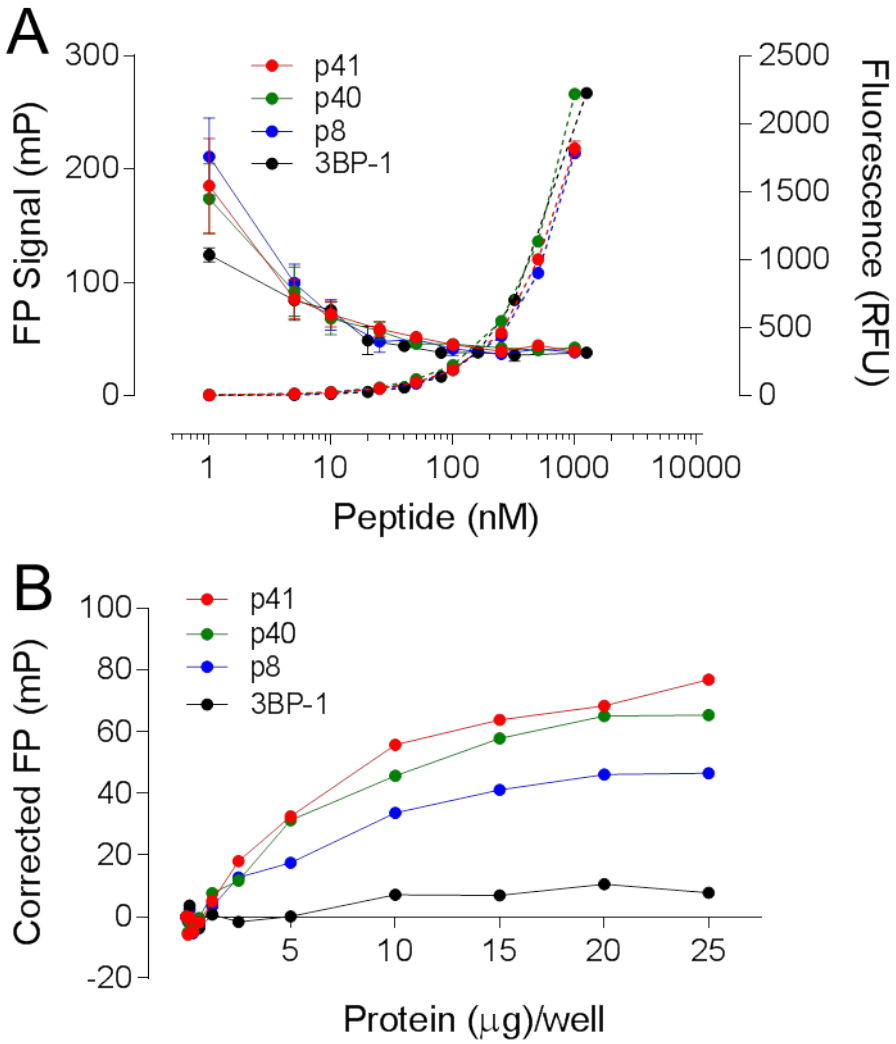

Figure 17. Identification of p41 as optimal probe peptide for the Abl N32L FP assay.

A) To characterize the baseline FP signal, the 6-carboxy-fluorescein labeled probe peptides p41 (red), p40 (green), p8 (blue), and 3BP-1 (black) were serially diluted over the concentration range of 1-1000 nM. The FP signals (solid lines, left Y axis) and corresponding fluorescence intensities (dashed lines, right Y axis) were measured at ambient temperature and plotted as a function of peptide concentration. Average values are shown ± SE from four measurements per condition. B) To test for probe peptide interaction with Abl N32L by FP, each peptide (50 nM) was incubated with the Abl N32L protein over the range of 0.08-25 μg/well. The resulting FP signals were measured at ambient temperature, corrected for baseline FP signal recorded in the absence of the N32L protein, and plotted against the N32L protein concentration. Average FP values are shown ± SE from four measurements per condition; error bars are smaller than the diameter of the data points.

3.4.5 Abl N32L FP assay development and optimization

We next investigated whether the FP signal obtained with the p41 probe peptide was due to interaction with SH3 domain of the recombinant Abl N32L target protein. For these experiments, we compared the FP signal produced from the wild-type Abl N32L protein with the SH3 domain mutant (W118A) as well as the high-affinity linker (HAL) protein. As shown in Figure 18A, the wild-type Abl N32L protein produced a concentration-dependent increase in the FP signal as observed previously. In contrast, the N32L W118A mutant failed to produce an FP signal with the p41 peptide over the same concentration range, indicating that the peptide requires this conserved SH3 domain tryptophan residue for binding as predicted from the crystal structure (see Figure 16). On the other hand, the Abl N32L HAL protein showed a greatly reduced FP signal in comparison to the wild-type protein with the p41 probe. This result is consistent with enhanced *cis*-interaction of the linker with SH3 domain in this protein as a result of the higher linker proline content (see Figure 16A for HAL sequence). Results with these control proteins demonstrate that the p41 probe peptide interacts with the Abl N32L target protein through its SH3 domain. FP experiments with the recombinant purified Abl SH3 domain alone also produced a very similar FP response, supporting this conclusion. Findings with these Abl N32L mutants support the idea that small molecules that disrupt or stabilize intramolecular interaction between the SH3 domain and linker will also reduce probe peptide binding and loss of the FP signal.

We next tested the stability of the FP signal as a function of time (Figure 18B). For this experiment, the p41 probe peptide (50 nM) and Abl N32L protein (12.8 μg/well) concentrations were held constant. Under these conditions, no significant variation in the FP signal was

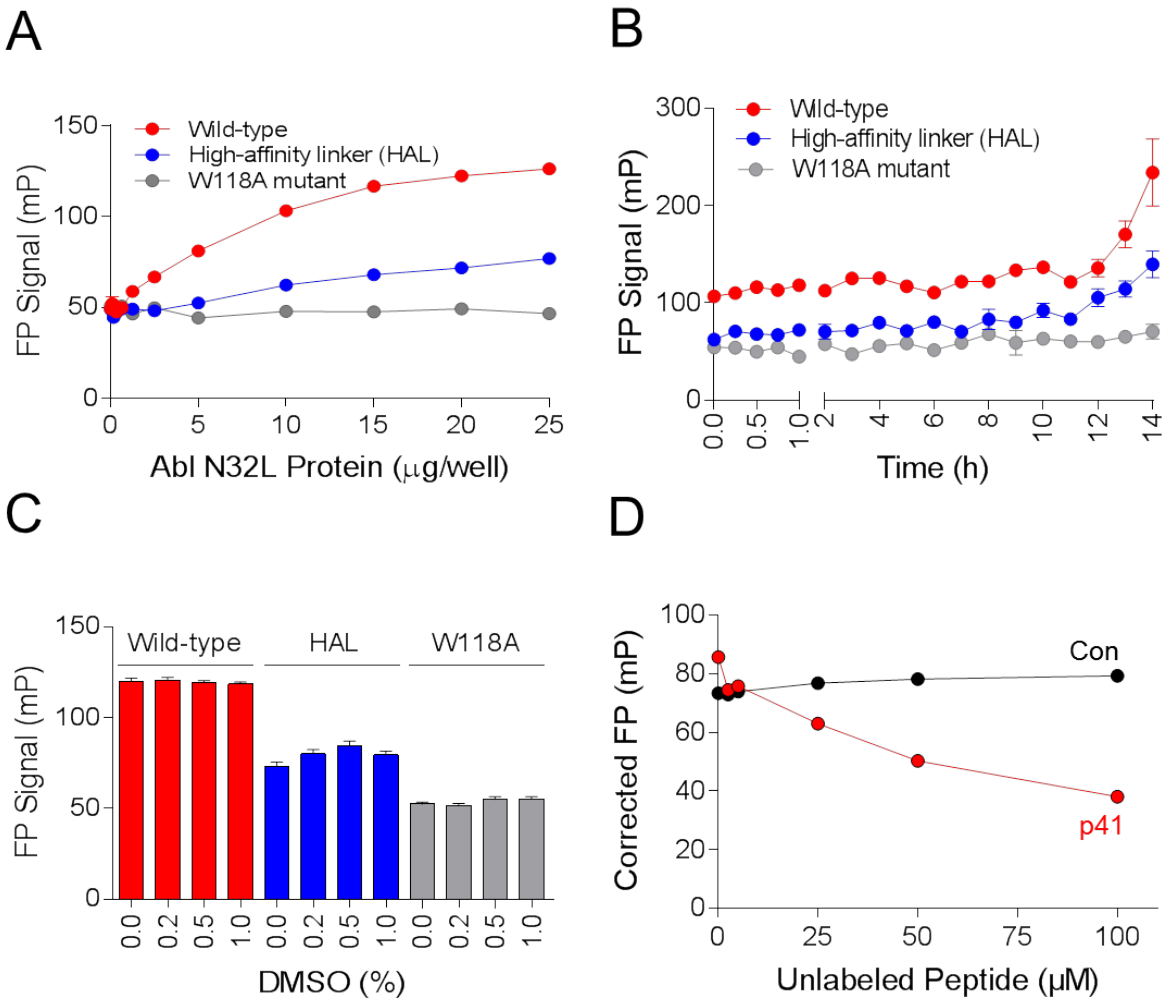

Figure 18. Abl N32L FP assay development and optimization.

A) *The p41 FP probe binds the Abl N32L protein through the SH3 domain.* The p41 probe peptide (50 nM) was combined with wild-type, HAL, and W118A Abl N32L proteins over the range of concentrations shown. The resulting FP signals were measured and plotted as a function of N32L protein concentration. B) *FP assay stability*. The p41 probe peptide (50 nM) was combined with the three Abl N32L proteins (12.8 μg/well) and FP signals were recorded over the time course shown. C) *DMSO tolerance*. FP assays consisting of the p41 probe peptide (50 nM) and each Abl N32L protein (25 μg/well) were incubated with the DMSO concentrations shown, and FP signals were recorded 1 h later. D) *Unlabeled peptide competition*. For the competition assay, the p41 probe peptide (50 nM) was mixed with unlabeled p41 peptide or a negative control peptide (Con) of similar length over the range of concentrations shown. The Abl N32L protein (20 μg/well) was then added, and FP signals were recorded. FP signals were corrected for the background p41 peptide FP signal and plotted as a function of the unlabeled peptide concentration. In all experiments (A through D), FP signal was measured at ambient temperature and average FP values are shown ± SE from four measurements per condition.

observed up to 10 hours. We also found that DMSO, the carrier solvent for the screening library compounds, did not influence the FP signal or the negative controls even at the highest concentration tested (1%; Figure 18C).

In a final validation experiment, we tested the effect of unlabeled p41 peptide on the FP signal (Figure 18D). For this study, we fixed the p41 probe peptide concentration at 50 nM and the wild-type Abl N32L protein concentration at 20 μg/well. Unlabeled p41 peptide was added to the assay over the concentration range of 2.5 to 100 μM. The FP signal decreased as a function of unlabeled p41 peptide concentration, demonstrating competition for the labeled probe peptide binding to the N32L protein. As a negative control, the peptide competition experiment was repeated with a non-specific peptide of similar length. This peptide had no effect on the FP signal, even at a concentration of 100 μM, demonstrating the specificity of p41 peptide recognition by the SH3 domain in the N32L target protein.

3.4.6 Identification of inhibitors of p41 interaction with Abl N32L

To test the performance of the Abl N32L FP assay under screening conditions, we performed pilot screens with two small molecule libraries – a collection of 1200 FDA-approved compounds, and a diversity set consisting of 1600 chemical scaffolds. The wild-type Abl N32L protein (25 μg) was added to each well together with the p41 probe peptide (50 nM). The compounds were then added to a final concentration of 10 μM in 1% DMSO. Each plate contained twenty-eight wells with the wild-type N32L target protein plus DMSO as positive controls, and twenty-eight wells with the non-binding W118A mutant protein plus DMSO as negative controls. The overall Z factors were 0.57 and 0.36 for the FDA-approved library and the diversity set, respectively, indicative of a reliable screening assay [203]. The average FP signals

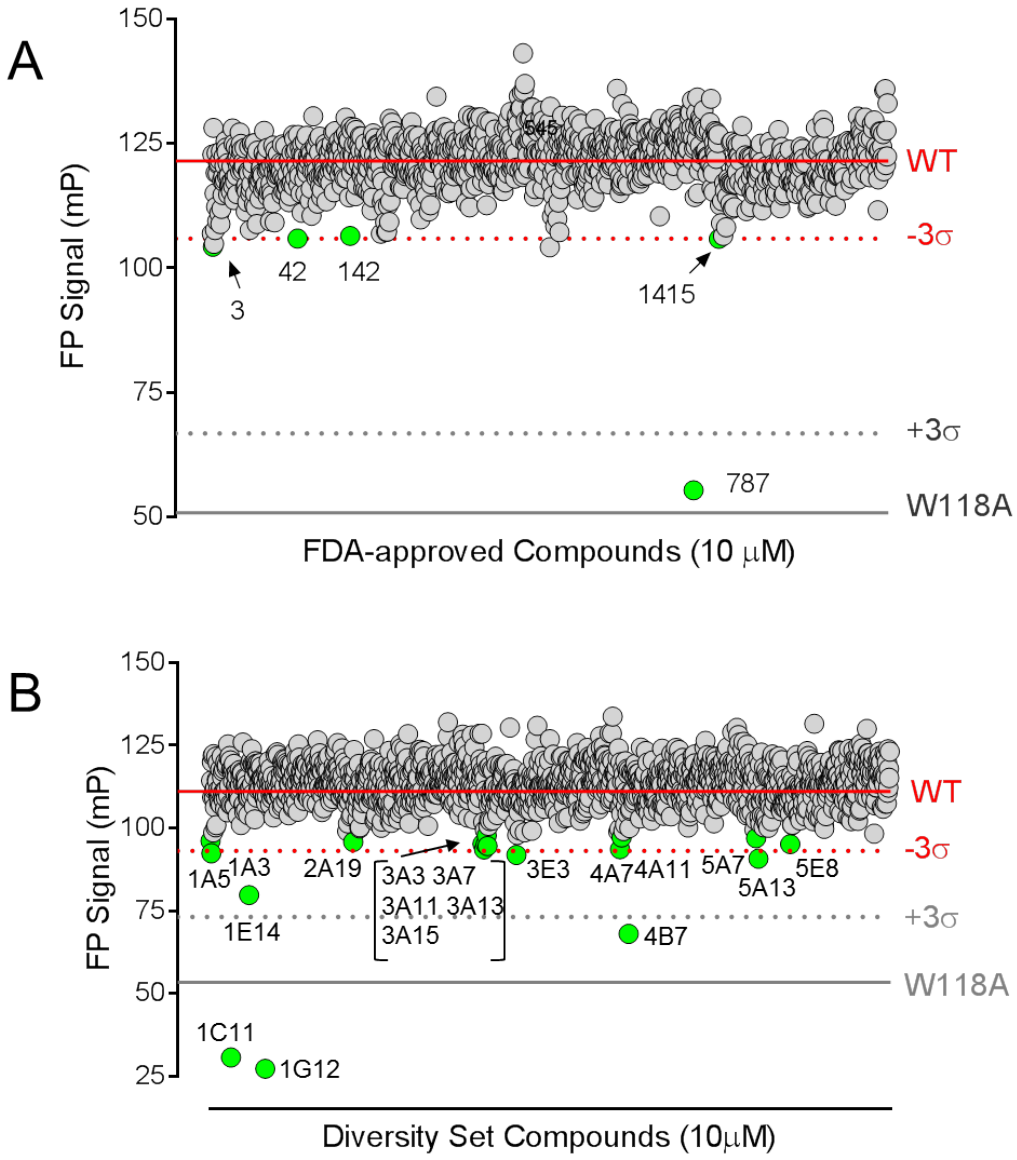

Figure 19. Pilot screens identify inhibitors of p41 interaction with the Abl N32L protein.

Two small molecule libraries were screened using the Abl N32L protein (25 μg/well) and the p41 probe peptide (50 nM) in the FP assay. Screening data from a library of 1200 FDA-approved compounds (A) and a diversity set of 1600 compounds from NCI (B) are shown. For both (A) and (B), the solid lines correspond to the mean FP signals for the wild-type (WT) and negative control (W118A) control N32L proteins across all assay plates, with the dotted lines indicating three standard deviations from the means (± 3σ). Each compound was tested at 10 μM, and each of the resulting 2800 FP signals is represented as an individual circle. Twenty-three putative hit compounds were identified (green circles), five from the FDA-approved compounds library (A) and eighteen from the NCI Diversity Set III (B).

observed with the controls as well as the readings observed with each of the test compounds are presented in Figure 19.

The FP signals for each compound were ranked by three different methods: increasing raw FP signal, decreasing normalized percent inhibition, and increasing Z score (described in section 3.3.4). For each library screen, we then compared the top 1% of compounds present ineach of these three rankings. In the FDA-approved compounds library, five compounds were present in at least two of these rankings, and were selected for follow-up assays (compound numbers 3, 42, 142, 787, and 1415; Figure 19A). From the diversity set, eighteen compounds were identified from at least two of the rankings and selected for follow-up assays (compounds 1A3, 1A5, 1C11, 1E14, 1G12, 2A19, 3A3, 3A7, 3A11, 3A13, 3A15, 3E3, 4A7, 4A11, 4B7, 5A7, 5A13, and 5E8; Figure 19B). These hit compounds are represented as green circles in Figure 19. Each of the raw hit compounds was then retested in multiple wells under screening assay conditions (Figure 20). Out of the five compounds identified from the FDA-approved compounds library, four compounds produced a significant inhibition of the FP signal relative to the DMSO controls (compounds 42, 142, 787, and 1415; Figure 20A). From the diversity set, thirteen out of eighteen compounds significantly inhibited the FP signal in comparison to the DMSO controls (compounds 1A3, 1C11, 1E14, 1G12, 3A3, 3A7, 3A11, 3A15, 4A11, 4B7, 5A7, 5A13, and 5E8; Figure 20B). We then performed control FP experiments with each of these compounds under the same conditions but in the absence of the N32L target protein (Figure 21). This counter-screen showed that compounds 787, 1C11, 1E14, and 1G12 reduced the baseline FP signal produced by the p41 probe peptide by at least three standard deviations from the DMSO control, thus indicating non-specific quenching of the FP signal (Figure 21). These

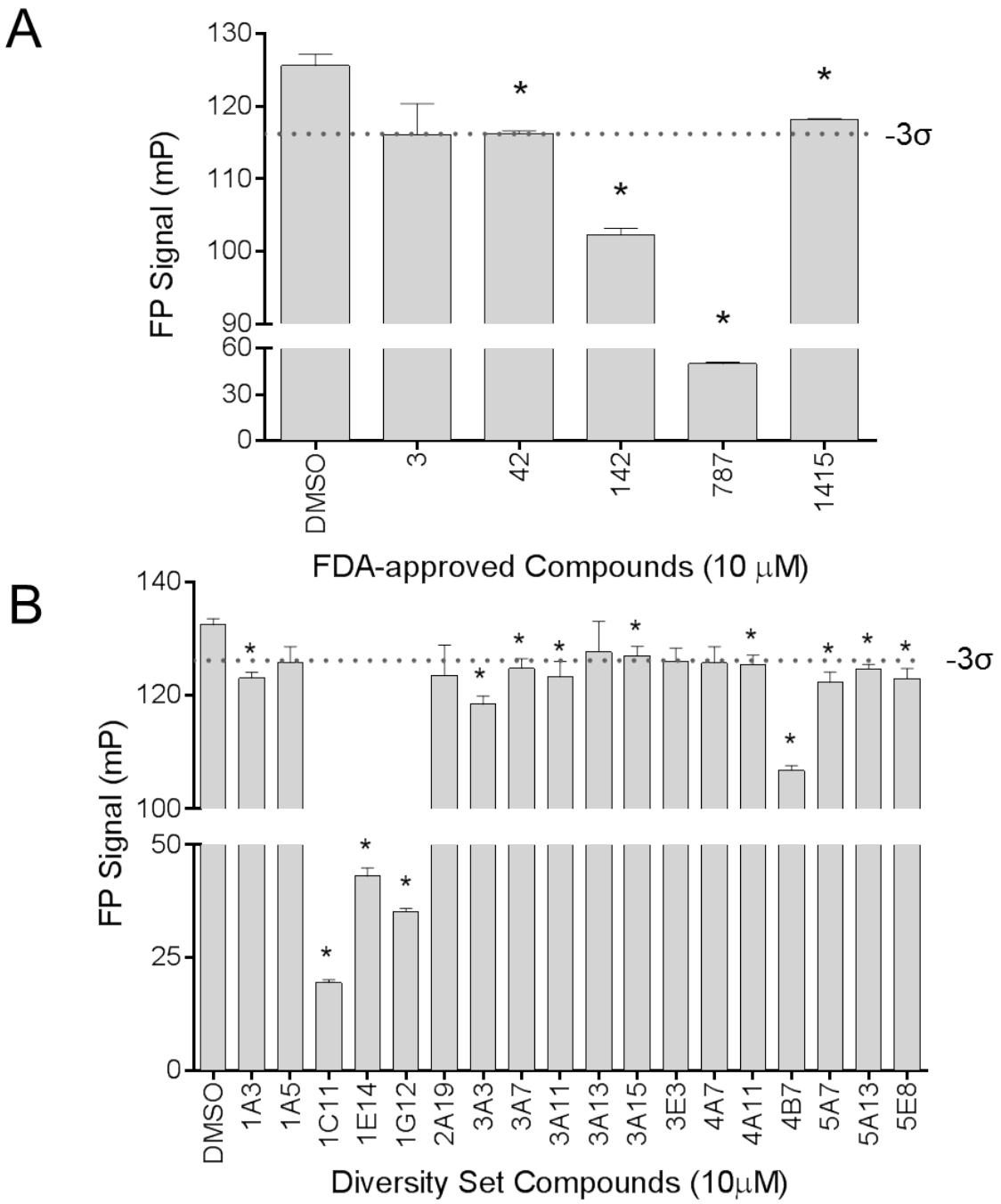

Figure 20. Confirmation of reproducible inhibition of p41 interaction with the Abl N32L protein.

Five potential hit compounds from the FDA-approved compounds library (A), and eighteen hit compounds from the NCI Diversity Set III (B) were re-tested in quadruplicate at 10 μM vs. the DMSO control under FP screening assay conditions, and the mean FP values are shown ± SE. Seventeen of these compounds significantly inhibited the FP signal relative to the DMSO control as indicated by the asterisk ($p < 0.05$; 2-tailed t-test). The dotted line (-3σ) shows FP value three standard deviations below the DMSO control FP signal.

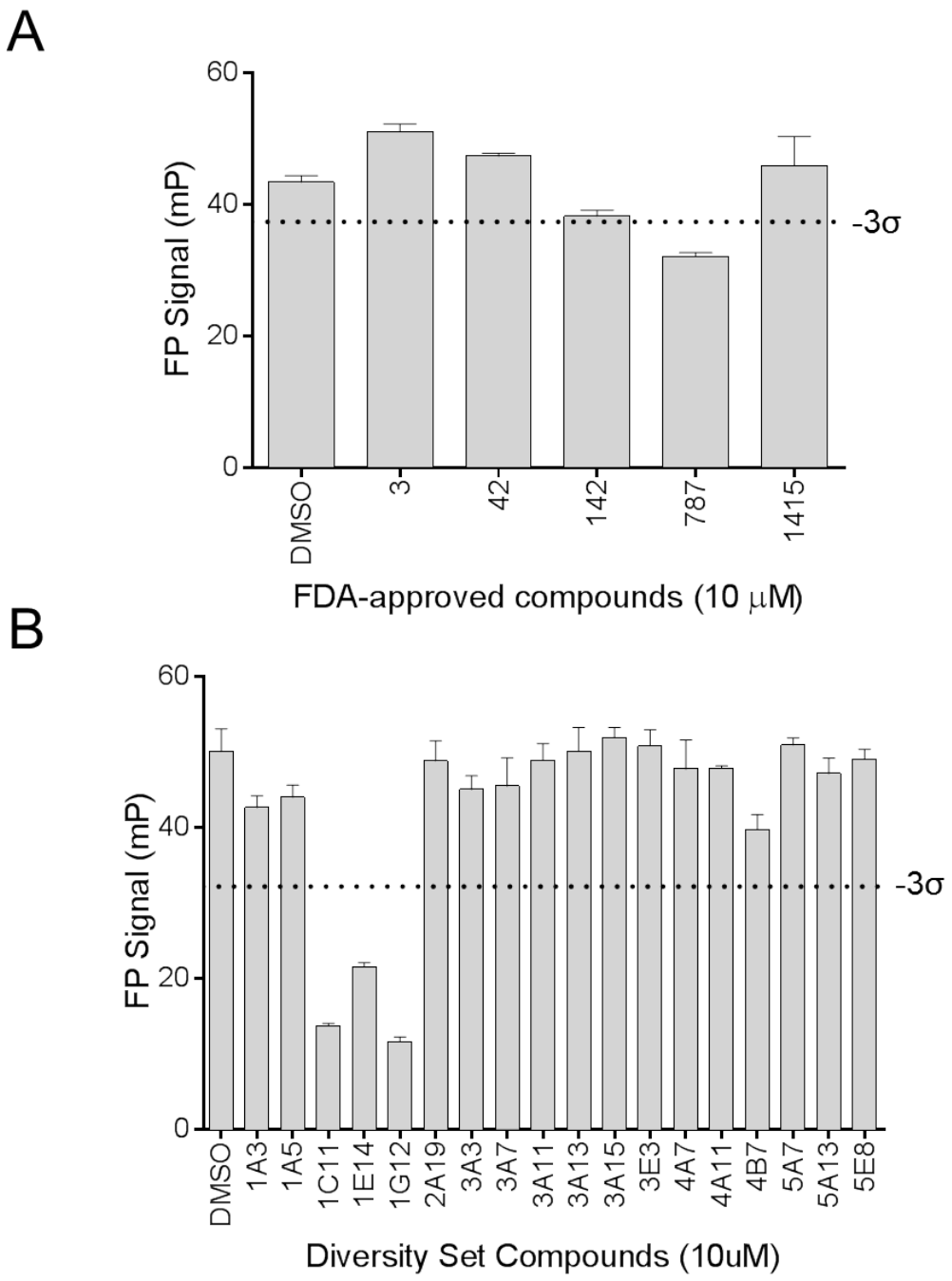

Figure 21. Identification of non-specific inhibitors of p41 FP signal.

Five potential hit compounds from the FDA-approved compounds library (A), and eighteen hit compounds from the NCI Diversity Set III (B) were tested with the p41 peptide in the absence of Abl N32L proteins. These compounds were tested in quadruplicate at 10 μM vs. the DMSO control, and the mean FP values are shown ± SE. The dotted line (-3σ) shows FP value three standard deviations below the DMSO control FP signal. Four of these compounds caused a decrease in FP signal greater than 3σ relative to the DMSO control.

compounds were not considered further. None of the other compounds affected the baseline p41 probe peptide fluorescence, and were therefore moved forward into secondary assays.

3.4.7 Compounds identified in the Abl N32L FP screen interact directly with the Abl N32L protein in orthogonal assays

As an independent measure of hit compound interaction with the Abl N32L target protein, we performed differential scanning fluorimetry assays [182]. For these experiments, the Abl N32L protein was heated with a molar excess of each compound in the presence of the reporter dye, SYPRO orange. As the temperature rises and the N32L protein unfolds, the reporter dye accesses the hydrophobic interior of the protein, resulting in an increase in dye fluorescence. The resulting protein 'melt curve' is then fit by regression analysis to obtain a T_m value, the temperature at which half-maximal thermal denaturation is observed. Small molecule binding to a target protein can either increase or decrease the T_m value, depending upon the effect of the compound on protein stability. Differential scanning fluorimetry was performed with the wild-type N32L protein in the presence of each of the hit compounds from the FP assay, and the change in T_m value (ΔT_m) was determined compared to DMSO as the reference control. As shown in Figure 22A, the three hit compounds from the FDA-approved drugs library resulted in a decrease in the T_m value. Compound 142 had the largest impact on N32L thermal stability, producing a decrease of more than 2 °C in the T_m, consistent with its effect in the FP assay (Figure 20A). Ten compounds from the diversity set were tested in this assay, and three of these led to a decrease of at least 1 °C in the T_m value (3A7, 3A11, and 4B7; Figure 22B). One compound, 3A3, was found to interfere with this assay and the T_m value could not be determined. Since compounds 142 and

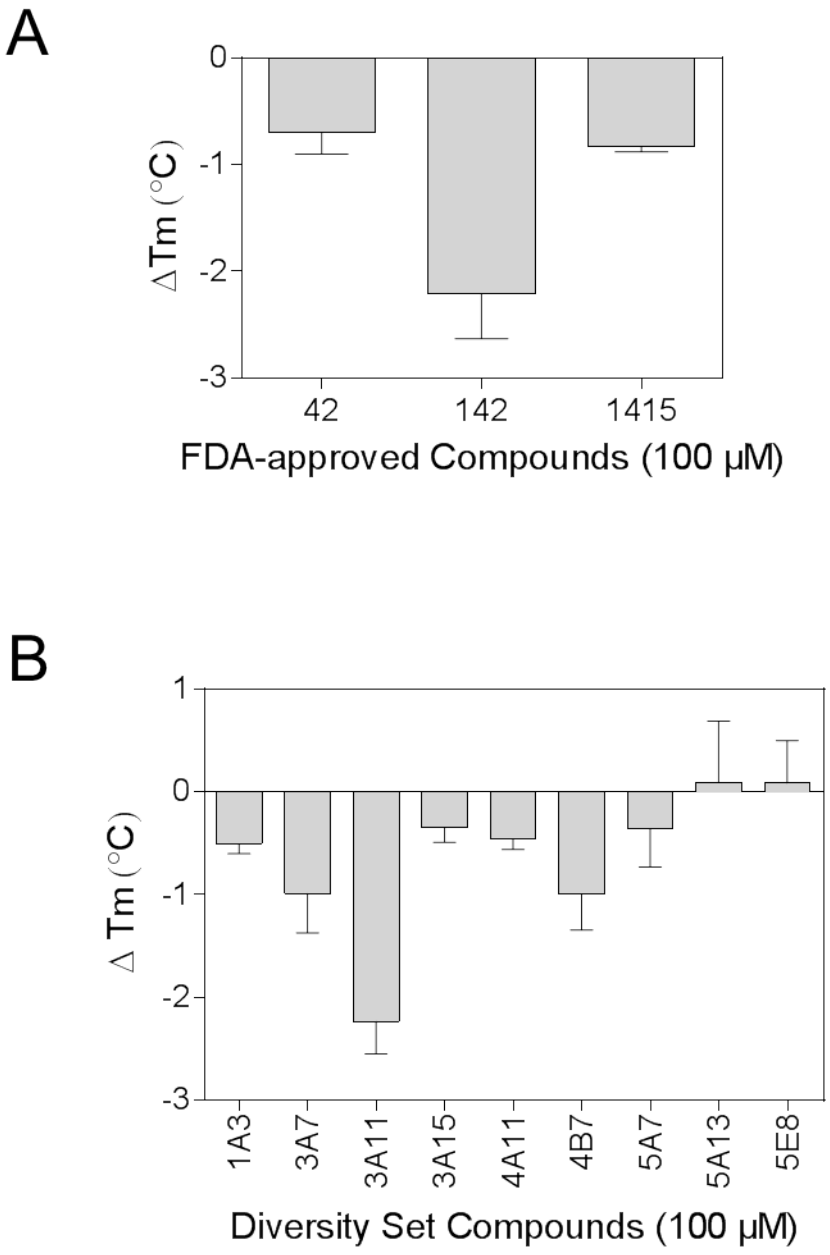

Figure 22. Six hit compounds directly interact with the Abl N32L protein.

Differential scanning fluorimetry assays were performed on the Abl N32L protein in the presence of the thirteen confirmed hit compounds, three from the FDA-approved compounds library (A) and ten from the NCI Diversity Set III (B), as described under Materials and Methods. The average change in the mid-point of the thermal melt profile (ΔT_m) is plotted on the Y-axis ± S.E. (n = 2). One compound from the diversity set, 3A3, interfered with the assay and is not shown here.

4B7 had a robust effect in the FP assay (Figure 20) and exhibited direct interaction with the Abl N32L protein in the DSF assay (Figure 22), we tested the effect of these compounds in the secondary assays discussed below.

Compounds that inhibit the FP signal in the Abl N32L assay may either interfere directly with probe peptide binding to the SH3 domain or allosterically tighten the *cis*-interaction of the SH3 with the linker, indirectly reducing probe peptide interaction. To distinguish between these two possibilities with compounds, we performed FP experiments with the isolated Abl SH3 domain as well. We performed FP assays with the Abl N32L protein as well as the isolated Abl SH3 domain over a range of compound concentrations. As shown in Figure 23, compounds 142 and 4B7 resulted in a concentration-dependent decrease in the FP signal with both the Abl N32L and SH3 proteins, suggesting that both compounds bind directly to the Abl SH3 domain.

To confirm direct interaction of hit compounds with the Abl N32L protein and explore the binding kinetics, we next performed surface plasmon resonance (SPR) assays. For these experiments, the Abl N32L protein was immobilized on the biosensor surface while compounds were flowed past the immobilized protein over a range of concentrations. As shown in Figure 24A, concentration-dependent interaction of compound 142 with Abl N32L was readily detected by this approach, yielding an association rate constant of $3.87 \pm 0.59 \times 10^{3}$ $M^{-1}s^{-1}$ and a dissociation rate constant of $2.70 \pm 0.72 \times 10^{-2}$ s^{-1}. The equilibrium dissociation constant (K_D) for this interaction, calculated as the ratio of k_d/k_a, is $6.90 \pm 0.78 \times 10^{-6}$ M.

We observed that compounds 142 and 4B7 inhibit p41 interaction with the Abl SH3 domain, indicating that they directly interact with the Abl SH3 domain. To confirm this direct interaction, we performed SPR experiments with the isolated Abl SH3 domain as well. In these

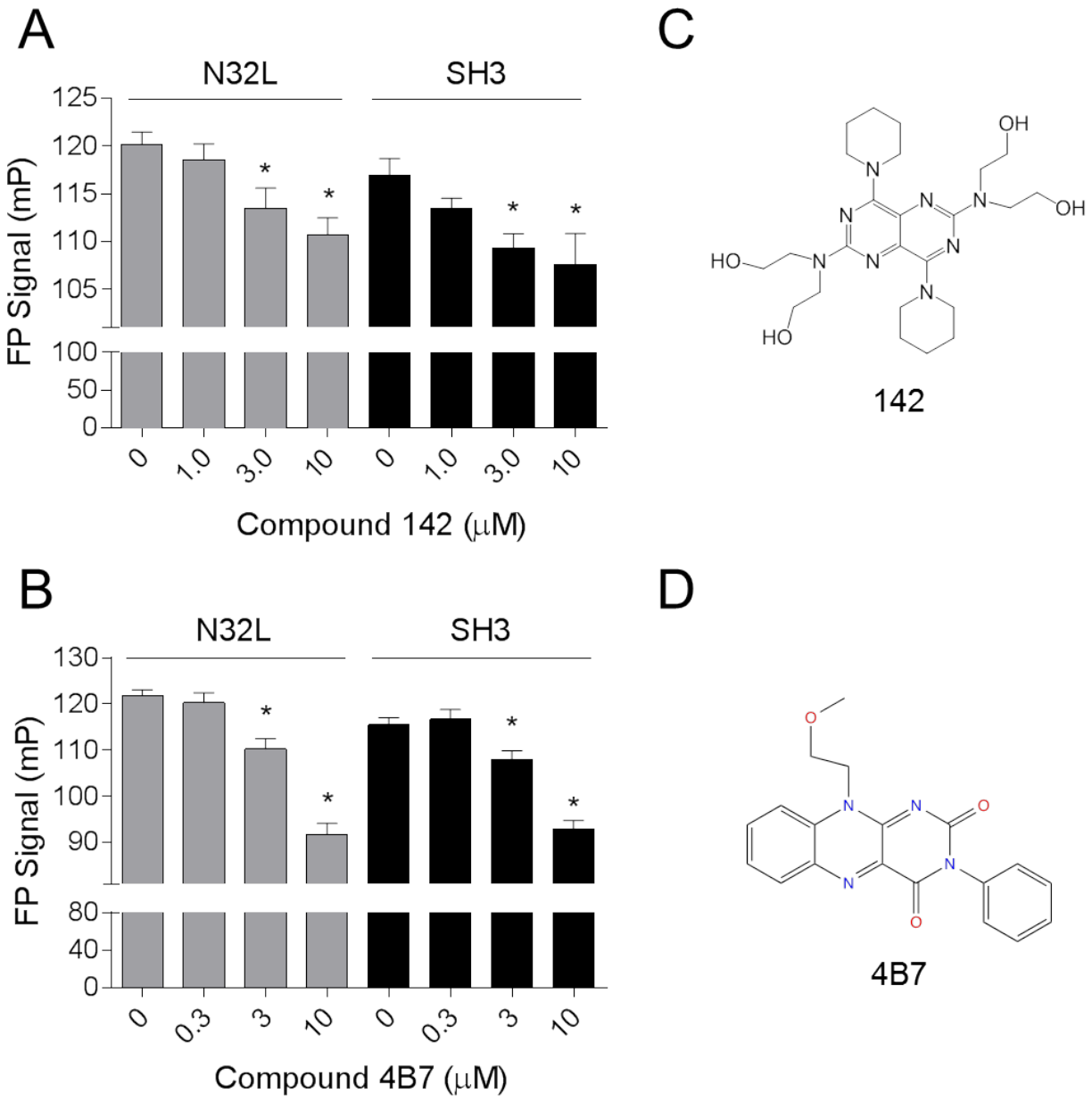

Figure 23. Hit compounds 142 and 4B7 inhibit interaction of p41 peptide with the Abl N32L and Abl SH3 proteins.

Compounds 142 (A) and 4B7 (B) inhibit p41 peptide binding to the Abl N32L and SH3 proteins in the FP assay. Compounds were added to N32L and SH3 FP assays over the range of concentrations shown, and the resulting FP signals are presented as the mean ± S.E. Significant inhibition for both N32L and SH3 was observed at 3 and 10 μM ($p < 0.05$ by 2-tailed t-test; columns marked with an asterisk). C) Chemical structure of compound 142 (dipyridamole). D) Chemical structure of compound 4B7 (10-(2-methoxyethyl)-3-phenyl-Benzo[g]pteridine-2,4(3H,10H)-dione).

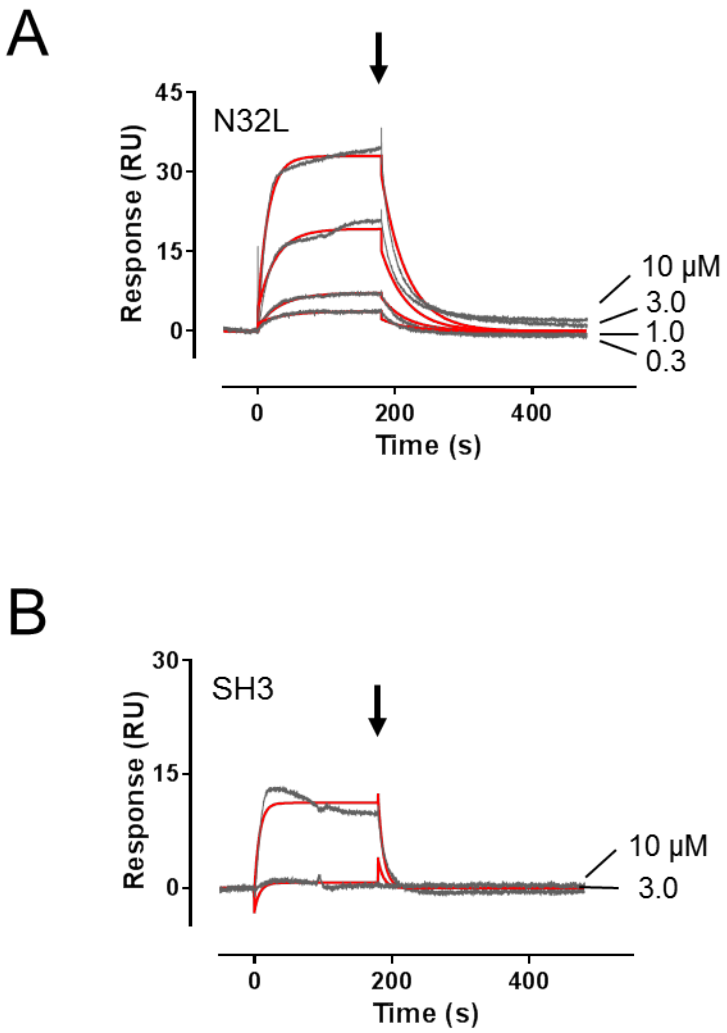

Figure 24. Hit compound 142 interacts directly with the Abl N32L and Abl SH3 proteins.

Surface plasmon resonance (SPR) was performed with the Abl N32L (A) or Abl SH3 (B) proteins immobilized on the biosensor chip and compound 142 as analyte. Responses were recorded for the indicated compound concentrations, and the flow path was switched back to buffer after 180 s to induce dissociation (*arrow*). The resulting sensorgrams (black lines) were fit by a 1:1 Langmuir binding model (red lines) to generate kinetic constants.

SPR experiments were performed and analyzed by Haibin Shi, Smithgall lab, Department of Microbiology and Molecular Genetics, University of Pittsburgh.

experiments, the Abl SH3 protein was immobilized on the biosensor surface while a range of compound concentrations were flowed past the immobilized protein. As shown in Figure 24B, compound 142 interacts with the Abl SH3 protein, albeit only at higher concentrations and the response is weaker in comparison to the Abl N32L protein. The association rate constant for this interaction is $3.83 \pm 0.37 \times 10^{3}$ $M^{-1}s^{-1}$ while the dissociation rate constant is $1.15 \pm 0.18 \times 10^{-1}$ s^{-1}. The equilibrium dissociation constant (K_D) for this interaction is $2.99 \pm 0.40 \times 10^{-5}$ M, which is nearly 5-fold higher than the K_D with the Abl N32L protein. This suggests that the presence of the N-cap, SH2 domain, and the SH2-kinase linker in addition to the SH3 domain enhance the binding of the compound 142.

We also tested binding of compound 4B7 to the Abl N32L and Abl SH3 in SPR assays. Unlike compound 142, we were unable to detect a binding response, suggesting that the change in FP produced by this compound in the screening assay may be due to non-specific adsorption to the Abl N32L protein.

3.4.8 Allosteric activation of Abl kinase by compound 142

Compound 142 reproducibly scored as a hit in the Abl N32L FP assay and demonstrated direct interaction with the Abl N32L protein by both differential scanning fluorimetry and SPR. This compound, a symmetrically substituted pyrimido-pyrimidine known as dipyridamole (Figure 23C), is a selective inhibitor of phosphodiesterase V and also an adenosine transport inhibitor used clinically for its antithrombotic activity [204]. However its potential impact on protein kinase function has not been reported. Because compound 142 interacts with the regulatory region of Abl, we investigated its effects on Abl kinase activity using three purified recombinant forms of Abl in a kinetic kinase assay. The first of these included the wild-type Abl core region,

consisting of the Ncap, the SH3 and SH2 domains, the SH2-kinase linker, and the kinase domain. This Abl protein was produced in Sf9 insect cells, which results in myristoylation of the N-cap and interaction with the C-lobe of the kinase domain, thereby assembling the downregulated state (Figure 14A). In addition to the wild-type core, we also tested a high-affinity linker (HAL) mutant version of the Abl protein, which has a modified proline-rich linker that packs more tightly against the SH3 domain [30]. Additionally, we tested the Abl kinase domain protein, which lacks all the regulatory features present in the Abl core proteins. The structure of each Abl kinase protein is illustrated in Figure 25.

Baseline kinase activities and kinetic parameters of each recombinant Abl kinase protein were determined first using ADP Quest assay, a fluorimetric assay that measures the kinase reaction rate as the generation of ADP [176]. For wild-type Abl, we obtained K_m values of 9.8 ± 0.1 μM and 144.6 ± 1.6 μM for ATP and peptide substrate, respectively. The Abl HAL core yielded a similar K_m value for substrate (150.2 ± 5.4 μM), with a higher value for ATP (21.2 ± 1.6 μM). For the Abl kinase domain, the K_m value for the substrate (20.9 $\pm$ 0.4 μM) is much lower than the wild-type Abl core, while the K_m value for ATP is higher (36.0 $\pm$ 3.5 μM). These observations are consistent with the allosteric effects of the regulatory domains on the conformation of the active site in the kinase domain. In subsequent experiments with compounds, the ATP and peptide substrate concentrations were set to their respective K_m values, and input kinase concentrations were adjusted to yield similar basal reaction rates (7 pmol ADP produced per minute for Abl core proteins, and 2.5 pmol ADP produced per minute for Abl kinase domain).

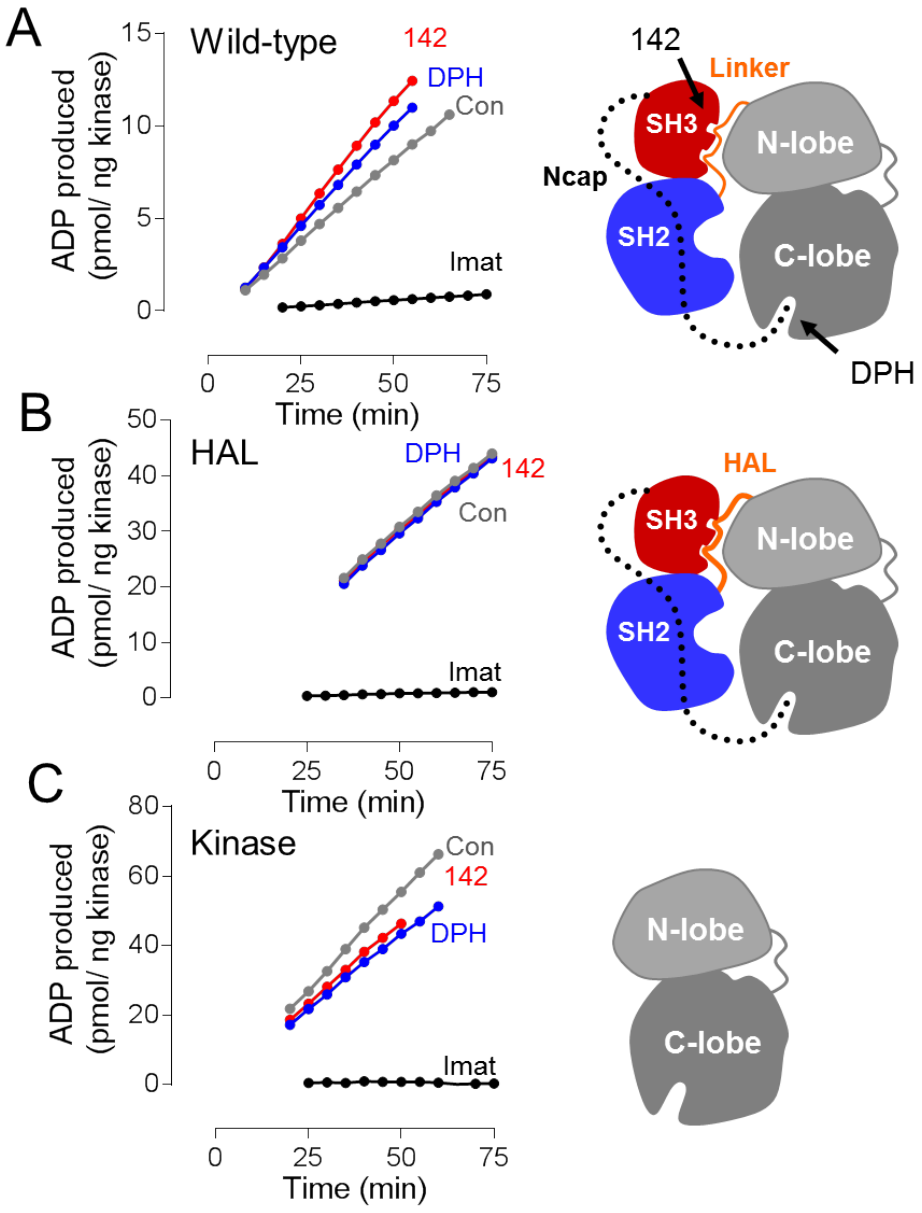

Figure 25. Compound 142 activates the Abl kinase core *in vitro*.

A) The recombinant Abl core protein, consisting of the Ncap, SH3, SH2 and kinase domains, was assayed in the presence of compound 142 (10 µM), the known Abl activator DPH (10 µM), and imatinib (1 µM) or with DMSO as control (Con) using the ADP Quest kinetic kinase assay (see Materials and Methods). Data are plotted as pmol ADP produced per ng kinase as a function of time. The cartoon (right) depicts the domain organization of the wild-type Abl core, and indicates the binding site for DPH (myristic acid binding pocket) as well as the predicted binding site for compound 142 (SH3 domain). B) and C) Kinase assays were performed using a Abl core protein with a high-affinity linker (HAL) (B) or the Abl kinase domain (C) in the presence of the same three compounds; the cartoons indicate the position of the modified linker (HAL) in (B) and the kinase domain in (C).

We first examined the effect of compound 142 on the activity of the wild-type Abl kinase core protein. As shown in Figure 25A, compound 142 stimulated wild-type Abl kinase activity by about 40% at a concentration of 10 μM relative to the DMSO control in this assay. As a positive control, we also assayed Abl core activity in the presence of the same concentration of a previously described Abl activator, DPH, and observed a similar degree of activation. DPH, unlike compound 142, stimulates Abl through the kinase domain via the myristic acid binding pocket in the C-lobe [185].

The mechanism of Abl activation by compound 142 may involve binding to the SH3 domain and subsequent displacement of its regulatory interaction with the SH2-kinase linker. Indeed, mutations that disrupt SH3:linker interaction also have a stimulatory effect on Abl kinase activity (discussed earlier in sections 1.2.1.2 and 1.2.1.4). To test this idea, we next examined the effect of this compound on the Abl core mutant with enhanced SH3:linker interaction. Unlike wild-type Abl, compound 142 did not affect the kinase activity of the Abl core with the HAL substitution (Figure 25B), consistent with the idea that enhanced SH3:linker interaction prevents compound 142 access to the Abl SH3 domain. Interestingly, DPH did not activate the Abl HAL core protein either, consistent with previous results showing that enhanced SH3:linker interaction overcomes Abl core activation by mutations in the myristic-acid binding pocket [30].

Additionally, we examined the effect of compound 142 and DPH on the Abl kinase domain that lacks all of the regulatory domains (Figure 25C). Unlike the wild-type Abl core protein, the reaction velocity of the kinase domain protein was not significantly affected by compound 142. This observation is consistent with the proposed allosteric mechanism of compound 142 acting through the SH3 and linker interface, which is lacking in this construct.

Interestingly, DPH also failed to activate the kinase domain in the absence of the regulatory domains, even though its binding pocket is present in the C-lobe of the kinase domain. This observation suggests that this kinase domain construct is maximally active and therefore no longer susceptible to regulation by compounds that bind through the myristic acid binding pocket.

To further characterize Abl activation by compound 142, we repeated kinetic kinase assays with the wild-type Abl core over a range of compound concentrations. As shown in Figure 26A, compound 142 activates the Abl core in a concentration-dependent manner, with an EC_{50} value of 0.63 ± 0.07 μM. This value compares favorably to that obtained with DPH, the myristic acid binding pocket agonist (EC_{50} = 1.11 ± 0.5 μM). We also calculated the activation constant (K_{act}) for each compound from these data (Figure 26B), which is defined as the concentration at which the reaction rate reaches half-maximum velocity (V_{act}). For compound 142, the K_{act} was calculated as 0.4 ± 0.02 μM, while DPH yielded a value of 1.02 ± 0.07 μM. The extent of Abl activation (V_{max}) by compound 142 was also higher than that for DPH.

Having established the activating effect of compound 142 in *in vitro* kinase assays, we proceeded to test its effect on Abl core kinase activity in cells. For this, we used an experimental system optimized in our lab where the phosphotyrosine content in HEK 293T cells transiently expressing Abl core proteins correlates with the catalytic activity of the Abl proteins [30]. Earlier studies from our lab as well as results shown in section 2.4.1 have shown that expression of the down-regulated wild-type or HAL Abl core proteins results in negligible phosphotyrosine levels (as observed by immunoblotting), while expression of the active Abl mutants (A356N, T315I, or ΔNcap-2PE) results in an increase in phosphotyrosine levels. On treatment with compound 142 at three different concentrations (1, 3, and 10 μM), we did not observe any significant increase in

the total phosphotyrosine levels of cells expressing wild-type or A356N Abl core proteins. In addition to the total phosphotyrosine levels, we also examined the phosphorylation levels of specific tyrosine residues involved in kinase regulation in the immunoprecipitated Abl protein fraction and did not observe any significant changes. While we observed a reproducible enhancement of kinase activity in the *in vitro* kinase assays in the presence of compound 142, we did not observe any effect on the total phosphotyrosine content in this cellular system. This discrepancy could be explained by a multitude of reasons. For example, compound 142 could potentially be binding to other proteins in cells with a higher affinity and getting sequestered, thus resulting in an insufficient concentration of the compound to activate Abl kinase. On the other hand, compound 142 could potentially be activating a small pool of Abl kinase and that effect may not be observable in the total phosphotyrosine blots. Future experiments to evaluate the effect of compound 142 on Abl activation in a different experimental setup could be helpful to confirm its effect in cellular assays.

Compound 4B7 reproducibly inhibited p41 interaction with the Abl N32L and SH3 proteins and demonstrated a direct interaction with Abl N32L protein in the differential scanning fluorimetry assay. The chemical name of this compound is 10-(2-Methoxyethyl)-3-phenylbenzo[g]pteridine-2,4-(3H,10H)-dione, and its structure is presented in Figure 23D. However, this compound failed to bind to the N32L or SH3 proteins by SPR, raising questions about the specificity of binding. To resolve this issue, we tested the effect of compound 4B7 on the wild-type Abl core protein as well as the Abl kinase domain in the kinetic kinase assay. At a concentration of 10 μM, compound 4B7 was found to inhibit wild-type Abl core kinase activity by about 15%. However, the compound had a similar inhibitory effect on the isolated Abl kinase

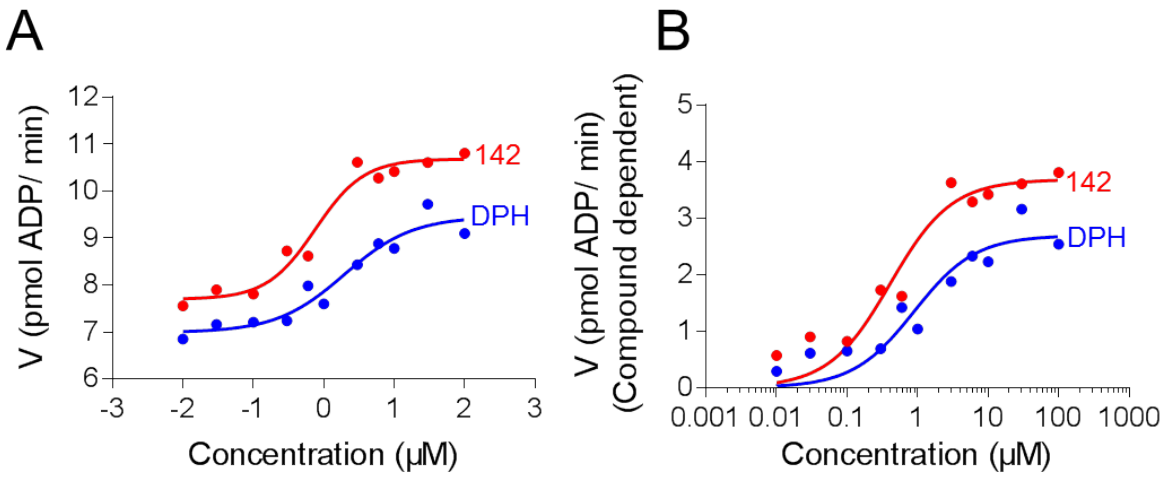

Compound:	142	DPH
EC_{50} (μM)	0.63 ± 0.07	1.11 ± 0.5
K_{act} (μM)	0.4 ± 0.02	1.02 ± 0.07
V_{max} (μM)	3.2 ± 0.28	1.90 ± 0.4

Figure 26. Concentration-dependent activation of the Abl kinase core protein by compound 142.

The wild-type Abl kinase core was assayed in the presence of compound 142 and DPH at the indicated concentrations using the ADP Quest kinetic kinase assay (see Materials and Methods). A) Reaction velocities are plotted as a function of compound concentrations. The resulting data were curve-fit to determine the EC_{50} for each activator as described under Materials and Methods. B) Compound dependent reaction rates, calculated by subtracting the basal rate of reaction in the absence of the compounds, are plotted as a function of concentration. These were curve-fit to determine the activation constant K_{act} and V_{max} for each activator as described under Materials and Methods. For both (A) and (B), each of the parameters was determined in triplicate, and the mean values ± SE are presented in the Table.

domain that lacks the presumptive binding site for this compound. This indicates that compound 4B7 has a weak, non-specific effect on Abl kinase activity that persists in the absence of the regulatory domains and thus, is not a consequence of the modulation of the SH3:linker interaction.

3.4.9 Molecular dynamics simulations and docking studies predict binding of compound 142 to the SH3:linker interface in the Abl kinase core

Data presented in the previous sections demonstrate that compound 142 interacts with the regulatory N32L region of Abl, resulting in a decrease in thermal stability and a concomitant increase in kinase activity. We used molecular dynamics (MD) simulations to explore the dynamics of the N32L region used in the assays. To model the effect of the linker being displaced from the SH3 domain, we manually pulled the linker a short distance away from the SH3 domain prior to the simulation (as described in section 3.3.8). After approximately 20 ns, the linker reconnected with the SH3 domain through the interaction of linker Pro249 and SH3 Trp118. To explore possible binding sites for this compound on the N32L region of the Abl kinase core, we used the computational docking tool *smina* [201] to dock 142 to snapshots of the simulation prior to the reconnection of the SH3:linker interface. As shown in Figure 27 (top panel), compound 142 fits into a surface pocket defined by the SH3:linker interface in the N32L protein. This predicted binding site involves an aromatic interaction between the pyrimido-pyrimidine moiety of 142 and the indole side chain of SH3 Trp118, as well as polar contacts involving all four hydroxyl groups on the ligand. This aromatic interaction is consistent with probe peptide displacement as well as the observed decrease in the FP signal produced by the W118A mutation (Figure 18C). Two of the hydroxyl groups of 142 make potential hydrogen

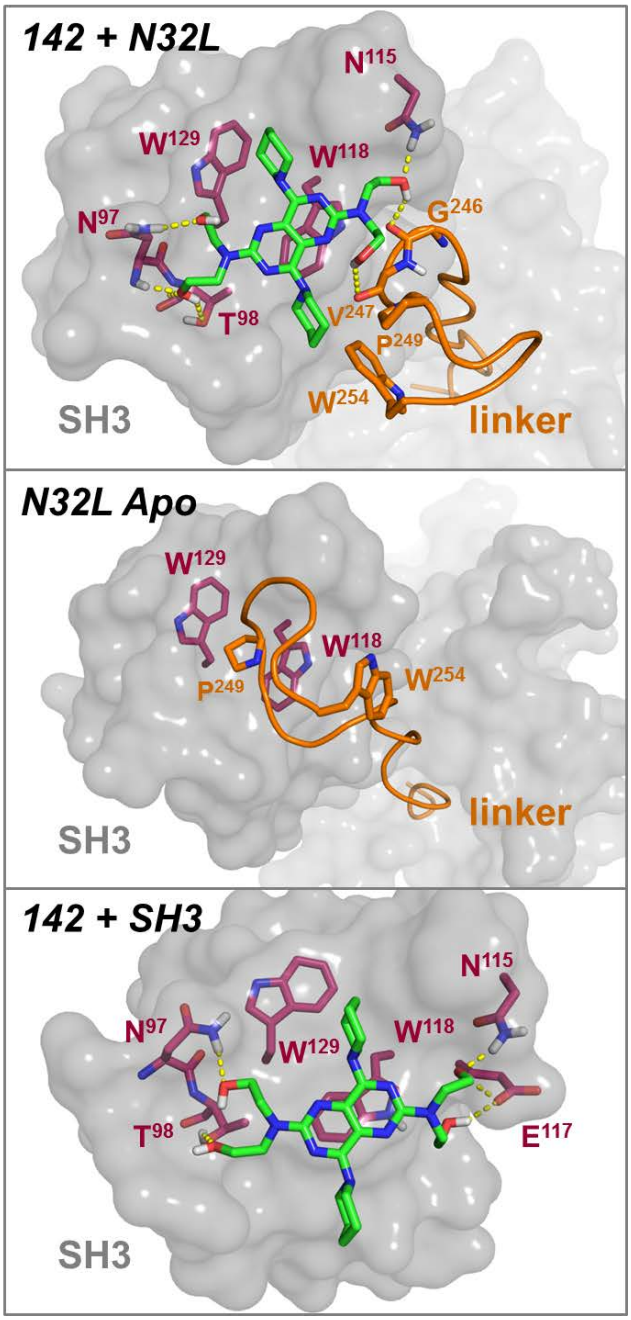

Figure 27. Computational docking predicts binding of hit compound 142 (dipyridimole) to the Abl SH3:linker interface.

Top: The lowest energy pose of the ligand (compound 142; carbon atoms rendered in green) is shown docked to a snapshot of an MD simulation of the Abl N32L structure. SH3 domain residues predicted to contribute to ligand binding include Asn97, Thr98, Asn115, Trp118, and Trp129 (carbons in red). The backbone of the linker is shown as an orange ribbon, with Gly246, Val247, Pro249 and Trp254 predicted to contribute to the binding pocket. One of the piperidine groups of compound 142 makes hydrophobic contacts with linker Pro249 and Trp254, while the

pyrimido-pyrimidine scaffold of compound 142 is π-stacking with Trp118. *Middle panel*: Model of the SH3:linker interface in the N32L region based on the crystal structure of the downregulated Abl core (PDB:2FO0), highlighting the interaction of linker Pro249 with SH3 Trp118 and Trp129. Ligand binding (top panel) is predicted to displace this regulatory interaction, leading to kinase activation. *Lower panel*: The lowest energy pose of compound 142 is shown docked to a snapshot of an MD simulation of the SH3 domain in the absence of the linker. The position of the 142 ligand is similar (within 1.5 Å RMSD) to that in the SH3 domain of N32L (top), except that the ligand contacts Glu117 rather than linker residues Gly246 and Val247. Without the linker, the potential hydrophobic stabilization of the 142 piperidine group is also lost.
Molecular dynamic simulations and docking were performed by Matthew Baumgartner and Carlos Camacho, Department of Computational Biology, University of Pittsburgh.

bonds with the side and main chains of SH3 Asn97 as well as the side chain of Thr98. The other two hydroxyl groups of 142 form hydrogen bonds with the main chain carbonyls of linker Gly246 and Val247 as well as the side chain of SH3 Asn115. In addition, one of the piperidine groups of compound 142 makes hydrophobic contacts with SH3 Trp129, while the other approaches the side chains of linker residues Pro249 and Trp254. Note that in the crystal structure of the fully assembled, downregulated conformation of the Abl core, linker Pro249 inserts between SH3 Trp118 and Trp129 (Figure 27, middle panel); displacement of this regulatory contact by compound 142 binding may contribute to kinase activation.

For comparison, we also ran unconstrained MD simulations of the SH3 domain in the absence of the linker. Our docked model to a snapshot from this simulation is shown in Figure 27 (bottom panel). The overall position of the ligand in this model is quite similar to that observed with the N32L snapshot (within 1.5 Å RMSD), and includes the potential stacking interaction with SH3 Trp118 and hydrogen bonding to SH3 Asn97, Thr98 and Asn115. Polar contacts of compound 142 with linker Gly246 and Val247 as well as hydrophobic interactions

with linker Trp254 and Pro249 are not possible. However, additional hydrogen bonds are observed with SH3 Glu117. Loss of these hydrophobic interactions in the SH3-only model helps to explain the lower binding affinity of compound 142 for the isolated SH3 domain (K_D = 2.99 ± 0.40 x 10^{-5} M) relative to the N32L protein (K_D = 6.90 ± 0.78 x 10^{-6} M) as determined by SPR (Figure 24).

3.5 SUMMARY AND CONCLUSIONS

In this study, we developed a screening strategy to identify allosteric small molecule modulators of Abl kinase activity that work outside of the kinase domain. Our FP-based assay targets the regulatory domains of Abl that control its kinase activity through intramolecular interactions. Specifically, this assay is based on a recombinant Abl protein comprising the complete regulatory apparatus (Ncap-SH3-SH2-linker) and a synthetic polyproline probe peptide (p41) that selectively binds the Abl SH3 domain. Interaction of the probe peptide with the Abl N32L protein results in a robust and reproducible FP signal. Mutation of the SH3 binding site (W118A) or introduction of a high-affinity linker both resulted in loss of the FP signal, demonstrating that probe access requires an intact and accessible SH3 domain. Small-scale pilot screens of two small molecule libraries (2800 total compounds) identified dipyridamole (compound 142) as an inhibitor of the FP signal observed with the N32L:p41 complex, and direct interaction of this compound with the Abl N32L protein was confirmed by SPR and DSF assays. Dipyridamole was observed to stimulate the kinase activity of downregulated Abl kinase *in vitro*, and was more potent than the previously described Abl agonist DPH which targets the myristic acid binding pocket in the kinase domain. In contrast to wild-type Abl, dipyridamole

had no effect on a modified Abl core protein with a high-affinity linker, suggesting that it works by binding to the SH3 domain and disrupting the SH3:linker interface. Molecular dynamics simulations in combination with molecular docking support this proposed mechanism of action: dipyridamole was predicted to interact with the Abl core through a pocket defined by the SH3:linker interface. This interaction involved the Trp residue 118 the SH3 domain binding surface, potentially disrupting a key regulatory interaction with Pro249 in the linker. The identification and characterization of dipyridamole as an allosteric modulator of Abl kinase activity required multiple secondary assays, and the hit validation and characterization strategy is summarized in Figure 28.

Discovery of dipyridamole as an Abl agonist provides an important proof of concept that small molecules altering SH3:linker interaction represent allosteric modulators of Abl kinase activity. Selective agonists of Abl function have potential as chemical probes to better understand the role of Abl kinase activity in solid tumors and in response to genotoxic stress. Conversely, allosteric antagonists may also be discovered by this approach and have the potential to complement current ATP-competitive inhibitors of Bcr-Abl in the context of CML and other cancers. The allosteric inhibitor discovery concept may also be extended to the discovery of allosteric modulators of other kinases systems with multidomain regulatory interactions, including members of the Src and Tec kinase families.

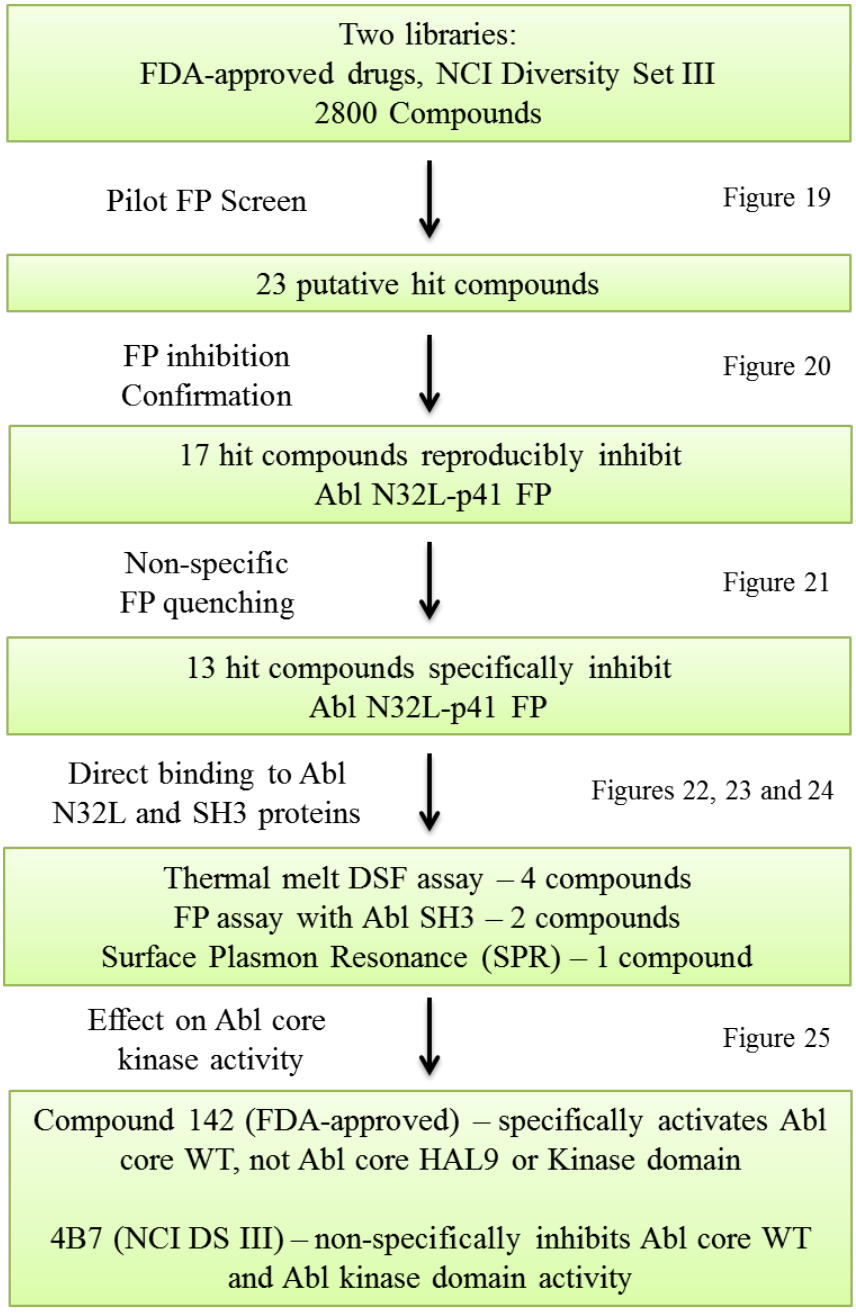

Figure 28. A summary of the hit selection and validation strategy.

Hit compounds identified from the pilot screens were first confirmed for reproducible FP inhibition of p41 interaction with Abl N32L protein. Compounds that quenched FP signal in a non-specific manner were then eliminated by testing for FP inhibition in the absence of the Abl N32L protein. The remaining 13 hit compounds were then tested for direct binding to the Abl N32L and SH3 proteins using a combination of DSF, FP, and SPR assays. Finally, the hit compounds were tested in functional assays where their effect on Abl kinase activity was examined in an *in vitro* kinetic kinase assay. This led to the identification of compound 142 (dipyridamole) that allosterically activates wild-type Abl core through the SH3:linker interface.

4.0 OVERALL DISCUSSION

The role of intramolecular interactions in maintaining the down-regulated conformation of the Abl core has been well established, though their status in the context of kinase activation is less clear. In this study, we have shown that Abl core kinase activation does not require complete disruption of intramolecular interactions or total rearrangement of regulatory domains. Moreover, we show that enhancing the interaction between the SH3 domain and the SH2-kinase linker has a dominant effect on the conformation and stability of active Abl core mutants. In the second part of this study, we have developed a novel biochemical assay, which is amenable to high throughput screening, to identify small molecules targeting the regulatory interaction between the SH3 domain and the SH2-kinase linker in the Abl protein. Using this screening assay, we have identified a small molecule that activates Abl kinase through a remarkably subtle disruption of the SH3:linker interaction. The data presented in this study provide important insights into Abl kinase conformation on activation, and alteration of intramolecular interactions to identify allosteric modulators of kinase activity.

4.1 EFFECT OF ACTIVATING AND STABILIZING MUTATIONS ON ABL KINASE ACTIVITY, STABILITY, AND CONFORMATION

In chapter 2, we investigated the effect of activating and stabilizing conformations on the kinase activity, enzyme kinetics, thermal stability, and conformation of Abl core proteins. The relative orientation of the regulatory SH3 and SH2 domains has been previously established for both the down-regulated conformation and a maximally activated conformation of the Abl core by X-ray crystallography [9,12]. We hypothesized that Abl kinase activation does not require complete disruption of all intra-molecular interactions and reorientation of regulatory domains. To test this hypothesis, we created the following four recombinant proteins modeling a graded range of active states: 1) the wild-type Abl core; 2) Abl core A356N that has a mutation in the myristic acid binding pocket leading to kinase activation; 3) Abl core T315I that has a mutation in the gatekeeper residue and exhibits enhanced kinase activity and resistance to imatinib; 4) Abl ΔNcap-2PE that lacks the N-cap region and includes mutations in two proline residues in the linker that disrupt the SH3:linker interaction. We observed that the kinase activity of these proteins spans a broad range of intrinsic catalytic activities both *in vitro* and in cells, with the following rank order: wild-type < A356N < T315I < ΔNcap-2PE. We next investigated the effect of these mutations on the Abl core protein stability in the DSF assay. We found that the ΔNcap-2PE exhibits a significantly lower melt temperature (T_m) in comparison to the wild-type Abl core protein. Interestingly, while the A356N Abl core mutant showed a moderate decrease in T_m (5 °C), the T315I mutant showed only a 2 °C decrease in T_m indicating that this protein adopts a relatively stable conformation despite its relatively high kinase activity. Data from X-ray scattering experiments demonstrated that the A356N mutant adopts a similar conformation as the wild-type Abl core protein. On the other hand, the T315I mutant adopted a unique ‘squashed

pear' conformation with an increased radius of gyration. Shape reconstructions based on the X-ray scattering indicated a rearrangement of the overall core structure in the T315I mutant, with the SH2 domain reoriented to the top of the kinase domain and the SH3 domain next to the kinase domain. It is remarkable that a single point mutation in the kinase domain causes such a dramatic rearrangement of regulatory domains in the Abl core protein. This rearranged conformation could explain the enhanced kinase activity and altered substrate selectivity of the Abl T315I protein in the context of Bcr-Abl [45,138]. The ΔNcap-2PE mutant of Abl exhibited an elongated conformation with a linear rearrangement of the kinase domain followed by the SH2 and SH3 domains, which is consistent with the lack of all regulatory interactions in this protein.

A recent study from our lab has shown that a high affinity linker (HAL) that results in enhanced SH3:linker interaction is able to overcome the effect of activating mutations A356N and T315I on Abl kinase activity [30]. To examine the effect of enhanced SH3:linker interaction on Abl core protein stability and conformation, we introduced the HAL mutations into the three Abl core proteins described above. We observed that the HAL mutation has a stabilizing effect on the Abl core protein, and results in an increased T_m for the wild-type Abl core as well as the A356N and T315I mutant Abl core proteins. Molecular reconstruction from the X-ray scattering data shows that the conformation of the Abl core HAL is similar to the wild-type Abl core, thus indicating that the addition of proline residues to the linker does not distort the downregulated Abl core conformation. Remarkably, the introduction of HAL into the T315I Abl core mutant resulted in a restoration of the regulatory domains to their observed positions in the downregulated core conformation. These observations indicate that enhanced SH3:linker interaction has a dominant effect on the conformation and thermal stability of Abl core mutants.

These results are in agreement with the earlier study from our lab that reported a dominant effect of enhanced SH3:linker interaction on kinase activity and conformational dynamics of Abl core mutants [30]. Based on these observations, a small molecule that strengthens the SH3:linker interaction is predicted to overcome the effect of activating mutations in the Abl core protein. These observations contributed to the rationale for assay development and small molecule discovery discussed in Chapter 3.

Ponatinib is the only current ATP-competitive inhibitor that can bind the Bcr-Abl T315I mutant and inhibit its kinase activity [159]. To examine its effect on the conformation of the Abl core proteins, we examined the effect of ponatinib and imatinib on Abl core thermal stability in the DSF assay. Ponatinib has a robust stabilizing effect on all three Abl core proteins (WT, A356N, and T315), while imatinib only stabilizes the WT and A356N Abl core proteins as expected. Future studies will determine the X-ray scattering patterns of Abl core proteins in the presence of these small molecules to further understand the effect of these inhibitors on the Abl core conformation. Specifically, X-ray scattering analysis of a complex of Abl core T315I and ponatinib could provide valuable insight into the relative orientation of the regulatory domains. Additionally, HXMS analysis of Abl core T315I in complex with ponatinib can be used to elucidate the effect of ponatinib on Abl core conformational dynamics. In particular, it would be very interesting to determine whether the addition of ponatinib is sufficient to restore the positions of the N-cap, SH3 and SH2 domains to those observed in the assembled, downregulated state, similar to what we observed with HAL substitution.

Though molecular reconstruction of the X-ray scattering patterns was used to indicate the positions of the SH2 and SH3 domains in the Abl core T315I protein, the position of the SH2-kinase linker or the status of the SH3:linker interaction could not be established. The SH2-kinase

linker may still be bound to the SH3 domain, or this interaction could have been allosterically disrupted by the T315I mutation and reorientation of the SH2 and SH3 domains. One way to test for the presence of the SH3:linker interaction in the Abl core T315I mutant is by introducing the 2PE mutation into this protein. A comparison of the two Abl core T315I proteins (with or without 2PE) in terms of their kinase activity, thermal stability, and X-ray scattering patterns could be useful in this context. If the SH3:linker interaction persists in the Abl core T315I mutant, disruption of this interaction by the 2PE mutation could result in a potential change in kinase activity, thermal stability, and overall protein conformation. As discussed in section 1.2.2.2, HXMS has been utilized to examine the effects of mutations (including A356N and T315I) on the conformational dynamics of Abl core proteins in solution [30,46]. An increase in protein dynamics manifests as a specific increase in deuterium uptake that can be measured by mass spectrometry. A change in deuterium uptake in the SH3 domain on introduction of the 2PE mutation in the Abl core T315I protein would indicate that the SH3:linker interaction persists in the Abl T315I protein. Moreover, it would be interesting to see if the 2PE mutation results in deuterium uptake changes in other parts of the protein, as these changes would indicate allosteric effects of the SH3:linker interaction in the Abl T315I protein.

DSF (thermal melt) data suggest that the Abl core T315I protein is relatively stable in solution, in comparison to the active A356N and ΔNcap-2PE mutants, and therefore maybe amenable to crystallization. An X-ray crystal structure of the Abl core T315I protein would unequivocally identify the locations of the regulatory SH2 and SH3 domains as well as the SH2-kinase linker in the most stable state of this protein. Moreover, SAXS analysis of the Abl T315I protein in complex with ponatinib (proposed above) could present useful information on the utility of ponatinib as a stabilizing ligand for these crystallization studies.

The intensive investigation of the conformation and dynamics of the Abl core T315I protein can provide valuable information to therapeutically target the clinically relevant Bcr-Abl T315I protein. The reorientation of the SH2 domain in the Abl core T315I protein could be partially responsible for its enhanced kinase activity and altered substrate specificity [45,138]. Moreover, the diversity observed in the mechanisms of Abl kinase activation may also be present in other multi-domains kinase families such as Src and Tec family kinases. This diversity can be used to identify small molecules that act through allosteric mechanisms and selectively modulate kinase activity.

4.2 IDENTIFICATION OF ALLOSTERIC MODULATORS OF ABL KINASE FUNCTION

The interaction between the SH3 domain and the SH2-kinase linker of Abl has been shown to be critical for regulation of the Abl kinase. We hypothesized that a small molecule that influences the SH3:linker interaction may be a potential agonist or antagonist of Abl kinase activity. In chapter 3, we focused on discovering small molecule allosteric modulators of Abl kinase activity that act through the regulatory domains. Specifically, we developed a novel fluorescence polarization (FP) screening assay to identify small molecules that target the SH3:linker regulatory interaction in Abl. This assay is based on a recombinant Abl protein that includes the complete regulatory apparatus (Ncap-SH3-SH2-linker, N32L) and a synthetic polyproline probe peptide (p41) that selectively binds the Abl SH3 domain. Interaction of the probe peptide with the Abl N32L protein results in a robust and reproducible FP signal. Mutation of the SH3

binding site (W118A) or introduction of a high-affinity linker both resulted in loss of the FP signal, demonstrating that probe access requires an intact and accessible SH3 domain.

We performed pilot screens with two small molecules libraries (2800 compounds total) and identified dipyridamole (‘compound 142’, an antithrombotic drug) as a hit compound. The interaction of dipyridamole to the Abl N32L protein was validated by SPR and DSF assays. In subsequent experiments with the wild-type Abl core, we observed that dipyridamole stimulates Abl kinase activity *in vitro* through an allosteric mechanism. Interestingly, dipyridamole had no effect on a modified Abl core protein with a high-affinity linker, suggesting that it acts through the SH3:linker interface. Moreover, molecular dynamics simulations in combination with molecular docking predicted that the compound interacts with the Abl core through a pocket defined by the SH3:linker interface. This predicted interaction involved a highly conserved residue on the binding surface of the SH3 domain (Trp118), in addition to other residues in the SH3 domain and the SH2-kinase linker, potentially disrupting a key regulatory interaction with Pro249 in the linker.

The discovery of dipyridamole as an Abl agonist shows that screening assays based on the non-catalytic domains of Abl can identify allosteric small molecule regulators of kinase function. Moreover, this compound provides an important proof of concept that small molecules that alter the SH3:linker interaction represent allosteric modulators of Abl kinase activity. Robust assay performance in our pilot screens predicts that this FP assay should be readily scalable to screen larger chemical libraries. In collaboration with Dr. Paul Johnston and David Close at the School of Pharmacy, University of Pittsburgh, we are in the process of screening two larger chemical libraries using the FP assay described in this study (60,000 diverse compounds in total). These fully automated library screens will potentially identify additional chemical scaffolds that

modulate the SH3:linker interaction and allosterically influence Abl kinase activity. Putative hit compounds identified from these screens will need to be first validated for binding and activity as described in Chapter 3 of this study. Lead selection must also consider drug-like properties of the hit compounds. Lipinski and colleagues analyzed over 2000 clinically available drugs and identified important properties that signify 'drug-likeness' in chemical compounds, and these include criteria for molecular weight, lipophilicity, and the number of hydrogen bond donor and acceptor groups [205]. Hit compounds identified from the FP screens that exhibit these properties, in addition to an optimum number of rotatable bonds and the possibility of chemical modifications, will be considered as strong lead compounds. Additional structure activity relationship studies can be utilized to improve the pharmacokinetic properties as well as specificity of these putative hit compounds.

Future studies can explore the effect of allosteric lead compounds on Abl as well as Bcr-Abl kinase activity in cells. Our lab has optimized experimental conditions where the phosphotyrosine content in HEK 293T cells transiently expressing Abl core proteins correlates with their intrinsic catalytic activity [30]. While expression of the down-regulated wild-type or HAL Abl core proteins results in negligible phosphotyrosine levels (as observed by immunoblotting), expression of the active Abl mutants (A356N, T315I, or ΔNcap-2PE) results in an increase in phosphotyrosine levels. Treatment with putative allosteric lead compounds that specifically affect the Abl core conformation and lead to a consequent increase or decrease in kinase activity could be assessed using this system. While the effect of agonists can be assessed on the wild-type and HAL Abl core proteins, the effect of antagonists can be assessed on the active Abl core mutants. In addition to the total phosphotyrosine levels, we can also examine the phosphorylation levels of specific tyrosine residues involved in kinase regulation. These include

pTyr89 (SH3 domain), pTyr245 (SH2-kinase linker) and pTyr412 (activation loop) [30]. In addition to the experimental system described above, we could also examine the effect of putative allosteric modulators on Bcr-Abl kinase activity in TF-1 cells. TF-1 cells are human myeloid cells that require granulocyte-macrophage colony stimulating factor (GM-CSF) for proliferation, and Bcr-Abl expression transforms these cells to GM-CSF-independent growth [206,207]. The effect of putative lead compounds on Bcr-Abl's transforming potential as well as kinase activity can be assessed by soft agar colony assays and immunoblotting for phosphotyrosine levels, respectively.

Data presented in this study as well as an earlier study from our lab has shown that enhancement of SH3:linker interaction overcomes the effects of activating mutations in Abl kinase [30]. Moreover, incorporation of the engineered HAL into Bcr-Abl proteins sensitizes Bcr-Abl to both ATP-competitive and allosteric inhibitors. Thus, a small molecule that strengthens the SH3:linker interaction in Abl may be a potential allosteric inhibitor of Bcr-Abl. Such allosteric antagonists may be discovered by the FP assay discussed in Chapter 3 and have the potential to complement current ATP-competitive and allosteric inhibitors of the Bcr-Abl kinase domain in the context of CML. Initial studies could focus on the effect of putative allosteric inhibitors on sensitization of Bcr-Abl transformed cells to imatinib or GNF-2 induced apoptosis. It will also be interesting to examine the effect of such inhibitors on imatinib-resistant Bcr-Abl mutants such as T315I. Furthermore, it would be crucial to identify any potential resistance mutations that develop following treatment with allosteric inhibitors acting through the SH3:linker interface, both alone and in combination with ATP-competitive inhibitors. While mutations in the regulatory domains including the SH3:linker interface could give rise to resistance against the putative allosteric inhibitor alone, we predict a decreased incidence of

resistance mutations against a combination of allosteric and ATP-competitive inhibitors that target multiple structural regions in the Abl kinase. This prediction is consistent with earlier studies where a combination of allosteric and ATP-competitive inhibitors was found to result in a decrease in the incidence of resistance mutations [55].

Several biophysical approaches can be utilized to characterize the effect of allosteric modulators on Abl protein dynamics and kinase conformation. As discussed in section 1.2.2.2, HXMS studies have been utilized to examine the effect of small molecule inhibitors of Abl (e.g. GNF-5, dasatinib) on the conformational dynamics of Abl core proteins [54]. The effect of lead allosteric compounds on SH3:linker interaction in the Abl N32L protein, and the deuterium uptake in different regions of the Abl core protein could provide useful information about the mechanism of action of these allosteric modulators. Additionally, SAXS analysis can provide useful information about the overall conformation of the Abl core proteins in complex with a lead compound that disrupts or enhances the SH3:linker interaction. It would be especially interesting to examine the effect of an allosteric antagonist on the conformation of the Abl core T315I mutant, to see if it mimics the 'HAL effect' and restores the regulatory domains to the positions observed in the downregulated Abl core conformation.

Small molecules that selectively activate Abl kinase can potentially be used as chemical probes to better understand the role of Abl kinase activity in response to genotoxic stresses. As discussed in section 1.3, Abl is activated in response to several genotoxic agents and has been shown to interact with proteins involved in both DNA damage repair as well as apoptotic induction pathways. While Abl has been clearly shown to induce apoptotic death in response to genotoxic agents, its effect on the outcome of DNA damage repair processes is less clear. Small molecules that selectively activate the Abl kinase may help to clarify the effect of Abl activation

on the DNA-damage repair pathways. Moreover, inhibition of Abl kinase activity has been shown to induce resistance to apoptosis in cells treated with ionizing radiation [93]. Selective Abl agonists may therefore cause the opposite effect, and represent useful therapeutic agents to sensitize radio-resistant tumor cells to ionizing radiation-induced apoptosis.

As discussed in section 1.5, the role of Abl kinases in solid tumors is not well defined, with conflicting reports in terms of its contribution to tumor growth and spread. Abl has been shown to promote anchorage-independent growth in breast, gastric, and hepatocellular carcinoma cells [169,170]. In contrast, a few studies found that Abl activation suppresses the growth of certain breast cancer xenografts [172,173]. Clinical studies investigating the treatment of solid tumors with imatinib, nilotinib, and dasatinib have yielded mixed results, which can partially be explained by the limited selectivity of these inhibitors [165,208,209]. An added complexity is the discrepancy in the effect of Abl in promoting vs. suppressing growth or invasiveness of solid tumors due to their heterogeneity. Selective allosteric modulators of Abl may be useful to delineate the effect of Abl kinase activity in diverse cancer cell types and tumor microenvironments. These small molecules may represent useful probes to identify tumor microenvironment and cellular biomarkers in which Abl kinase acts as a tumor promoter vs. suppressor.

In addition to Abl, the Src and Tec kinase families have a similar multidomain organization and mechanisms of intramolecular interactions that are important for regulation of kinase activity [210,211]. On one hand, since some of the residues in the SH3:linker interaction are conserved (e.g. SH3 domain Trp118), it will be important to evaluate the selectivity of putative allosteric modulators by testing them against related kinases for both binding as well as effects on kinase activity. On the other hand, there is enough sequence and structural diversity

between these kinase families that it may be possible to identify allosteric compounds that are selective for specific kinases. Moreover, chemical modifications of putative lead allosteric hits in combination with structure activity relationship studies can be utilized to further enhance specificity for Abl over related kinase families. Furthermore, this allosteric inhibitor discovery concept developed using the Abl kinase can be extended to the discovery of allosteric modulators of other similar kinases systems.

4.3 CLOSING REMARKS

Results presented in this study provide valuable insight into the importance of allosteric interactions on Abl kinase activity. The first part of the study demonstrates that Abl kinases can adopt diverse active conformations, while the second part of the study presents a platform to discover small molecules that specifically modulate allosteric interactions in Abl. These studies thus present a new approach to selective drug discovery for this important kinase system. Allosteric modulators may help us better understand the function of Abl kinase in response to DNA damage agents and potentially overcome radioresistance observed in certain tumors in the future. Additionally, such compounds may identify cellular contexts in solid tumors where Abl activity can be exploited for therapeutic gain. Finally, selective allosteric antagonists of Abl can complement the existing ATP-competitive inhibitors and present important therapeutic agents to counter the high incidence of resistance mutations observed in Bcr-Abl positive CML patients.

APPENDIX A

LIST OF ABBREVIATIONS

Abl	Abelson tyrosine kinase
Arg	Abl related gene
Bcr	Breakpoint cluster region
CML	Chronic myelogenous leukemia
DDR	DNA damage repair
DSF	Differential scanning fluorimetry
EC_{50}	Half-maximal effective concentration
EGFR	Epidermal growth factor receptor
FP	Fluorescence polarization
GM-CSF	Granulocyte monocyte colony stimulating factor
HAL	High affinity linker
HXMS	Hydrogen exchange mass spectrometry
K_{act}	Activation constant
K_D	Equilibrium dissociation constant
MD	Molecular dynamics

N32L	Ncap-SH3-SH2-Linker
N-cap	N terminal cap
NMR	Nuclear magnetic resonance
PDGFR	Platelet derived growth factor receptor
PP II	Poly-proline type II
R_g	Radius of gyration
SAXS	Small angle X-ray scattering
SH	Src homology
SPR	Surface plasmon resonance
TKI	Tyrosine kinase inhibitor
T_m	Thermal melt temperature

BIBLIOGRAPHY

1. Wang JY, Ledley F, Goff S, Lee R, Groner Y, Baltimore D (1984) The mouse c-abl locus: molecular cloning and characterization. Cell 36: 349-356. 0092-8674(84)90228-9 [pii].

2. Reddy EP, Smith MJ, Srinivasan A (1983) Nucleotide sequence of Abelson murine leukemia virus genome: structural similarity of its transforming gene product to other onc gene products with tyrosine-specific kinase activity. Proc Natl Acad Sci U S A 80: 3623-3627.

3. Srinivasan A, Dunn CY, Yuasa Y, Devare SG, Reddy EP, Aaronson SA (1982) Abelson murine leukemia virus: structural requirements for transforming gene function. Proc Natl Acad Sci U S A 79: 5508-5512.

4. Shtivelman E, Lifshitz B, Gale RP, Canaani E (1985) Fused transcript of *abl* and *bcr* genes in chronic myelogenous leukemia. Nature 315: 550-554.

5. Ben-Neriah Y, Daley GQ, Mes-Masson AM, Witte ON, Baltimore D (1986) The chronic myelogenous leukemia-specific p210 protein is the product of the *bcr/abl* hybrid gene. Science 233: 212-214.

6. Shtivelman E, Lifshitz B, Gale RP, Roe BA, Canaani E (1986) Alternative splicing of RNAs transcribed from the human abl gene and from the bcr-abl fused gene. Cell 47: 277-284. 0092-8674(86)90450-2 [pii].

7. Pendergast AM (2002) The Abl family kinases: mechanisms of regulation and signaling. Adv Cancer Res 85: 51-100.

8. Colicelli J (2010) ABL tyrosine kinases: evolution of function, regulation, and specificity. Sci Signal 3: re6. scisignal.3139re6 [pii];10.1126/scisignal.3139re6 [doi].

9. Nagar B, Hantschel O, Seeliger M, Davies JM, Weis WI, Superti-Furga G, Kuriyan J (2006) Organization of the SH3-SH2 unit in active and inactive forms of the c-Abl tyrosine kinase. Mol Cell 21: 787-798.

10. Van Etten RA (1999) Cycling, stressed-out and nervous: cellular functions of c-Abl. Trends Cell Biol 9: 179-186.

11. Superti-Furga G, Courtneidge SA (1995) Structure-function relationships in Src family and related protein tyrosine kinases. BioEssays 17: 321-330. 10.1002/bies.950170408 [doi].

12. Nagar B, Hantschel O, Young MA, Scheffzek K, Veach D, Bornmann W, Clarkson B, Superti-Furga G, Kuriyan J (2003) Structural basis for the autoinhibition of c-Abl tyrosine kinase. Cell 112: 859-871.

13. Pluk H, Dorey K, Superti-Furga G (2002) Autoinhibition of c-Abl. Cell 108: 247-259.

14. Hantschel O, Nagar B, Guettler S, Kretzschmar J, Dorey K, Kuriyan J, Superti-Furga G (2003) A myristoyl/phosphotyrosine switch regulates c-Abl. Cell 112: 845-857.

15. Kuriyan J, Cowburn D (1997) Modular peptide recognition domains in eukaryotic signaling. Annu Rev Biophys Biomol Struct 26: 259-288.

16. Musacchio A, Saraste M, Wilmanns M (1994) High-resolution crystal structures of tyrosine kinase SH3 domains complexed with proline-rich peptides. Nat Struct Biol 1: 546-551.

17. Yu H, Rosen MK, Sin TB, Seidel-Dugan C, Brugge JS, Schreiber SL (1992) Solution structure of the SH3 domain of Src and identification of its ligand binding site. Science 258: 1665-1668.

18. Cicchetti P, Mayer BJ, Thiel G, Baltimore D (1992) Identification of a protein that binds to the SH3 domain of Abl and is similar to Bcr and GAP-rho. Science 257: 803-806.

19. Ren R, Mayer BJ, Cicchetti P, Baltimore D (1993) Identification of a ten-amino acid proline-rich SH3 binding site. Science 259: 1157-1161.

20. Franz WM, Berger P, Wang JYJ (1989) Deletion of an N-terminal regulatory domain of the c-abl tyrosine kinase activates its oncogenic potential. EMBO J 8: 137-147.

21. Jackson PK, Baltimore D (1989) N-terminal mutations activate the leukemogenic potential of the myristoylated form of c-Abl. EMBO J 8: 449-456.

22. Brasher BB, Roumiantsev S, Van Etten RA (2001) Mutational analysis of the regulatory function of the c-Abl Src homology 3 domain. Oncogene 20: 7744-7752. 10.1038/sj.onc.1204978 [doi].

23. Barila D, Superti-Furga G (1998) An intramolecular SH3-domain interaction regulates c-Abl activity. Nat Genet 18: 280-282. 10.1038/ng0398-280 [doi].

24. Chen S, O'Reilly LP, Smithgall TE, Engen JR (2008) Tyrosine phosphorylation in the SH3 domain disrupts negative regulatory interactions within the c-Abl kinase core. J Mol Biol 383: 414-423. S0022-2836(08)01046-2 [pii];10.1016/j.jmb.2008.08.040 [doi].

25. Meyn MA, III, Wilson MB, Abdi FA, Fahey N, Schiavone AP, Wu J, Hochrein JM, Engen JR, Smithgall TE (2006) Src family kinases phosphorylate the Bcr-Abl SH3-SH2 region and modulate Bcr-Abl transforming activity. J Biol Chem 281: 30907-30916.

26. Sadowski I, Stone JC, Pawson T (1986) A noncatalytic domain conserved among cytoplasmic protein-tyrosine kinases modifies the kinase function and transforming activity of Fujinami sarcoma virus $p130^{gag\text{-}fps}$. Mol Cell Biol 6: 4396-4408.

27. Waksman G, Shoelson SE, Pant N, Cowburn D, Kuriyan J (1993) Binding of a high affinity phosphotyrosyl peptide to the Src SH2 domain: Crystal structures of the complexed and peptide-free forms. Cell 72: 779-790.

28. Chen S, Brier S, Smithgall TE, Engen JR (2007) The Abl SH2-kinase linker naturally adopts a conformation competent for SH3 domain binding. Protein Sci 16: 572-581. ps.062631007 [pii];10.1110/ps.062631007 [doi].

29. Brasher BB, Van Etten RA (2000) c-Abl has high intrinsic tyrosine kinase activity that is stimulated by mutation of the Src homology 3 domain and by autophosphorylation at two distinct regulatory tyrosines. J Biol Chem 275: 35631-35637.

30. Panjarian S, Iacob RE, Chen S, Wales TE, Engen JR, Smithgall TE (2013) Enhanced SH3/linker interaction overcomes Abl kinase activation by gatekeeper and myristic acid binding pocket mutations and increases sensitivity to small molecule inhibitors. J Biol Chem 288: 6116-6129. M112.431312 [pii];10.1074/jbc.M112.431312 [doi].

31. Taylor SS, Kornev AP (2011) Protein kinases: evolution of dynamic regulatory proteins. Trends Biochem Sci 36: 65-77. S0968-0004(10)00183-0 [pii];10.1016/j.tibs.2010.09.006 [doi].

32. Nagar B, Bornmann WG, Pellicena P, Schindler T, Veach DR, Miller WT, Clarkson B, Kuriyan J (2002) Crystal Structures of the Kinase Domain of c-Abl in Complex with the Small Molecule Inhibitors PD173955 and Imatinib (STI-571). Cancer Res 62: 4236-4243.

33. Schindler T, Bornmann W, Pellicena P, Miller WT, Clarkson B, Kuriyan J (2000) Structural mechanism for STI-571 inhibition of abelson tyrosine kinase. Science 289: 1938-1942.

34. Zhang J, Yang PL, Gray NS (2009) Targeting cancer with small molecule kinase inhibitors. Nat Rev Cancer 9: 28-39. nrc2559 [pii];10.1038/nrc2559 [doi].

35. Nagar B (2007) c-Abl tyrosine kinase and inhibition by the cancer drug imatinib (Gleevec/STI-571). J Nutr 137: 1518S-1523S. 137/6/1518S [pii].

36. Tokarski JS, Newitt JA, Chang CY, Cheng JD, Wittekind M, Kiefer SE, Kish K, Lee FY, Borzillerri R, Lombardo LJ, Xie D, Zhang Y, Klei HE (2006) The structure of Dasatinib (BMS-354825) bound to activated ABL kinase domain elucidates its inhibitory activity against imatinib-resistant ABL mutants. Cancer Res 66: 5790-5797. 66/11/5790 [pii];10.1158/0008-5472.CAN-05-4187 [doi].

37. Levinson NM, Kuchment O, Shen K, Young MA, Koldobskiy M, Karplus M, Cole PA, Kuriyan J (2006) A Src-like inactive conformation in the abl tyrosine kinase domain. PLoS Biol 4: e144. 05-PLBI-RA-1226R3 [pii];10.1371/journal.pbio.0040144 [doi].

38. Alaimo PJ, Knight ZA, Shokat KM (2005) Targeting the gatekeeper residue in phosphoinositide 3-kinases. Bioorg Med Chem 13: 2825-2836. S0968-0896(05)00136-7 [pii];10.1016/j.bmc.2005.02.021 [doi].

39. Blencke S, Zech B, Engkvist O, Greff Z, Orfi L, Horvath Z, Keri G, Ullrich A, Daub H (2004) Characterization of a conserved structural determinant controlling protein kinase sensitivity to selective inhibitors. Chem Biol 11: 691-701. 10.1016/j.chembiol.2004.02.029 [doi];S1074552104001164 [pii].

40. Liu Y, Shah K, Yang F, Witucki L, Shokat KM (1998) A molecular gate which controls unnatural ATP analogue recognition by the tyrosine kinase v-Src. Bioorg Med Chem 6: 1219-1226. S0968-0896(98)00099-6 [pii].

41. Liu Y, Bishop A, Witucki L, Kraybill B, Shimizu E, Tsien J, Ubersax J, Blethrow J, Morgan DO, Shokat KM (1999) Structural basis for selective inhibition of Src family kinases by PP1. Chem Biol 6: 671-678. cm6911 [pii].

42. Bell DW, Gore I, Okimoto RA, Godin-Heymann N, Sordella R, Mulloy R, Sharma SV, Brannigan BW, Mohapatra G, Settleman J, Haber DA (2005) Inherited susceptibility to lung cancer may be associated with the T790M drug resistance mutation in EGFR. Nat Genet 37: 1315-1316. ng1671 [pii];10.1038/ng1671 [doi].

43. Kobayashi S, Boggon TJ, Dayaram T, Janne PA, Kocher O, Meyerson M, Johnson BE, Eck MJ, Tenen DG, Halmos B (2005) EGFR mutation and resistance of non-small-cell lung cancer to gefitinib. N Engl J Med 352: 786-792. 352/8/786 [pii];10.1056/NEJMoa044238 [doi].

44. Azam M, Seeliger MA, Gray NS, Kuriyan J, Daley GQ (2008) Activation of tyrosine kinases by mutation of the gatekeeper threonine. Nat Struct Mol Biol 15: 1109-1118. nsmb.1486 [pii];10.1038/nsmb.1486 [doi].

45. Skaggs BJ, Gorre ME, Ryvkin A, Burgess MR, Xie Y, Han Y, Komisopoulou E, Brown LM, Loo JA, Landaw EM, Sawyers CL, Graeber TG (2006) Phosphorylation of the ATP-binding loop directs oncogenicity of drug-resistant BCR-ABL mutants. Proc Natl Acad Sci U S A 103: 19466-19471.

46. Iacob RE, Pene-Dumitrescu T, Zhang J, Gray NS, Smithgall TE, Engen JR (2009) Conformational disturbance in Abl kinase upon mutation and deregulation. Proc Natl Acad Sci U S A 106: 1386-1391.

47. Grant TD, Luft JR, Wolfley JR, Tsuruta H, Martel A, Montelione GT, Snell EH (2011) Small angle X-ray scattering as a complementary tool for high-throughput structural studies. Biopolymers 95: 517-530. 10.1002/bip.21630 [doi].

48. Hura GL, Menon AL, Hammel M, Rambo RP, Poole FL, Tsutakawa SE, Jenney FE, Jr., Classen S, Frankel KA, Hopkins RC, Yang SJ, Scott JW, Dillard BD, Adams MW, Tainer JA (2009) Robust, high-throughput solution structural analyses by small angle X-ray scattering (SAXS). Nat Methods 6: 606-612. nmeth.1353 [pii];10.1038/nmeth.1353 [doi].

49. Jacques DA, Trewhella J (2010) Small-angle scattering for structural biology--expanding the frontier while avoiding the pitfalls. Protein Sci 19: 642-657. 10.1002/pro.351 [doi].

50. Svergun DI, Petoukhov MV, Koch MH (2001) Determination of domain structure of proteins from X-ray solution scattering. Biophys J 80: 2946-2953. S0006-3495(01)76260-1 [pii];10.1016/S0006-3495(01)76260-1 [doi].

51. Skora L, Mestan J, Fabbro D, Jahnke W, Grzesiek S (2013) NMR reveals the allosteric opening and closing of Abelson tyrosine kinase by ATP-site and myristoyl pocket inhibitors. Proc Natl Acad Sci U S A 110: E4437-E4445. 1314712110 [pii];10.1073/pnas.1314712110 [doi].

52. Marcsisin SR, Engen JR (2010) Hydrogen exchange mass spectrometry: what is it and what can it tell us? Anal Bioanal Chem 397: 967-972. 10.1007/s00216-010-3556-4 [doi].

53. Chen S, Dumitrescu TP, Smithgall TE, Engen JR (2008) Abl N-terminal cap stabilization of SH3 domain dynamics. Biochemistry 47: 5795-5803.

54. Iacob RE, Zhang J, Gray NS, Engen JR (2011) Allosteric interactions between the myristate- and ATP-site of the Abl kinase. PLoS One 6: e15929. 10.1371/journal.pone.0015929 [doi].

55. Zhang J, Adrian FJ, Jahnke W, Cowan-Jacob SW, Li AG, Iacob RE, Sim T, Powers J, Dierks C, Sun F, Guo GR, Ding Q, Okram B, Choi Y, Wojciechowski A, Deng X, Liu G, Fendrich G, Strauss A, Vajpai N, Grzesiek S, Tuntland T, Liu Y, Bursulaya B, Azam M, Manley PW, Engen JR, Daley GQ, Warmuth M, Gray NS (2010) Targeting Bcr-Abl by combining allosteric with ATP-binding-site inhibitors. Nature 463: 501-506. nature08675 [pii];10.1038/nature08675 [doi].

56. Marion D (2013) An introduction to biological NMR spectroscopy. Mol Cell Proteomics 12: 3006-3025. O113.030239 [pii];10.1074/mcp.O113.030239 [doi].

57. Baldwin AJ, Kay LE (2009) NMR spectroscopy brings invisible protein states into focus. Nat Chem Biol 5: 808-814. nchembio.238 [pii];10.1038/nchembio.238 [doi].

58. Gosser YQ, Zheng J, Overduin M, Mayer BJ, Cowburn D (1995) The solution structure of Abl SH3, and its relationship to SH2 in the SH(32) construct. Structure 3: 1075-1086.

59. Overduin M, Rios CB, Mayer BJ, Baltimore D, Cowburn D (1992) Three-dimensional solution structure of the src homology 2 domain of c-abl. Cell 70: 697-704.

60. Fushman D, Xu R, Cowburn D (1999) Direct determination of changes of interdomain orientation on ligation: use of the orientational dependence of 15N NMR relaxation in Abl SH(32). Biochemistry 38: 10225-10230. 10.1021/bi990897g [doi];bi990897g [pii].

61. Hantschel O, Wiesner S, Guttler T, Mackereth CD, Rix LL, Mikes Z, Dehne J, Gorlich D, Sattler M, Superti-Furga G (2005) Structural basis for the cytoskeletal association of Bcr-Abl/c-Abl. Mol Cell 19: 461-473. S1097-2765(05)01433-4 [pii];10.1016/j.molcel.2005.06.030 [doi].

62. Donaldson LW, Gish G, Pawson T, Kay LE, Forman-Kay JD (2002) Structure of a regulatory complex involving the Abl SH3 domain, the Crk SH2 domain, and a Crk-derived phosphopeptide. Proc Natl Acad Sci U S A 99: 14053-14058. 10.1073/pnas.212518799 [doi];212518799 [pii].

63. Strauss A, Bitsch F, Fendrich G, Graff P, Knecht R, Meyhack B, Jahnke W (2005) Efficient uniform isotope labeling of Abl kinase expressed in Baculovirus-infected insect cells. J Biomol NMR 31: 343-349. 10.1007/s10858-005-2451-3 [doi].

64. Vajpai N, Strauss A, Fendrich G, Cowan-Jacob SW, Manley PW, Grzesiek S, Jahnke W (2008) Solution conformations and dynamics of ABL kinase-inhibitor complexes determined by NMR substantiate the different binding modes of imatinib/nilotinib and dasatinib. J Biol Chem 283: 18292-18302. M801337200 [pii];10.1074/jbc.M801337200 [doi].

65. Grebien F, Hantschel O, Wojcik J, Kaupe I, Kovacic B, Wyrzucki AM, Gish GD, Cerny-Reiterer S, Koide A, Beug H, Pawson T, Valent P, Koide S, Superti-Furga G (2011) Targeting the SH2-kinase interface in Bcr-Abl inhibits leukemogenesis. Cell 147: 306-319. S0092-8674(11)01067-1 [pii];10.1016/j.cell.2011.08.046 [doi].

66. Plattner R, Kadlec L, DeMali KA, Kazlauskas A, Pendergast AM (1999) c-Abl is activated by growth factors and Src family kinases and has a role in the cellular response to PDGF. Genes Dev 13: 2400-2411.

67. Dorey K, Engen JR, Kretzschmar J, Wilm M, Neubauer G, Schindler T, Superti-Furga G (2001) Phosphorylation and structure-based functional studies reveal a positive

and a negative role for the activation loop of the c-Abl tyrosine kinase. Oncogene 20: 8075-8084. 10.1038/sj.onc.1205017 [doi].

68. Birge RB, Kalodimos C, Inagaki F, Tanaka S (2009) Crk and CrkL adaptor proteins: networks for physiological and pathological signaling. Cell Commun Signal 7: 13. 1478-811X-7-13 [pii];10.1186/1478-811X-7-13 [doi].

69. Dai Z, Pendergast AM (1995) Abi-2, a novel SH3-containing protein interacts with the c-Abl tyrosine kinase and modulates c-Abl transforming activity. Genes and Development 9: 2569-2582.

70. Shi Y, Alin K, Goff SP (1995) Abl-interactor-1, a novel SH3 protein binding to the carboxy-terminal portion of the Abl protein, suppresses v-abl transforming activity. Genes Dev 9: 2583-2597.

71. Xiong X, Cui P, Hossain S, Xu R, Warner B, Guo X, An X, Debnath AK, Cowburn D, Kotula L (2008) Allosteric inhibition of the nonMyristoylated c-Abl tyrosine kinase by phosphopeptides derived from Abi1/Hssh3bp1. Biochim Biophys Acta 1783: 737-747. S0167-4889(08)00045-1 [pii];10.1016/j.bbamcr.2008.01.028 [doi].

72. Cao X, Tanis KQ, Koleske AJ, Colicelli J (2008) Enhancement of ABL kinase catalytic efficiency by a direct binding regulator is independent of other regulatory mechanisms. J Biol Chem 283: 31401-31407. M804002200 [pii];10.1074/jbc.M804002200 [doi].

73. Wen ST, Van Etten RA (1997) The PAG gene product, a stress-induced protein with antioxidant properties, is an Abl SH3-binding protein and a physiological inhibitor of c-Abl tyrosine kinase activity. Genes Dev 11: 2456-2467.

74. Lin J, Sun T, Ji L, Deng W, Roth J, Minna J, Arlinghaus R (2007) Oncogenic activation of c-Abl in non-small cell lung cancer cells lacking FUS1 expression: inhibition of c-Abl by the tumor suppressor gene product Fus1. Oncogene 26: 6989-6996. 1210500 [pii];10.1038/sj.onc.1210500 [doi].

75. Plattner R, Koleske AJ, Kazlauskas A, Pendergast AM (2004) Bidirectional signaling links the Abelson kinases to the platelet-derived growth factor receptor. Mol Cell Biol 24: 2573-2583.

76. Tanis KQ, Veach D, Duewel HS, Bornmann WG, Koleske AJ (2003) Two distinct phosphorylation pathways have additive effects on abl family kinase activation. Mol Cell Biol 23: 3884-3896.

77. Plattner R, Irvin BJ, Guo S, Blackburn K, Kazlauskas A, Abraham RT, York JD, Pendergast AM (2003) A new link between the c-Abl tyrosine kinase and phosphoinositide signalling through PLC-gamma1. Nat Cell Biol 5: 309-319. 10.1038/ncb949 [doi];ncb949 [pii].

78. Plattner R, Pendergast AM (2003) Activation and signaling of the Abl tyrosine kinase: bidirectional link with phosphoinositide signaling. Cell Cycle 2: 273-274.

79. Jones RB, Gordus A, Krall JA, MacBeath G (2006) A quantitative protein interaction network for the ErbB receptors using protein microarrays. Nature 439: 168-174. nature04177 [pii];10.1038/nature04177 [doi].

80. Srinivasan D, Plattner R (2006) Activation of Abl tyrosine kinases promotes invasion of aggressive breast cancer cells. Cancer Res 66: 5648-5655. 66/11/5648 [pii];10.1158/0008-5472.CAN-06-0734 [doi].

81. Tanos B, Pendergast AM (2006) Abl tyrosine kinase regulates endocytosis of the epidermal growth factor receptor. J Biol Chem 281: 32714-32723. M603126200 [pii];10.1074/jbc.M603126200 [doi].

82. Kharbanda S, Ren R, Pandey P, Shafman TD, Feller SM, Weichselbaum RR, Kufe DW (1995) Activation of the c-Abl tyrosine kinase in the stress response to DNA-damaging agents. Nature 376: 785-788. 10.1038/376785a0 [doi].

83. Kharbanda S, Pandey P, Ren R, Mayer B, Zon L, Kufe D (1995) c-Abl activation regulates induction of the SEK1/stress-activated protein kinase pathway in the cellular response to 1-beta-D-arabinofuranosylcytosine. J Biol Chem 270: 30278-30281.

84. Liu ZG, Baskaran R, Lea-Chou ET, Wood LD, Chen Y, Karin M, Wang JY (1996) Three distinct signalling responses by murine fibroblasts to genotoxic stress. Nature 384: 273-276. 10.1038/384273a0 [doi].

85. Baskaran R, Wood LD, Whitaker LL, Canman CE, Morgan SE, Xu Y, Barlow C, Baltimore D, Wynshaw-Boris A, Kastan MB, Wang JY (1997) Ataxia telangiectasia mutant protein activates c-Abl tyrosine kinase in response to ionizing radiation. Nature 387: 516-519. 10.1038/387516a0 [doi].

86. Shafman T, Khanna KK, Kedar P, Spring K, Kozlov S, Yen T, Hobson K, Gatei M, Zhang N, Watters D, Egerton M, Shiloh Y, Kharbanda S, Kufe D, Lavin MF (1997) Interaction between ATM protein and c-Abl in response to DNA damage. Nature 387: 520-523. 10.1038/387520a0 [doi].

87. Kharbanda S, Pandey P, Jin S, Inoue S, Bharti A, Yuan ZM, Weichselbaum R, Weaver D, Kufe D (1997) Functional interaction between DNA-PK and c-Abl in response to DNA damage. Nature 386: 732-735. 10.1038/386732a0 [doi].

88. Yuan ZM, Huang Y, Ishiko T, Nakada S, Utsugisawa T, Kharbanda S, Wang R, Sung P, Shinohara A, Weichselbaum R, Kufe D (1998) Regulation of Rad51 function by c-Abl in response to DNA damage. J Biol Chem 273: 3799-3802.

89. Shimizu H, Popova M, Fleury F, Kobayashi M, Hayashi N, Sakane I, Kurumizaka H, Venkitaraman AR, Takahashi M, Yamamoto K (2009) c-ABL tyrosine kinase

stabilizes RAD51 chromatin association. Biochem Biophys Res Commun 382: 286-291. S0006-291X(09)00460-4 [pii];10.1016/j.bbrc.2009.03.020 [doi].

90. Kharbanda S, Yuan ZM, Weichselbaum R, Kufe D (1997) Functional role for the c-Abl protein tyrosine kinase in the cellular response to genotoxic stress. Biochim Biophys Acta 1333: O1-O7. S0304-419X(97)00020-6 [pii].

91. Cheng WH, von KC, Opresko PL, Fields KM, Ren J, Kufe D, Bohr VA (2003) Werner syndrome protein phosphorylation by abl tyrosine kinase regulates its activity and distribution. Mol Cell Biol 23: 6385-6395.

92. Foray N, Marot D, Randrianarison V, Venezia ND, Picard D, Perricaudet M, Favaudon V, Jeggo P (2002) Constitutive association of BRCA1 and c-Abl and its ATM-dependent disruption after irradiation. Mol Cell Biol 22: 4020-4032.

93. Meltser V, Ben-Yehoyada M, Reuven N, Shaul Y (2010) c-Abl downregulates the slow phase of double-strand break repair. Cell Death Dis 1: e20. cddis200921 [pii];10.1038/cddis.2009.21 [doi].

94. Wang X, Zeng L, Wang J, Chau JF, Lai KP, Jia D, Poonepalli A, Hande MP, Liu H, He G, He L, Li B (2011) A positive role for c-Abl in Atm and Atr activation in DNA damage response. Cell Death Differ 18: 5-15. cdd2010106 [pii];10.1038/cdd.2010.106 [doi].

95. Yuan ZM, Huang Y, Ishiko T, Kharbanda S, Weichselbaum R, Kufe D (1997) Regulation of DNA damage-induced apoptosis by the c-Abl tyrosine kinase. Proc Natl Acad Sci U S A 94: 1437-1440.

96. Roger R, Issaad C, Pallardy M, Leglise MC, Turhan AG, Bertoglio J, Breard J (1996) BCR-ABL does not prevent apoptotic death induced by human natural killer or lymphokine-activated killer cells. Blood 87: 1113-1122.

97. Sawyers CL, McLaughlin J, Goga A, Havlik M, Witte ON (1994) The nuclear tyrosine kinase c-Abl negatively regulates cell growth. Cell 77: 121-131.

98. Truong T, Sun G, Doorly M, Wang JY, Schwartz MA (2003) Modulation of DNA damage-induced apoptosis by cell adhesion is independently mediated by p53 and c-Abl. Proc Natl Acad Sci U S A 100: 10281-10286. 10.1073/pnas.1635435100 [doi];1635435100 [pii].

99. Vella V, Zhu J, Frasca F, Li CY, Vigneri P, Vigneri R, Wang JY (2003) Exclusion of c-Abl from the nucleus restrains the p73 tumor suppression function. J Biol Chem 278: 25151-25157. 10.1074/jbc.M301962200 [doi];M301962200 [pii].

100. Goldberg Z, Vogt SR, Berger M, Zwang Y, Perets R, Van Etten RA, Oren M, Taya Y, Haupt Y (2002) Tyrosine phosphorylation of Mdm2 by c-Abl: implications for p53 regulation. EMBO J 21: 3715-3727. 10.1093/emboj/cdf384 [doi].

101. Sionov RV, Moallem E, Berger M, Kazaz A, Gerlitz O, Ben-Neriah Y, Oren M, Haupt Y (1999) c-Abl neutralizes the inhibitory effect of Mdm2 on p53. J Biol Chem 274: 8371-8374.

102. Agami R, Blandino G, Oren M, Shaul Y (1999) Interaction of c-Abl and p73alpha and their collaboration to induce apoptosis. Nature 399: 809-813. 10.1038/21697 [doi].

103. Gong JG, Costanzo A, Yang HQ, Melino G, Kaelin WG, Jr., Levrero M, Wang JY (1999) The tyrosine kinase c-Abl regulates p73 in apoptotic response to cisplatin-induced DNA damage. Nature 399: 806-809. 10.1038/21690 [doi].

104. White E, Prives C (1999) DNA damage enables p73. Nature 399: 734-5, 737. 10.1038/21539 [doi].

105. Yuan ZM, Shioya H, Ishiko T, Sun X, Gu J, Huang YY, Lu H, Kharbanda S, Weichselbaum R, Kufe D (1999) p73 is regulated by tyrosine kinase c-Abl in the apoptotic response to DNA damage. Nature 399: 814-817. 10.1038/21704 [doi].

106. Levy D, Adamovich Y, Reuven N, Shaul Y (2008) Yap1 phosphorylation by c-Abl is a critical step in selective activation of proapoptotic genes in response to DNA damage. Mol Cell 29: 350-361. S1097-2765(08)00064-6 [pii];10.1016/j.molcel.2007.12.022 [doi].

107. American Cancer Society (2015) Cancer Facts and Figures 2015. Atlanta: American Cancer Society .

108. Ren R (2005) Mechanisms of BCR-ABL in the pathogenesis of chronic myelogenous leukaemia. Nat Rev Cancer 5: 172-183. nrc1567 [pii];10.1038/nrc1567 [doi].

109. Apperley JF (2014) Chronic myeloid leukaemia. Lancet . S0140-6736(13)62120-0 [pii];10.1016/S0140-6736(13)62120-0 [doi].

110. Sokal JE, Baccarani M, Russo D, Tura S (1988) Staging and prognosis in chronic myelogenous leukemia. Semin Hematol 25: 49-61.

111. Rowley JD (1973) A new consistent chromosomal abnormality in chronic myelogenous leukemia identified by quinacrine fluorescence and G Giemsa staining. Nature 243: 290-293.

112. NOWELL PC (1962) The minute chromosome (Phl) in chronic granulocytic leukemia. Blut 8: 65-66.

113. NOWELL PC (2007) Discovery of the Philadelphia chromosome: a personal perspective. J Clin Invest 117: 2033-2035. 10.1172/JCI31771 [doi].

114. Groffen J, Stephenson JR, Heisterkamp N, de Klein A, Bartram CR, Grosfeld G (1984) Philadelphia chromosomal breakpoints are clustered within a limited region, *bcr*, on chromosome 22. Cell 36: 93-99.

115. Advani AS, Pendergast AM (2002) Bcr-Abl variants: biological and clinical aspects. Leuk Res 26: 713-720. S0145212601001977 [pii].

116. McWhirter JR, Wang JYJ (1991) Activation of tyrosine kinase and microfilament-binding functions of c-*abl* by *bcr* sequences in *bcr/abl* fusion proteins. Mol Cell Biol 11: 1553-1565.

117. Pendergast AM, Muller AJ, Havlik MH, Maru Y, Witte ON (1991) BCR sequences essential for transformation by the BCR-ABL oncogene bind to the ABL SH2 regulatory domain in a non-phosphotyrosine-dependent manner. Cell 66: 161-171.

118. McWhirter JR, Galasso DL, Wang JYJ (1993) A coiled-coil oligomerization domain of *bcr* is essential for the transforming function of *bcr-abl* oncoproteins. Mol Cell Biol 13: 7587-7595.

119. Zhao X, Ghaffari S, Lodish H, Malashkevich VN, Kim PS (2002) Structure of the Bcr-Abl oncoprotein oligomerization domain. Nat Struct Biol 9: 117-120. 10.1038/nsb747 [doi];nsb747 [pii].

120. Azam M, Latek RR, Daley GQ (2003) Mechanisms of autoinhibition and STI-571/imatinib resistance revealed by mutagenesis of BCR-ABL. Cell 112: 831-843.

121. Ren R (2002) The molecular mechanism of chronic myelogenous leukemia and its therapeutic implications: studies in a murine model. Oncogene 21: 8629-8642. 10.1038/sj.onc.1206090 [doi];1206090 [pii].

122. Ramaraj P, Singh H, Niu N, Chu S, Holtz M, Yee JK, Bhatia R (2004) Effect of mutational inactivation of tyrosine kinase activity on BCR/ABL-induced abnormalities in cell growth and adhesion in human hematopoietic progenitors. Cancer Res 64: 5322-5331. 10.1158/0008-5472.CAN-03-3656 [doi];64/15/5322 [pii].

123. Zhao RC, Jiang Y, Verfaillie CM (2001) A model of human p210(bcr/ABL)-mediated chronic myelogenous leukemia by transduction of primary normal human CD34(+) cells with a BCR/ABL-containing retroviral vector. Blood 97: 2406-2412.

124. Daley GQ, Van Etten RA, Baltimore D (1990) Induction of chronic myelogenous leukemia in mice by the $p210^{bcr-abl}$ gene of the Philadelphia chromosome. Science 247: 824-830.

125. Deininger MW, Goldman JM, Melo JV (2000) The molecular biology of chronic myeloid leukemia. Blood 96: 3343-3356.

126. Yaish P, Gazit A, Gilon C, Levitzki A (1988) Blocking of EGF-dependent cell proliferation by EGF receptor kinase inhibitors. Science 242: 933-935.

127. Buchdunger E, Zimmermann J, Mett H, Meyer T, Muller M, Regenass U, Lydon NB (1995) Selective inhibition of the platelet-derived growth factor signal transduction pathway by a protein-tyrosine kinase inhibitor of the 2-phenylaminopyrimidine class. Proc Natl Acad Sci U S A 92: 2558-2562.

128. Buchdunger E, Zimmermann J, Mett H, Meyer T, Muller M, Druker BJ, Lydon NB (1996) Inhibition of the Abl protein-tyrosine kinase in vitro and in vivo by a 2-phenylaminopyrimidine derivative. Cancer Res 56: 100-104.

129. Druker BJ, Tamura S, Buchdunger E, Ohno S, Segal GM, Fanning S, Zimmermann J, Lydon NB (1996) Effects of a selective inhibitor of the Abl tyrosine kinase on the growth of Bcr-Abl positive cells. Nat Med 2: 561-566.

130. Druker BJ, Talpaz M, Resta DJ, Peng B, Buchdunger E, Ford JM, Lydon NB, Kantarjian H, Capdeville R, Ohno-Jones S, Sawyers CL (2001) Efficacy and safety of a specific inhibitor of the BCR-ABL tyrosine kinase in chronic myeloid leukemia. N Engl J Med 344: 1031-1037.

131. Druker BJ (2004) Imatinib as a paradigm of targeted therapies. Adv Cancer Res 91: 1-30. 10.1016/S0065-230X(04)91001-9 [doi];S0065230X04910019 [pii].

132. Quintas-Cardama A, Kantarjian HM, Cortes JE (2009) Mechanisms of primary and secondary resistance to imatinib in chronic myeloid leukemia. Cancer Control 16: 122-131.

133. La RP, Deininger MW (2010) Resistance to imatinib: mutations and beyond. Semin Hematol 47: 335-343. S0037-1963(10)00079-X [pii];10.1053/j.seminhematol.2010.06.005 [doi].

134. Gorre ME, Mohammed M, Ellwood K, Hsu N, Paquette R, Rao PN, Sawyers CL (2001) Clinical resistance to STI-571 cancer therapy caused by BCR-ABL gene mutation or amplification. Science 293: 876-880.

135. Hochhaus A, Kreil S, Corbin AS, La RP, Muller MC, Lahaye T, Hanfstein B, Schoch C, Cross NC, Berger U, Gschaidmeier H, Druker BJ, Hehlmann R (2002) Molecular and chromosomal mechanisms of resistance to imatinib (STI571) therapy. Leukemia 16: 2190-2196. 10.1038/sj.leu.2402741 [doi].

136. Sherbenou DW, Hantschel O, Kaupe I, Willis S, Bumm T, Turaga LP, Lange T, Dao KH, Press RD, Druker BJ, Superti-Furga G, Deininger MW (2010) BCR-ABL SH3-SH2 domain mutations in chronic myeloid leukemia patients on imatinib. Blood . blood-2008-10-183665 [pii];10.1182/blood-2008-10-183665 [doi].

137. Deininger MW (2004) Basic science going clinical: molecularly targeted therapy of chronic myelogenous leukemia. J Cancer Res Clin Oncol 130: 59-72. 10.1007/s00432-003-0502-2 [doi].

138. Griswold IJ, MacPartlin M, Bumm T, Goss VL, O'Hare T, Lee KA, Corbin AS, Stoffregen EP, Smith C, Johnson K, Moseson EM, Wood LJ, Polakiewicz RD, Druker BJ, Deininger MW (2006) Kinase domain mutants of Bcr-Abl exhibit altered transformation potency, kinase activity, and substrate utilization, irrespective of sensitivity to imatinib. Mol Cell Biol 26: 6082-6093.

139. Vaidya S, Ghosh K, Vundinti BR (2011) Recent developments in drug resistance mechanism in chronic myeloid leukemia: a review. Eur J Haematol 87: 381-393. 10.1111/j.1600-0609.2011.01689.x [doi].

140. Donato NJ, Wu JY, Stapley J, Gallick G, Lin H, Arlinghaus R, Talpaz M (2003) BCR-ABL independence and LYN kinase overexpression in chronic myelogenous leukemia cells selected for resistance to STI571. Blood 101: 690-698. 10.1182/blood.V101.2.690 [doi];101/2/690 [pii].

141. Ptasznik A, Nakata Y, Kalota A, Emerson SG, Gewirtz AM (2004) Short interfering RNA (siRNA) targeting the Lyn kinase induces apoptosis in primary, and drug-resistant, BCR-ABL1(+) leukemia cells. Nat Med 10: 1187-1189. nm1127 [pii];10.1038/nm1127 [doi].

142. Wu J, Meng F, Kong LY, Peng Z, Ying Y, Bornmann WG, Darnay BG, Lamothe B, Sun H, Talpaz M, Donato NJ (2008) Association between imatinib-resistant BCR-ABL mutation-negative leukemia and persistent activation of LYN kinase. J Natl Cancer Inst 100: 926-939. djn188 [pii];10.1093/jnci/djn188 [doi].

143. Grosso S, Puissant A, Dufies M, Colosetti P, Jacquel A, Lebrigand K, Barbry P, Deckert M, Cassuto JP, Mari B, Auberger P (2009) Gene expression profiling of imatinib and PD166326-resistant CML cell lines identifies Fyn as a gene associated with resistance to BCR-ABL inhibitors. Mol Cancer Ther 8: 1924-1933. 1535-7163.MCT-09-0168 [pii];10.1158/1535-7163.MCT-09-0168 [doi].

144. Ban K, Gao Y, Amin HM, Howard A, Miller C, Lin Q, Leng X, Munsell M, Bar-Eli M, Arlinghaus RB, Chandra J (2008) BCR-ABL1 mediates up-regulation of Fyn in chronic myelogenous leukemia. Blood 111: 2904-2908. blood-2007-05-091769 [pii];10.1182/blood-2007-05-091769 [doi].

145. Singh MM, Howard A, Irwin ME, Gao Y, Lu X, Multani A, Chandra J (2012) Expression and activity of Fyn mediate proliferation and blastic features of chronic myelogenous leukemia. PLoS One 7: e51611. 10.1371/journal.pone.0051611 [doi];PONE-D-12-18436 [pii].

146. Pene-Dumitrescu T, Peterson LF, Donato NJ, Smithgall TE (2008) An inhibitor-resistant mutant of Hck protects CML cells against the antiproliferative and apoptotic

effects of the broad-spectrum Src family kinase inhibitor A-419259. Oncogene 27: 7055-7069.

147. Pene-Dumitrescu T, Smithgall TE (2010) Expression of a Src family kinase in chronic myelogenous leukemia cells induces resistance to imatinib in a kinase-dependent manner. J Biol Chem 285: 21446-21457. M109.090043 [pii];10.1074/jbc.M109.090043 [doi].

148. O'Hare T, Zabriskie MS, Eiring AM, Deininger MW (2012) Pushing the limits of targeted therapy in chronic myeloid leukaemia. Nat Rev Cancer 12: 513-526. nrc3317 [pii];10.1038/nrc3317 [doi].

149. Chu S, McDonald T, Lin A, Chakraborty S, Huang Q, Snyder DS, Bhatia R (2011) Persistence of leukemia stem cells in chronic myelogenous leukemia patients in prolonged remission with imatinib treatment. Blood 118: 5565-5572. blood-2010-12-327437 [pii];10.1182/blood-2010-12-327437 [doi].

150. Corbin AS, Agarwal A, Loriaux M, Cortes J, Deininger MW, Druker BJ (2011) Human chronic myeloid leukemia stem cells are insensitive to imatinib despite inhibition of BCR-ABL activity. J Clin Invest 121: 396-409. 35721 [pii];10.1172/JCI35721 [doi].

151. Hamilton A, Helgason GV, Schemionek M, Zhang B, Myssina S, Allan EK, Nicolini FE, Muller-Tidow C, Bhatia R, Brunton VG, Koschmieder S, Holyoake TL (2012) Chronic myeloid leukemia stem cells are not dependent on Bcr-Abl kinase activity for their survival. Blood 119: 1501-1510. blood-2010-12-326843 [pii];10.1182/blood-2010-12-326843 [doi].

152. Weisberg E, Manley PW, Breitenstein W, Bruggen J, Cowan-Jacob SW, Ray A, Huntly B, Fabbro D, Fendrich G, Hall-Meyers E, Kung AL, Mestan J, Daley GQ, Callahan L, Catley L, Cavazza C, Azam M, Neuberg D, Wright RD, Gilliland DG, Griffin JD (2005) Characterization of AMN107, a selective inhibitor of native and mutant Bcr-Abl. Cancer Cell 7: 129-141. S1535-6108(05)00028-0 [pii];10.1016/j.ccr.2005.01.007 [doi].

153. Weisberg E, Manley P, Mestan J, Cowan-Jacob S, Ray A, Griffin JD (2006) AMN107 (nilotinib): a novel and selective inhibitor of BCR-ABL. Br J Cancer 94: 1765-1769. 6603170 [pii];10.1038/sj.bjc.6603170 [doi].

154. O'Hare T, Walters DK, Deininger MW, Druker BJ (2005) AMN107: tightening the grip of imatinib. Cancer Cell 7: 117-119. S1535-6108(05)00035-8 [pii];10.1016/j.ccr.2005.01.020 [doi].

155. Lombardo LJ, Lee FY, Chen P, Norris D, Barrish JC, Behnia K, Castaneda S, Cornelius LA, Das J, Doweyko AM, Fairchild C, Hunt JT, Inigo I, Johnston K, Kamath A, Kan D, Klei H, Marathe P, Pang S, Peterson R, Pitt S, Schieven GL, Schmidt RJ, Tokarski J, Wen ML, Wityak J, Borzilleri RM (2004) Discovery of N-(2-chloro-6-methyl- phenyl)-2-(6-(4-(2-hydroxyethyl)- piperazin-1-yl)-2-methylpyrimidin-

4- ylamino)thiazole-5-carboxamide (BMS-354825), a dual Src/Abl kinase inhibitor with potent antitumor activity in preclinical assays. J Med Chem 47: 6658-6661. 10.1021/jm049486a [doi].

156. O'Hare T, Walters DK, Stoffregen EP, Jia T, Manley PW, Mestan J, Cowan-Jacob SW, Lee FY, Heinrich MC, Deininger MW, Druker BJ (2005) In vitro activity of Bcr-Abl inhibitors AMN107 and BMS-354825 against clinically relevant imatinib-resistant Abl kinase domain mutants. Cancer Res 65: 4500-4505. 65/11/4500 [pii];10.1158/0008-5472.CAN-05-0259 [doi].

157. Golas JM, Arndt K, Etienne C, Lucas J, Nardin D, Gibbons J, Frost P, Ye F, Boschelli DH, Boschelli F (2003) SKI-606, a 4-anilino-3-quinolinecarbonitrile dual inhibitor of Src and Abl kinases, is a potent antiproliferative agent against chronic myelogenous leukemia cells in culture and causes regression of K562 xenografts in nude mice. Cancer Res 63: 375-381.

158. Puttini M, Coluccia AM, Boschelli F, Cleris L, Marchesi E, Donella-Deana A, Ahmed S, Redaelli S, Piazza R, Magistroni V, Andreoni F, Scapozza L, Formelli F, Gambacorti-Passerini C (2006) In vitro and in vivo activity of SKI-606, a novel Src-Abl inhibitor, against imatinib-resistant Bcr-Abl+ neoplastic cells. Cancer Res 66: 11314-11322. 0008-5472.CAN-06-1199 [pii];10.1158/0008-5472.CAN-06-1199 [doi].

159. O'Hare T, Shakespeare WC, Zhu X, Eide CA, Rivera VM, Wang F, Adrian LT, Zhou T, Huang WS, Xu Q, Metcalf CA, III, Tyner JW, Loriaux MM, Corbin AS, Wardwell S, Ning Y, Keats JA, Wang Y, Sundaramoorthi R, Thomas M, Zhou D, Snodgrass J, Commodore L, Sawyer TK, Dalgarno DC, Deininger MW, Druker BJ, Clackson T (2009) AP24534, a pan-BCR-ABL inhibitor for chronic myeloid leukemia, potently inhibits the T315I mutant and overcomes mutation-based resistance. Cancer Cell 16: 401-412. S1535-6108(09)00339-0 [pii];10.1016/j.ccr.2009.09.028 [doi].

160. Cortes JE, Kim DW, Pinilla-Ibarz J, le CP, Paquette R, Chuah C, Nicolini FE, Apperley JF, Khoury HJ, Talpaz M, DiPersio J, DeAngelo DJ, Abruzzese E, Rea D, Baccarani M, Muller MC, Gambacorti-Passerini C, Wong S, Lustgarten S, Rivera VM, Clackson T, Turner CD, Haluska FG, Guilhot F, Deininger MW, Hochhaus A, Hughes T, Goldman JM, Shah NP, Kantarjian H (2013) A phase 2 trial of ponatinib in Philadelphia chromosome-positive leukemias. N Engl J Med 369: 1783-1796. 10.1056/NEJMoa1306494 [doi].

161. Quintas-Cardama A (2014) Ponatinib in Philadelphia chromosome-positive leukemias. N Engl J Med 370: 577. 10.1056/NEJMc1315234#SA1 [doi].

162. Chan WW, Wise SC, Kaufman MD, Ahn YM, Ensinger CL, Haack T, Hood MM, Jones J, Lord JW, Lu WP, Miller D, Patt WC, Smith BD, Petillo PA, Rutkoski TJ, Telikepalli H, Vogeti L, Yao T, Chun L, Clark R, Evangelista P, Gavrilescu LC, Lazarides K, Zaleskas VM, Stewart LJ, Van Etten RA, Flynn DL (2011)

Conformational control inhibition of the BCR-ABL1 tyrosine kinase, including the gatekeeper T315I mutant, by the switch-control inhibitor DCC-2036. Cancer Cell 19: 556-568. S1535-6108(11)00092-4 [pii];10.1016/j.ccr.2011.03.003 [doi].

163. Adrian FJ, Ding Q, Sim T, Velentza A, Sloan C, Liu Y, Zhang G, Hur W, Ding S, Manley P, Mestan J, Fabbro D, Gray NS (2006) Allosteric inhibitors of Bcr-abl-dependent cell proliferation. Nat Chem Biol 2: 95-102.

164. Beissert T, Hundertmark A, Kaburova V, Travaglini L, Mian AA, Nervi C, Ruthardt M (2008) Targeting of the N-terminal coiled coil oligomerization interface by a helix-2 peptide inhibits unmutated and imatinib-resistant BCR/ABL. Int J Cancer 122: 2744-2752. 10.1002/ijc.23467 [doi].

165. Greuber EK, Smith-Pearson P, Wang J, Pendergast AM (2013) Role of ABL family kinases in cancer: from leukaemia to solid tumours. Nat Rev Cancer 13: 559-571. nrc3563 [pii];10.1038/nrc3563 [doi].

166. Mader CC, Oser M, Magalhaes MA, Bravo-Cordero JJ, Condeelis J, Koleske AJ, Gil-Henn H (2011) An EGFR-Src-Arg-cortactin pathway mediates functional maturation of invadopodia and breast cancer cell invasion. Cancer Res 71: 1730-1741. 0008-5472.CAN-10-1432 [pii];10.1158/0008-5472.CAN-10-1432 [doi].

167. Sirvent A, Boureux A, Simon V, Leroy C, Roche S (2007) The tyrosine kinase Abl is required for Src-transforming activity in mouse fibroblasts and human breast cancer cells. Oncogene 26: 7313-7323. 1210543 [pii];10.1038/sj.onc.1210543 [doi].

168. Smith-Pearson PS, Greuber EK, Yogalingam G, Pendergast AM (2010) Abl kinases are required for invadopodia formation and chemokine-induced invasion. J Biol Chem 285: 40201-40211. M110.147330 [pii];10.1074/jbc.M110.147330 [doi].

169. Srinivasan D, Sims JT, Plattner R (2008) Aggressive breast cancer cells are dependent on activated Abl kinases for proliferation, anchorage-independent growth and survival. Oncogene 27: 1095-1105. 1210714 [pii];10.1038/sj.onc.1210714 [doi].

170. Furlan A, Stagni V, Hussain A, Richelme S, Conti F, Prodosmo A, Destro A, Roncalli M, Barila D, Maina F (2011) Abl interconnects oncogenic Met and p53 core pathways in cancer cells. Cell Death Differ 18: 1608-1616. cdd201123 [pii];10.1038/cdd.2011.23 [doi].

171. Sirvent A, Benistant C, Roche S (2008) Cytoplasmic signalling by the c-Abl tyrosine kinase in normal and cancer cells. Biol Cell 100: 617-631. BC20080020 [pii];10.1042/BC20080020 [doi].

172. Noren NK, Foos G, Hauser CA, Pasquale EB (2006) The EphB4 receptor suppresses breast cancer cell tumorigenicity through an Abl-Crk pathway. Nat Cell Biol 8: 815-825. ncb1438 [pii];10.1038/ncb1438 [doi].

173. Allington TM, Galliher-Beckley AJ, Schiemann WP (2009) Activated Abl kinase inhibits oncogenic transforming growth factor-beta signaling and tumorigenesis in mammary tumors. FASEB J 23: 4231-4243. fj.09-138412 [pii];10.1096/fj.09-138412 [doi].

174. Hantschel O, Superti-Furga G (2004) Regulation of the c-Abl and Bcr-Abl tyrosine kinases. Nat Rev Mol Cell Biol 5: 33-44.

175. Wong S, Witte ON (2004) The BCR-ABL story: bench to bedside and back. Annu Rev Immunol 22: 247-306. 10.1146/annurev.immunol.22.012703.104753 [doi].

176. Charter NW, Kauffman L, Singh R, Eglen RM (2006) A generic, homogenous method for measuring kinase and inhibitor activity via adenosine 5'-diphosphate accumulation. J Biomol Screen 11: 390-399. 1087057106286829 [pii];10.1177/1087057106286829 [doi].

177. Moroco JA, Craigo JK, Iacob RE, Wales TE, Engen JR, Smithgall TE (2014) Differential sensitivity of Src-family kinases to activation by SH3 domain displacement. PLoS One 9: e105629. 10.1371/journal.pone.0105629 [doi];PONE-D-14-20866 [pii].

178. Allaire M, Yang L (2011) Biomolecular solution X-ray scattering at the National Synchrotron Light Source. J Synchrotron Radiat 18: 41-44. S0909049510036022 [pii];10.1107/S0909049510036022 [doi].

179. Konarev PV, Petoukhov MV, Volkov VV, Svergun DI (2006) ATSAS 2.1, a program package for small-angle scattering data analysis. Journal of Applied Crystallography 39: 277-286.

180. Svergun DI (1992) Determination of the regularization parameter in indirect-transform methods using perceptual criteria. Journal of Applied Crystallography 25: 495-503.

181. Kozin MB, Svergun DI (2001) Automated matching of high- and low-resolution structural models. Journal of Applied Crystallography 34: 33-41.

182. Niesen FH, Berglund H, Vedadi M (2007) The use of differential scanning fluorimetry to detect ligand interactions that promote protein stability. Nat Protoc 2: 2212-2221. nprot.2007.321 [pii];10.1038/nprot.2007.321 [doi].

183. Konarev PV, Volkov VV, Sokolova AV, Koch MHJ, Svergun DI (2003) PRIMUS: a Windows PC-based system for small-angle scattering data analysis. Journal of Applied Crystallography 36: 1277-1282.

184. Filippakopoulos P, Kofler M, Hantschel O, Gish GD, Grebien F, Salah E, Neudecker P, Kay LE, Turk BE, Superti-Furga G, Pawson T, Knapp S (2008) Structural coupling of SH2-kinase domains links Fes and Abl substrate recognition and kinase activation. Cell 134: 793-803. S0092-8674(08)01013-1 [pii];10.1016/j.cell.2008.07.047 [doi].

185. Yang J, Campobasso N, Biju MP, Fisher K, Pan XQ, Cottom J, Galbraith S, Ho T, Zhang H, Hong X, Ward P, Hofmann G, Siegfried B, Zappacosta F, Washio Y, Cao P, Qu J, Bertrand S, Wang DY, Head MS, Li H, Moores S, Lai Z, Johanson K, Burton G, Erickson-Miller C, Simpson G, Tummino P, Copeland RA, Oliff A (2011) Discovery and characterization of a cell-permeable, small-molecule c-Abl kinase activator that binds to the myristoyl binding site. Chem Biol 18: 177-186. S1074-5521(10)00486-2 [pii];10.1016/j.chembiol.2010.12.013 [doi].

186. Heller WT (2005) Influence of multiple well defined conformations on small-angle scattering of proteins in solution. Acta Crystallogr D Biol Crystallogr 61: 33-44. S0907444904025855 [pii];10.1107/S0907444904025855 [doi].

187. Cowan-Jacob SW, Fendrich G, Manley PW, Jahnke W, Fabbro D, Liebetanz J, Meyer T (2005) The Crystal Structure of a c-Src Complex in an Active Conformation Suggests Possible Steps in c-Src Activation. Structure (Camb) 13: 861-871.

188. Maiani E, Diederich M, Gonfloni S (2011) DNA damage response: the emerging role of c-Abl as a regulatory switch? Biochem Pharmacol 82: 1269-1276. S0006-2952(11)00430-8 [pii];10.1016/j.bcp.2011.07.001 [doi].

189. Panjarian S, Iacob RE, Chen S, Engen JR, Smithgall TE (2013) Structure and dynamic regulation of Abl kinases. J Biol Chem 288: 5443-5450. R112.438382 [pii];10.1074/jbc.R112.438382 [doi].

190. Seeliger MA, Young M, Henderson MN, Pellicena P, King DS, Falick AM, Kuriyan J (2005) High yield bacterial expression of active c-Abl and c-Src tyrosine kinases. Protein Sci 14: 3135-3139.

191. Pisabarro MT, Serrano L (1996) Rational design of specific high-affinity peptide ligands for the Abl-SH3 domain. Biochemistry 35: 10634-10640. 10.1021/bi960203t [doi];bi960203t [pii].

192. Pisabarro MT, Serrano L, Wilmanns M (1998) Crystal structure of the abl-SH3 domain complexed with a designed high-affinity peptide ligand: implications for SH3-ligand interactions. J Mol Biol 281: 513-521. S0022-2836(98)91932-5 [pii];10.1006/jmbi.1998.1932 [doi].

193. Dragiev P, Nadon R, Makarenkov V (2012) Two effective methods for correcting experimental high-throughput screening data. Bioinformatics 28: 1775-1782. bts262 [pii];10.1093/bioinformatics/bts262 [doi].

194. Shun TY, Lazo JS, Sharlow ER, Johnston PA (2011) Identifying actives from HTS data sets: practical approaches for the selection of an appropriate HTS data-processing method and quality control review. J Biomol Screen 16: 1-14. 1087057110389039 [pii];10.1177/1087057110389039 [doi].

195. Murphy M, Jason-Moller L, Bruno J (2006) Using Biacore to measure the binding kinetics of an antibody-antigen interaction. Curr Protoc Protein Sci Chapter 19: Unit 19.14. 10.1002/0471142301.ps1914s45 [doi].

196. Jason-Moller L, Murphy M, Bruno J (2006) Overview of Biacore systems and their applications. Curr Protoc Protein Sci Chapter 19: Unit 19.13. 10.1002/0471140864.ps1913s45 [doi].

197. Champ PC, Camacho CJ (2007) FastContact: a free energy scoring tool for protein-protein complex structures. Nucleic Acids Res 35: W556-W560. gkm326 [pii];10.1093/nar/gkm326 [doi].

198. Gotz AW, Williamson MJ, Xu D, Poole D, Le GS, Walker RC (2012) Routine Microsecond Molecular Dynamics Simulations with AMBER on GPUs. 1. Generalized Born. J Chem Theory Comput 8: 1542-1555. 10.1021/ct200909j [doi].

199. Case DA, Babib V, Berryman JT, Betz RM, Cai Q et al. (2014) AMBER 14, University of California San Francisco, version 14 [computer program].

200. Wang J, Wolf RM, Caldwell JW, Kollman PA, Case DA (2004) Development and testing of a general amber force field. J Comput Chem 25: 1157-1174. 10.1002/jcc.20035 [doi].

201. Koes DR, Baumgartner MP, Camacho CJ (2013) Lessons learned in empirical scoring with smina from the CSAR 2011 benchmarking exercise. J Chem Inf Model 53: 1893-1904. 10.1021/ci300604z [doi].

202. Pisabarro MT, Serrano L, Wilmanns M (1998) Crystal structure of the abl-SH3 domain complexed with a designed high-affinity peptide ligand: implications for SH3-ligand interactions. J Mol Biol 281: 513-521.

203. Zhang JH, Chung TDY, Oldenburg KR (1999) A simple statistical parameter for use in evaluation and validation of high throughput screening assays. J Biomol Screen 4: 67-73.

204. Balakumar P, Nyo YH, Renushia R, Raaginey D, Oh AN, Varatharajan R, Dhanaraj SA (2014) Classical and pleiotropic actions of dipyridamole: Not enough light to illuminate the dark tunnel? Pharmacol Res 87: 144-150. S1043-6618(14)00074-7 [pii];10.1016/j.phrs.2014.05.008 [doi].

205. Lipinski CA (2004) Lead- and drug-like compounds: the rule-of-five revolution. Drug Discov Today Technol 1: 337-341. S1740-6749(04)00055-1 [pii];10.1016/j.ddtec.2004.11.007 [doi].

206. Kitamura T, Tange T, Terasawa T, Chiba S, Kuwaki T, Miyagawa K, Piao YF, Miyazono K, Urabe A, Takaku F (1989) Establishment and characterization of a unique

human cell line that proliferates dependently on GM-CSF, IL-3, or erythropoietin. J Cell Physiol 140: 323-334. 10.1002/jcp.1041400219 [doi].

207. Nakajima A, Tauchi T, Ohyashiki K (2001) ABL-specific tyrosine kinase inhibitor, STI571 in vitro, affects Ph-positive acute lymphoblastic leukemia and chronic myelogenous leukemia in blastic crisis. Leukemia 15: 989-990.

208. Ganguly SS, Plattner R (2012) Activation of abl family kinases in solid tumors. Genes Cancer 3: 414-425. 10.1177/1947601912458586 [doi];10.1177_1947601912458586 [pii].

209. Puls LN, Eadens M, Messersmith W (2011) Current status of SRC inhibitors in solid tumor malignancies. Oncologist 16: 566-578. theoncologist.2010-0408 [pii];10.1634/theoncologist.2010-0408 [doi].

210. Berg LJ, Finkelstein LD, Lucas JA, Schwartzberg PL (2005) Tec family kinases in T lymphocyte development and function. Annu Rev Immunol 23: 549-600. 10.1146/annurev.immunol.22.012703.104743 [doi].

211. Sicheri F, Kuriyan J (1997) Structures of Src-family tyrosine kinases. Curr Opin Struct Biol 7: 777-785.